Cover Page



Universiteit Leiden



The handle http://hdl.handle.net/1887/19035 holds various files of this Leiden University dissertation.

Author: Andrea, Carlos Eduardo de
Title: The epiphyseal growth plate and peripheral cartilaginous tumours : the neighbours matter
Issue Date: 2012-05-30

The Epiphyseal Growth Plate and Peripheral Cartilaginous Tumours: The Neighbours Matter

The Epiphyseal Growth Plate and Peripheral Cartilaginous Tumours: The Neighbours Matter
©2012, Carlos E. de Andrea, Leiden, the Netherlands. All rights reserved.

ISBN:

Printed by:

The work presented in this thesis was financially supported by EuroBoNeT, a European Commission-granted European Network of excellence for studying the pathology and genetics of bone tumours.
Grant Number: LSHC-CT-2006-018814

The Epiphyseal Growth Plate and Peripheral Cartilaginous Tumours: The Neighbours Matter

Proefschrift

ter verkrijging van de graad van Doctor aan de Universiteit Leiden,
op gezag van Rector Magnificus prof. mr. P.F. van der Heijden,
volgens besluit van het College voor Promoties
te verdedigen op woensdag 30 mei 2012
klokke 11.15 uur

door

Carlos Eduardo de Andrea
geboren te Curitiba (Brazilië)
in 1978

Promotiecommissie

Promotor:	Prof. Dr. P.C.W. Hogendoorn
Co-promotor:	Dr. J.V.M.G. Bovée
Overige leden:	Prof. Dr. A.J. Koster Prof. Dr. H. Spaink Prof. Dr. H.J. Tanke Prof. Dr. N.A. Athanasou (Nuffield Department of Orthopaedics, Rheumatology and Musculoskeletal Sciences, University of Oxford, Oxford, UK)

“Omnis cellula e cellula”
Rudolf Ludwig Karl Virchow (1858)

CONTENTS

Chapter 1 09
General Introduction

Chapter 2 19
Epiphyseal growth plate and secondary peripheral chondrosarcoma:
the neighbours matter
J Pathol. 2012;226:219-28

Chapter 3 41
Cartilage ultrastructure in proteoglycan-deficient zebrafish mutants brings
to light new candidate genes for human skeletal disorders
J Pathol. 2011;223:531-42

Chapter 4 61
Heparan sulphate upholds osteoblastic lineage

Chapter 5 73
Growth plate regulation and osteochondroma formation: insights from
tracing proteoglycans in zebrafish models and human cartilage
J Pathol. 2011;224:160-8

Chapter 6 91
Primary cilia organization reflects polarity in the growth plate and implies
loss of polarity and mosaicism in osteochondroma
Lab Invest. 2010;90:1091-101

Chapter 7 109
Secondary peripheral chondrosarcoma evolving from osteochondroma as
a result of outgrowth of cells with functional *EXT*
Oncogene. 2012;31:1095-104

Chapter 8 129
Interobserver Reliability in the Histopathological Diagnosis of Cartilaginous Tumors in Patients with Multiple Osteochondromas
Mod Pathol. *in press*

Chapter 9 143
Peripheral chondrosarcoma progression is associated with increased type X collagen and vascularisation
Virchows Archiv. 2012;460:95-102

Chapter 10 157
Summary and concluding remarks

Nederlandse samenvatting 165
List of publications 171
Curriculum Vitae 173
Acknowledgments 175

Chapter 1

General Introduction

I. Developmental regulation of the growth plate
II. Peripheral cartilaginous bone tumours
III. Zebrafish as a model system to study human skeletal disorders
IV. Scope of the study and outline of the thesis

I. Developmental regulation of the growth plate

Skeletal development is a highly orchestrated process in which all the players involved ought to be perfectly co-ordinated and regulated in order to achieve harmonious and symmetrical growth. Most of the skeleton is formed by endochondral ossification, including the long, short, and irregular bones (1;2). In the process of endochondral ossification, mesenchymal cells differentiate into chondrocytes, which then provide a cartilage template for bone morphogenesis.

Endochondral ossification occurs at two distinct centres of ossification in the vertebrate long bone – the primary (diaphyseal) and the secondary (epiphyseal) centres (3). Bone development initiates at the primary centre. The secondary (epiphyseal) centre is ossified later. During this process, the segregation of chondrocytes at different stages of differentiation between the diaphysis and the epiphysis forms the growth plate.

The epiphyseal growth plate is regulated by a wide array of autocrine and paracrine molecules (3). Signalling through Indian hedgehog (Ihh), parathyroid hormone-related peptide (PTHrP; also known as PTHLH), bone morphogenetic proteins (BMPs), fibroblast growth factor (FGFs), and others, modulates and regulates chondrocyte proliferation and hypertrophy (3). Another important growth factor for both embryonic and post-natal development is insulin-like growth factors (IGF-1 and IGF-2). While IGF-2 is important for normal embryonic growth (4), IGF-1 appears to regulate post-natal growth (5). IGF-1 and IGF-2 are known to signal through the type I IGF receptor (IGF1R) in target tissues (6). Both circulating and locally produced IGF-1 stimulate chondrocyte proliferation in the growth plate (7).

The cartilaginous extracellular matrix produced by and surrounding the terminally differentiated hypertrophic chondrocytes is calcified. Following vascular invasion, osteogenic progenitors are recruited to this calcified area, replacing it by trabecular bone (3). Proteoglycans and collagens are the most abundant matrix components of the growth plate. Proteoglycans are localized intracellularly (usually in secretory granules), at the cell surface, or in the extracellular matrix (8). Their biological functions are highly diversified (8). Proteoglycans play an important role on various cellular processes, such as cell adhesion, motility, and proliferation, further to differentiation and tissue morphogenesis (8). Most of these effects depend on binding of signalling molecules to the glycosaminoglycan side chains. Proteoglycans influence the distribution of these signalling molecules in the extracellular matrix, their receptor binding affinity and the responses of cells to secreted protein factors (8;9).

Mutations affecting the biosynthesis of either proteoglycans or glycosaminoglycans alter the interaction between a cell and its micro-environment and are the cause of several human disorders. Several of these disorders are associated with a skeletal phenotype (10).

II. Peripheral cartilaginous bone tumours

Cartilaginous bone tumours are characterized by production of a chondroid matrix. They are classified based on their histological and radiological features, location, and clinical behaviour. Cartilaginous bone tumours can form on the surface of bones, as in sporadic or multiple osteochondromas, or within the bones, as in sporadic or multiple enchondromas. These originally benign tumours often carry significant morbidity and risk of developing chondrosarcoma.

Osteochondromas are the most common benign bone tumours of childhood and adolescence (11). They are characterized by sporadic (non-familial/solitary) or multiple (hereditary) cartilage-capped bony projections from the metaphyses of endochondral bones adjacent to the growth plate and develop during skeletal growth (12). Multiple osteochondromas, previously called hereditary multiple exostoses, is an autosomal dominant disorder with a prevalence of 1 in 18,000 (13). Patients with multiple osteochondromas are often short in stature and have bowed bones that can restrict movement and ultimately result in joint dislocation (13). In contrast, patients with sporadic lesions may develop symptoms on the affected side only. Sporadic and multiple lesions are histologically indistinguishable (12;14).

Multiple osteochondromas is characterized by genetic variability, which partially explains inter- and intra-familial phenotypic variation often found in these patients (15). The majority of the hereditary cases are caused by point mutations (70-75%). Small deletions involving single or multiple exons are found in about 10% of all hereditary cases (16-18). Large deletions have been identified in few cases (15). No genomic alterations are detected in about 10-15%. In some of these negative cases, somatic mosaicism with large genomic deletions of *EXT1* and *EXT2* has been described as the underlying mechanism of multiple osteochondromas formation (19). In sporadic osteochondromas, homozygous deletions of *EXT1* are often identified (20).

EXT1 and *EXT2* encode type II transmembrane glycosyltransferases (21;22), whose functions are not fully known. *EXT1* and *EXT2* form a hetero-oligomeric complex in the Golgi apparatus of most human cells that participate in chain elongation in heparan sulphate biosynthesis (23;24). During endochondral ossification, heparan sulphate regulates the range of Ihh signalling, and thus proliferation of growth plate chondrocytes (3).
Albeit the genetic correlation between mutations in *EXT1/EXT2* and osteochondromas, the mechanism by which alterations in heparan sulphate biosynthesis leads to osteochondroma is not entirely understood (25).

Neoplastic transformation of an osteochondroma occurs in less than 1% of patients with sporadic osteochondromas and 1-3% of patients with multiple osteochondromas (26). Neoplastic transformation usually occurs 20-60 years after the cessation of osteochondroma growth that happens at the time of the fusion of the epiphyseal growth plate at puberty (12;14).

III. Zebrafish as a model system to study human skeletal disorders

As a vertebrate, zebrafish, Danio rerio, is more closely related to humans than are yeast, worms or flies. Many features of zebrafish development have been characterized, including early embryonic patterning, development of the musculoskeletal system as well as aspects of cell fate and lineage determination. Zebrafish has several valuable features as a model organism for study of vertebrate development.

Zebrafish embryos are transparent and accessible throughout development. In live embryos, techniques for ablation and transplantation of individual cells have been used to explore questions about induction and cell fate (27). Because of their relatively short reproductive cycle, the large number of progeny that can be produced, and the relatively small space needed to maintain large numbers of offspring, zebrafish is an efficient model system for genetic analysis (28;29).

Mutations in exostosin genes, *dackel* (*dak/ext2*) and *boxer* (*box/exlt3*), cause in zebrafish cartilage defects that strongly resemble those seen in patients with multiple osteochondromas (27). As zebrafish cartilaginous skeleton develops by similar mechanisms to that of humans, *dak/ext2* and *box* may be a powerful model for the study of osteochondromagenesis.

IV. Scope of the study and outline of the thesis

In the past decades, our knowledge on the epiphyseal growth plate regulation and peripheral cartilaginous tumour formation has increased significantly. Although some milestones have been achieved to date, our studies address many remaining questions on these topics:

1. Zebrafish as a model system to study human skeletal disorders.
2. Developmental regulation of the epiphyseal growth plate in relation to the formation of osteochondroma.
3. The role of *EXT1* and *EXT2* genes in the formation of a secondary peripheral chondrosarcoma.
4. Clues to the mechanisms of neoplastic transformation of osteochondroma towards secondary peripheral chondrosarcoma.

The most relevant literature on the epiphyseal growth plate and peripheral cartilaginous tumours is reviewed in **Chapter 2**. Chondrocytes interact with each other and with their micro-environment. These interactions are modulated by proteoglycans and other molecules and lead to the formation of a polarized tissue, such as the epiphyseal growth plate. The zebrafish (*Danio rerio*) exhibits fast development, a growth plate-like organization of its craniofacial skeleton and an availability of various mutants, making it a powerful model for the study of human skeletal disorders with unknown aetiology. Five zebrafish lines with known mutations in genes involved in proteoglycan synthesis were studied in **Chapter 3**. Each mutant displays different phenotypes related to: (*a*) cartilage morphology; (*b*) composition of the extracellular matrix; (*c*) ultrastructure of the extracellular matrix; and (*d*) the intracellular ultrastructure of chondrocytes. In addition, these zebrafish mutants might bring to light new candidate genes for human skeletal disorders.

Mutations in exostosin genes in zebrafish - *dackel* (*dak/ext2*) - cause cartilage defects that strongly resemble those seen in patients with multiple osteochondromas, and lead to a heparan sulphate deficiency (27). Heparan sulphate modulates receptor-ligand binding of many growth factors. The impact of mutations in the *ext2* gene in the zebrafish craniofacial skeleton development was investigated in **Chapter 4**.

Several growth factors diffuse across the extracellular matrix creating short and long range signalling. The distribution of these signalling molecules in a gradient fashion is shown to be established by proteoglycans (30). Cytochemical staining with positively charged dyes (e.g., polyethyleneimine-PEI) allows visualisation of proteoglycans and provides a detailed description of how proteoglycans are distributed throughout the cartilage matrix. The distribution of proteoglycans was studied in the five zebrafish mutants described above and in the epiphyseal growth plate and osteochondroma (**Chapter 5**). In addition, the distribution of proteoglycans throughout the cartilage matrix might shed light on the regulation of the epiphyseal growth plate and the formation of osteochondroma.

Primary cilia are specialized cell surface projections present on most eukaryotic cells (31;32). They function as signalling apparatus of the cells that receives and transduces mechanical and chemical signals from the neighbouring cells and the extracellular matrix (33). Primary cilia have been associated with vertebrate planar cell polarity and loss of cell polarity has been hypothesised to be involved in osteochondroma formation. The link between primary cilia and cell polarity in the epiphyseal growth plate and osteochondroma was investigated in **Chapter 6**.

The role of *EXT1* and *EXT2* genes in secondary peripheral chondrosarcoma formation was studied in **Chapter 7**. The homozygous inactivation of the *EXT* genes required for osteochondromagenesis and the mixture of cells with distinct genetic background within the osteochondroma cap raised the possibility of non-involvement of the *EXT1/EXT2* genes in the genesis of peripheral chondrosarcoma. Moreover, the presence of wild-type cells in the osteochondroma cap is not just an incidental component (34) and they might play a role during neoplastic transformation of osteochondroma.

Clues to the mechanisms of neoplastic transformation of osteochondroma towards secondary peripheral chondrosarcoma may give reliable histological criteria to properly identify each tumour type. An initial step in the process of defining histological criteria for guiding the diagnosis of peripheral cartilaginous tumours is to assess diagnostic reliability among specialized bone-tumour pathologists, as measured by intraclass correlation coefficient (35). A second step is to identify common histological criteria among the concordant cases, aiming to have histological parameters that characterize each tumour type (**Chapter 8**).

Endochondral ossification is a multistep process in which a cartilaginous model is gradually replaced by bone (3). Like in the epiphyseal growth plate, endochondral ossification takes place deep to the cartilage cap of osteochondroma and secondary peripheral chondrosarcoma (12). Two critical steps of endochondral ossification are the deposition of collagen X-rich matrix and blood vessel attraction/invasion (3). Formation of a collagen X-rich matrix and vascularisation might be useful prognostic markers of neoplastic transformation of an osteochondroma and were studied in **Chapter 9**.

Finally, the achievements of the study are summarised and possible future directions of research are indicated in **Chapter 10**.

References

1. Campbell JT, Kaplan FS. The role of morphogens in endochondral ossification. Calcif Tissue Int 1992;50:283-9.
2. Mariani FV, Martin GR. Deciphering skeletal patterning: clues from the limb. Nature 2003;423:319-25.
3. Kronenberg HM. Developmental regulation of the growth plate. Nature 2003;423:332-6.
4. DeChiara TM, Efstratiadis A, Robertson EJ. A growth-deficiency phenotype in heterozygous mice carrying an insulin-like growth factor II gene disrupted by targeting. Nature 1990;345:78-80.
5. Baker J, Liu JP, Robertson EJ, Efstratiadis A. Role of insulin-like growth factors in embryonic and postnatal growth. Cell 1993;75:73-82.

6. Long F, Joeng KS, Xuan S, Efstratiadis A, McMahon AP. Independent regulation of skeletal growth by Ihh and IGF signaling. Dev Biol 2006;298:327-33.
7. Ballock RT, O'Keefe RJ. The biology of the growth plate. J Bone Joint Surg Am 2003;85-A:715-26.
8. Hacker U, Nybakken K, Perrimon N. Heparan sulphate proteoglycans: the sweet side of development. Nat Rev Mol Cell Biol 2005;6:530-41.
9. Bulow HE, Hobert O. The molecular diversity of glycosaminoglycans shapes animal development. Annu Rev Cell Dev Biol 2006;22:375-407.
10. Warman ML, Cormier-Daire V, Hall C, Krakow D, Lachman R, Lemerrer M, et al. Nosology and classification of genetic skeletal disorders: 2010 revision. Am J Med Genet A 2011;155A:943-68.
11. van den Berg H., Kroon HM, Slaar A, Hogendoorn P. Incidence of biopsy-proven bone tumors in children: a report based on the Dutch pathology registration "PALGA". J Pediatr Orthop 2008;28:29-35.
12. Khurana J, Abdul-Karim F, Bovée JVMG. Osteochondroma. In: Fletcher CDM, Unni KK, Mertens F, editors. World Health Organization classification of tumours. Pa thology and genetics of tumours of soft tissue and bone.Lyon (France): IARC Press; 2002. p. 234-6.
13. Stieber JR, Dormans JP. Manifestations of hereditary multiple exostoses. J Am Acad Orthop Surg 2005;13:110-20.
14. Romeo S, Hogendoorn PC, Dei Tos AP. Benign cartilaginous tumors of bone: from morphology to somatic and germ-line genetics. Adv Anat Pathol 2009;16:307-15.
15. Jennes I, de JD, Mees K, Hogendoorn PC, Szuhai K, Wuyts W. Breakpoint charac terization of large deletions in EXT1 or EXT2 in 10 Multiple Osteochondromas families. BMC Med Genet 2011;12:85.
16. Hameetman L, David G, Yavas A, White SJ, Taminiau AHM, Cleton-Jansen AM, et al. Decreased EXT expression and intracellular accumulation of HSPG in osteochon dromas and peripheral chondrosarcomas. J Pathol 2007;211:399-409.
17. Reijnders CM, Waaijer CJ, Hamilton A, Buddingh EP, Dijkstra SP, Ham J, et al. No haploinsufficiency but loss of heterozygosity for EXT in multiple osteochondromas. Am J Pathol 2010;177:1946-57.
18. Zuntini M, Pedrini E, Parra A, Sgariglia F, Gentile FV, Pandolfi M, et al. Genetic models of osteochondroma onset and neoplastic progression: evidence for mechanisms alternative to EXT genes inactivation. Oncogene 2010;29:3827-34.
19. Szuhai K, Jennes I, De Jong D, Bovée JVMG, Wiweger M, Wuyts W, et al. Tiling resolution array-CGH shows that somatic mosaic deletion of the EXT gene is causative in EXT gene mutation negative multiple osteochondromas patients. Hum Mutat 2011;32:2036-49.

20. Hameetman L, Szuhai K, Yavas A, Knijnenburg J, van Duin M, Van Dekken H, et al. The Role of EXT1 in non hereditary osteochondroma:identification of homozygous deletions. J Natl Cancer Inst 2007;99:396-406.
21. Stickens D, Clines G, Burbee D, Ramos P, Thomas S, Hogue D, et al. The EXT2 multiple exostoses gene defines a family of putative tumour suppressor genes. Nature Genet 1996;14:25-32.
22. Ahn J, Ludecke H-J, Lindow S, Horton WA, Lee B, Wagner MJ, et al. Cloning of the putative tumour suppressor gene for hereditary multiple exostoses (EXT1). Nature Genet 1995;11:137-43.
23. McCormick C, Duncan G, Goutsos KT, Tufaro F. The putative tumor suppressors EXT1 and EXT2 form a stable complex that accumulates in the golgi apparatus and catalyzes the synthesis of heparan sulfate. Proc Natl Acad Sci USA 2000;97:668-73.
24. Busse M, Feta A, Presto J, Wilen M, Gronning M, Kjellen L, et al. Contribution of EXT1, EXT2, and EXTL3 to heparan sulfate chain elongation. J Biol Chem 2007;282:32802-10.
25. Jones KB. Glycobiology and the growth plate: current concepts in multiple hereditary exostoses. J Pediatr Orthop 2011;31:577-86.
26. Bertoni F, Bacchini P, Hogendoorn PCW. Chondrosarcoma. In: Fletcher CDM, Unni KK, Mertens F, editors. World Health Organisation classification of tumours. Pathology and genetics of tumours of soft tissue and bone.Lyon: IARC Press; 2002. p. 247-51.
27. Clément A, Wiweger M, von der Hardt S., Rusch MA, Selleck SB, Chien CB, et al. Regulation of zebrafish skeletogenesis by ext2/dackel and papst1/pinscher. PLoS Genet 2008;4:e1000136.
28. Palstra AP, Tudorache C, Rovira M, Brittijn SA, Burgerhout E, Van den Thillart GE, et al. Establishing zebrafish as a novel exercise model: swimming economy, swimming-enhanced growth and muscle growth marker gene expression. PLoS ONE 2010;5:e14483.
29. Ali S, Champagne DL, Spaink HP, Richardson MK. Zebrafish embryos and larvae: a new generation of disease models and drug screens. Birth Defects Res C Embryo Today 2011;93:115-33.
30. Wu Y, Belenkaya TY, Lin X. Dual roles of Drosophila glypican Dally-like in Wingless/ Wnt signaling and distribution. Methods Enzymol 2010;480:33-50.
31. Wheatley DN, Feilen EM, Yin Z, Wheatley SP. Primary cilia in cultured mammalian cells: detection with an antibody against detyrosinated alpha-tubulin (ID5) and by electron microscopy. J Submicrosc Cytol Pathol 1994;26:91-102.

32. Poole CA, Flint MH, Beaumont BW. Analysis of the morphology and function of primary cilia in connective tissues: a cellular cybernetic probe? Cell Motil 1995;5:175-93.
33. Singla V, Reiter JF. The primary cilium as the cell's antenna: signaling at a sensory organelle. Science 2006;313:629-33.
34. Matsumoto K, Irie F, Mackem S, Yamaguchi Y. A mouse model of chondrocyte-specific somatic mutation reveals a role for Ext1 loss of heterozygosity in multiple hereditary exostoses. Proc Natl Acad Sci U S A 2010;107:10932-7.
35. Shrout PE, Fleiss JL. Intraclass correlations: uses in assessing rater reliability. Psychol Bull 1979;86:420-8.

Chapter 2

Epiphyseal growth plate and secondary peripheral chondrosarcoma: the neighbours matter

Carlos E. de Andrea and Pancras C.W. Hogendoorn
Journal of Pathology 2012; 226:219–228

Abstract

Chondrocytes interact with their neighbours through their cartilaginous extracellular matrix (ECM). Chondrocyte–matrix interactions compensate the lack of cell–cell contact and are modulated by proteoglycans and other molecules. The epiphyseal growth plate is a highly organized tissue responsible for long bone elongation. The growth plate is regulated by gradients of morphogens that are established by proteoglycans. Morphogens diffuse across the ECM, creating short- and long-range signalling that lead to the formation of a polarized tissue. Mutations affecting genes that modulate cell–matrix interactions are linked to several human disorders. Homozygous mutations of *EXT1/EXT2* result in reduced synthesis and shortened heparan sulphate chains on both cell surface and matrix proteoglycans. This disrupts the diffusion gradients of morphogens and signal transduction in the epiphyseal growth plate, contributing to loss of cell polarity and osteochondroma formation. Osteochondromas are cartilage-capped bony projections arising from the metaphyses of endochondral bones adjacent to the growth plate. The osteochondroma cap is formed by cells with homozygous mutation of *EXT1/EXT2* and committed stem cells/wild-type chondrocytes. Osteochondroma serves as a niche (a permissive environment), which facilitates the committed stem cells/wild-type chondrocytes to acquire secondary genetic changes to form a secondary peripheral chondrosarcoma. In such a scenario, the micro-environment is the site of the initiating processes that ultimately lead to cancer.

Keywords: growth plate; osteochondroma; gradients; polarity; primary cilia; proteoglycans; bone tumour

Introduction

Skeletal development is a highly orchestrated process in which all the players involved ought to be perfectly coordinated and regulated in order to achieve harmonious and symmetrical growth. During mammalian skeletal development, long, short and irregular bones are formed by endochondral ossification [1,2].

Endochondral ossification begins when progenitor chondrocytes derived from mesenchymal cells pack densely (so-called 'condensation'). Cells of condensation form a cartilaginous template that is ultimately replaced by bone (Figure 1). Cell–cell interactions and the transcription factor Sox9 regulate the formation of these condensations [3]. Cell adhesion molecules, such as N-cadherin and N-CAM, are important in establishing an aggregation centre by recruiting mesenchymal cells from surrounding tissue [2]. Sox9 plays a key role in the differentiation of progenitor chondrocytes into chondrocytes by modulating the expression of cartilage-specific genes, such as type II and type XI collagen genes [3]. Down-regulation of N-CAM by the binding of syndecan to fibronectin and activation of homeobox genes (ie *Msx-1* and *Msx-2*) by the presence of BMP-2 and BMP-4 stop condensation growth and initiate pre-chondrocyte differentiation (Figure 1) [3]. An abundant cartilaginous extracellular matrix (ECM) surrounds mature chondrocytes. Cell–cell interactions found in the condensations are now replaced by interactions between chondrocytes via their ECM. These interactions are mediated by proteoglycans and have important effects on chondrocyte functions [4,5].

Post-natal endochondral bone formation is found in the epiphyseal growth plate. The epiphyseal growth plate is a highly organized, cartilaginous template needed for the elongation of long bones. Structurally, the epiphyseal growth plate can be divided into three distinct zones [6]. In the resting zone, chondrocytes are non-polarized and irregularly arranged. Resting chondrocytes serve as precursors (committed stem cell pool) for proliferative chondrocytes. In the proliferating zone, cell division of chondrocytes occurs perpendicular to the long axis of the growing bone (Figure 1). Proliferating chondrocytes have to undertake a series of cell movements/rotations (intercalation) and shape changes to align one on top of the other to generate the typical chondrocyte columns of the growth plate (Figure 1) [7–9]. Once acquired, this columnar organization is maintained. Chondrocytes require adhesion to cartilaginous ECM for all types of shape changes. Integrins are an important family of receptors that mediate chondrocyte–matrix adhesion [10]. Integrins regulate centrosome function, the assembly of the mitotic spindle and cytokinesis [11]. In β1-null growth plates, chondrocytes display mitotic figures perpendicular to the long axis, but they stay side-by-side and failed to move over each other and form columns, suggesting that β1 integrins regulate chondrocyte shape and rotation [12]. In the hypertrophic zone, chondrocytes stop proliferating and change their expression profile to synthesize type X collagen and to prepare for mineralization of the surrounding cartilaginous ECM (Figure 1) [6].

The process of endochondral bone formation in the epiphyseal growth plate may be considered as a patterning process that begins with chondrocytes proliferation and ends with matrix ossification. The endochondral chondrocytes undergo successive sequences of cell division, matrix secretion, cell hypertrophy, apoptosis and matrix calcification/ mineralization.

Although many biological processes contribute to the formation and organization of the epiphyseal growth plate and the initiation of tumours related to the growth plate (osteochondromas and secondary peripheral chondrosarcomas), this review focus on how chondrocytes interact with their ECM to establish cell polarity or not, contributing to morphogenesis and, in the case of neoplastic growth, to tumourigenesis.

Gradients modulating the organization of the epiphyseal growth plate

According to positional information concepts, cells acquire 'positional values' in a three-dimensional (3D) coordinate system which are later interpreted as leading to the formation of the appropriated structure at that position [13–15]. 'Positional values' are conferred by morphogens [16]. Concentration gradients of morphogens allows for their diffusion into the developing tissue, generating short- and long-range signalling molecules. Subsequently, chondrocytes at different positions along the epiphyseal growth plate are exposed to different concentrations of morphogens. The transduction of these signalling molecules is crucial for the formation of distinct zones. Each zone has different patterns of proliferation, differentiation and cell morphology.

Several models explain the formation of morphogen gradients, such as passive diffusion, planar transcytosis and others [17]. In planar transcytosis, morphogens move from the source by active transport, through repeated endocytosis and re-secretion [17].

Throughout the ECM, the distribution of morphogens in a gradient fashion is shown to be established by proteoglycans [5,18,19]. Proteoglycans are found in the ECM and attached to the cell membrane in virtually all types of tissue. They are composed of highly diverse core proteins, to which one or more glycosaminoglycans chains are covalently linked. Proteoglycans influence the morphogens-receptor, binding affinity and responses of cells to secreted proteins [4].

Recently, by studying the distribution of the proteoglycans anionic sites, it has been shown that, in zebrafish cartilage and in the human epiphyseal growth plate, proteoglycans are distributed in a gradient fashion [20]. A concentration gradient of proteoglycans in the cartilaginous ECM is observed as a function of the distance from the cell surface. Therefore, proteoglycans regulate the distribution of morphogens across the ECM [17].

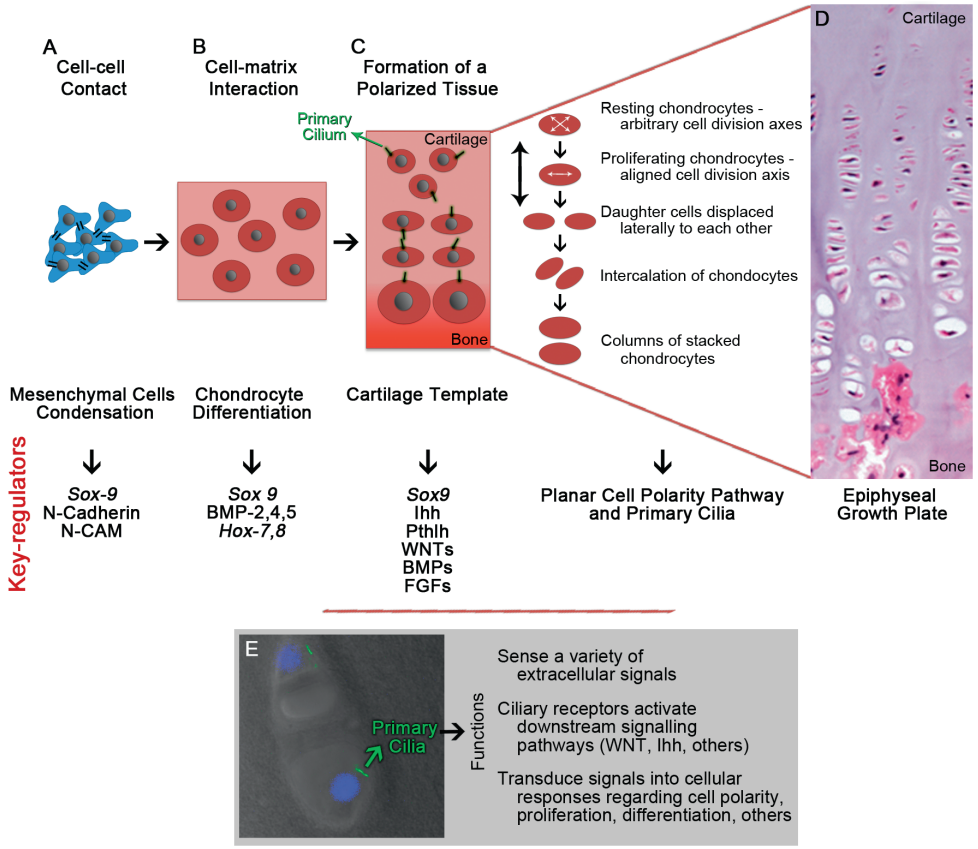


Figure 1. Endochondral bone formation and the epiphyseal growth plate. (A) Mesenchymal cells condense. (B) Cells of condensation become chondrocytes. (C) Several sequences of chondrocytes proliferation and hypertrophy regulated by highly coordinated signalling pathways form cartilage templates for bone formation. (D, E) Cell–matrix interactions, in part mediated by primary cilia, organize the cartilage templates (ie the epiphyseal growth plate); (D) in columns of proliferating and hypertrophic chondrocytes. The hypertrophic chondrocytes are ultimately replaced by bone. Double arrow-bar indicates long axis of the growing bone.

Proteoglycans, such as heparan and chondroitin sulphate, function in concert to establish an Indian hedgehog (Ihh) gradient, either through affecting its diffusion or by protecting it from degradation [19]. Ihh is a key regulator of the epiphyseal growth plate. The balance between chondrocyte proliferation and chondrocyte hypertrophy is regulated by a negative feedback loop involving Ihh and parathyroid hormone-related peptide (PTHrP; also known as PTHlH) [21,22]. Ihh is secreted by pre-hypertrophic chondrocytes and diffuses away from its site of synthesis regulating proliferation in a pool of cells that precedes them within the columns of stacked chondrocytes, namely chondrocytes from the resting and proliferating zone [6].

Additionally, Ihh signals to the cells of perichondrium and up-regulates their synthesis of PTHrP. PTHrP diffuses to the pre-hypertrophic zone and signals to the PTH/PTHrP receptor expressed on pre-hypertrophic chondrocytes to suppress their differentiation into hypertrophic chondrocytes [22].

Ihh induces the expression of several bone morphogenetic proteins (BMP) in the flaking perichondrium/ periosteum and the proliferating chondrocytes [21]. BMP is a group of proteins within the transforming growth factor-β (TGF-β) superfamily. BMP and Ihh signals act in parallel to induce chondrocyte proliferation [21]. Additionally, BMP signalling stimulates expression of Ihh [21,23]. Finally, BMP signals independent of the Ihh/PTHrP pathway delaying the process of hypertrophic differentiation [21].

The polarization of the epiphyseal growth plate

Cell polarity can be defined as a structurally and functionallyasymmetric organization in which the nonrandom positioning of each organelle, the function of which contributes to cell asymmetry, is preserved and transmitted through cell division [24]. Planar cell polarity coordinates cell behaviour in a two-dimensional (2D) plane. Spatial information that organizes planar polarity and ultimately a tissue is shown to be transmitted locally from one cell to the next [25]. Input from neighbouring cells can influence the behaviour of individual cells as well as the orientation of groups of cells that respond as a unit to 'positional values' [25].

The core planar cell polarity is regulated by Wingless-type (Wnt) molecules that comprise a family of 19 lipid-modified secreted glycoproteins, such as Wnt5A. Wnt molecules are diffusible morphogens, which interact with heparan sulphate proteoglycans to generate a gradient throughout the tissue [26]. By binding to frizzled (Fzd) cell surface receptors, Wnt molecules signal via different pathways, including the canonical Wnt/β-catenin, non canonical Wnt/Ca2+ and non-canonical Wnt/planar cell polarity pathways [27,28].

Planar cell polarity pathway has been demonstrated to regulate chondrocyte polarity in the epiphyseal growth plate [9]. Non-polarized resting chondrocytes, which are committed progenitor cells responsible for the generation of proliferating chondrocytes, become polarized proliferating chondrocytes assuming a precise position and orientation in the epiphyseal growth plate, creating columns of stacked cells (Figure 1). Planar cell polarity pathway comprises molecules such as Wnt5A, the Rho family of GTPases and Gpi-anchored proteins. These molecules are shown to regulate orientated cell division and movements (intercalation) of chondrocytes (Figure 1) [7–9].

Vertebrate planar cell polarity has been linked to primary cilia, which are specialized cell surface projections present on most eukaryotic cells [29,30]. The primary cilia function as the signalling 'antennae' of the cells that receives and transduces mechanical and chemical signals from the neighbouring cells and the ECM (Figure 1) [31].

During development, the positioning of the primary cilium of the hair cells in the sensory epithelium leads and predicts the polarity of each stereociliary bundle, supporting the hypothesis that primary cilia direct the polarization of hair cells [32,33].

In the resting growth plate chondrocytes, primary cilia do not acquire a clear pattern of orientation. However, in the proliferating and hypertrophic chondrocytes, primary cilia are orientated parallel to the longitudinal axis of the bone (Figure 1) [34]. The polarization of primary cilia in the proliferating and hypertrophic zones of the epiphyseal growth plate creates a virtual axis that crosses the centre of each column of stacked chondrocytes (Figure 1). The parallel ciliary axes across the epiphyseal growth plate seem to represent the planar polarity axis of the chondrocyte, and consequently of the entire epiphyseal growth plate [34].

In epithelial cells, the activation Rho GTPase takes place at the primary cilium's basal body [35]. In the mouse growth plate, Rho GTPase has been shown to control tissue polarity [9]. Moreover, conditional deletion of *Kif3a* in the growth plate chondrocytes results in the depletion of cilia and loss of columnar organization [8], suggesting the loss of tissue polarity. *Kif3a*, a subunit of the anterograde kinesin-II intraflagellar transport machinery, is required the formation of primary cilia [36]. Therefore, primary cilia seem to play a role in the polarization of the epiphyseal growth plate.

Taken together, the lack of cell–cell contact in the epiphyseal growth plate turns cell–matrix interaction critical. In such a scenario, chondrocytes interact with their neighbouring chondrocytes and distant cells. These interactions are shown to be partially mediated by primary cilia that regulate and modulate the functions of the epiphyseal growth plate (Figure 1).

The epiphyseal growth plate's fate is to be resorbed after the pubertal growth spurt, at the time of sexual maturation [37]. The resorption and fusion of the growth plate follow the cessation of growth and are regulated by both systemic mechanisms (ie oestrogen hormone) and local mechanisms, intrinsic to the growth plate [38,39]. It has been described that the growth plate chondrocytes have a finite proliferative capacity [39]. Therefore, the fusion of the growth plate is triggered when the proliferative potential of the chondrocytes is exhausted and finally all the remaining chondrocytes are replaced by bone, in which the epiphysis fuses with the metaphysic [37].

Osteochondromagenesis

Mutations affecting the biosynthesis of either proteoglycans or glycosaminoglycans alter the interaction between a cell and its micro-environment and are the cause of several human disorders. Several of these disorders are associated with a skeletal and articular phenotype [40].

Mutations in *EXT1* (8q24.1) and *EXT2* (11p11) genes are associated with osteochondromas [41–44]. *EXT1* and *EXT2* encode type II transmembrane glycosyltransferases [45,46], whose functions are not fully known. EXT1 and EXT2 form a hetero-oligomeric complex in the Golgi apparatus of most human cells that participate in chain elongation in heparan sulphate biosynthesis [47,48]. Albeit the genetic correlation between mutations in *EXT1/EXT2* and osteochondromas, the mechanism by which alterations in heparan sulphate biosynthesis leads to osteochondroma is not entirely understood. As heparan sulphate acts as a coreceptor for fibroblast growth factors and BMPs [49], and regulates the diffusion of Ihh [19] and members of the Wnt family [26], improper elongation of heparan sulphate chains may result in a variety of growth factor signalling defects and impaired cell–matrix interactions, which ultimately may result in osteochondroma formation (Figure 2).

Osteochondromas are the most common benign bone tumours of childhood and adolescence [50]. They are characterized by sporadic (non-familial/solitary) or multiple (hereditary) cartilage-capped bony projections from the metaphyses of endochondral bones adjacent to the growth plate and develop during skeletal growth [51]. Multiple osteochondromas, previously called hereditary multiple exostoses, is an autosomal dominant disorder with a prevalence of 1 in 18 000 [52]. Patients with multiple osteochondromas are often short in stature and have bowed bones that can restrict movement and ultimately result in joint dislocation [52]. In contrast, patients with sporadic lesions may develop symptoms on the affected side only. Sporadic and multiple lesions are morphologically indistinguishable [51,53].

Multiple osteochondromas is characterized by genetic variability, which partially explain inter- and intrafamilial phenotypic variation often found in these patients [54]. The majority of the hereditary cases are caused by point mutations (70–75%). Small deletions involving single or multiple exons are found in about 10% of all hereditary cases [55–57]. Large deletions have been identified in few cases [54]. No genomic alterations are detected in about 10–15%. In some of these negative cases, somatic mosaicism with large genomic deletions of *EXT1* and *EXT2* has been described as the underlying mechanism of multiple osteochondromas formation [58]. In sporadic osteochondromas, homozygous deletions of *EXT1* are often identified [42].

A propitious micro-environment for osteochondromagenesis

Model systems have provided significant insight into osteochondromagenesis. Zebrafish *dackel* (*dak/ext2*) mutant has cartilage defects that strongly resemble those seen in patients with multiple osteochondromas [59]. Interestingly, dak chondrocytes (chondrocytes with homozygous mutation in *ext2*) behave as wild-type cells when juxtaposed with heparan sulphate-secreting cells and form osteochondroma-like outgrowths when implanted at the edge of wild-type cartilage [60]. This shows that the secretion of heparan sulphate from the neighbouring wild-type chondrocytes is able to rescue the chondrocytes with homozygous mutation in *ext2*. Only, at the edge of the cartilage elements, where the level of heparan sulphate is decreased, chondrocytes with homozygous mutation in *ext2* are able to form outgrowths [60].

Studies using Cre recombinase drivers to generate *Ext1* knockouts in mouse skeletal cells show that somatic loss of the wild-type *Ext1* allele is needed for osteochondroma formation [61]. Recently, it has been shown that, in humans and in animal models, cells with functional *EXT* are being integrated into the osteochondroma cartilaginous cap [20,34,61,62]. These cells might be wild-type chondrocytes from the epiphyseal growth plate or stem cells from the neighbouring tissue. Recently, a subset of cells in the osteochondroma cap has been shown to express nestin, a protein marker for neural stem cells [63]. Although nestin levels are higher in younger patients, nestin-positive cells are also identified in older adults [63], suggesting the presence of committed stem cells or cells with stem cells properties in the osteochondroma cap. The occurrence of osteochondroma in childhood after haematopoietic stem cell transplantation has been reported in the literature [64]. Osteochondromas after stem cell transplantation are linked to total-body irradiation and their cause is still unclear. They might be the result of a prolonged duration of epiphyseal opening caused by damage to bone and cartilage at the epiphysis [64]. Alternatively, the growth hormone treatment that is often indicated to patients with total-body irradiation and haematopoietic stem cell transplantation [65] may disturb the process of endochondral ossification, triggering the committed stem cells from the epiphyseal growth plate or from the neighbouring tissue to form outgrowths.

The wild-type cells in the osteochondroma cap may create an environment conducive for chondrocytes with homozygous inactivation of *EXT1/EXT2* to proliferate and grow [66], probably providing a certain threshold level and distribution of heparan sulphate proteoglycans.

By studying the distribution of the anionic sites of proteoglycans, it has been shown that the mosaic mixture of wild-type chondrocytes and chondrocytes with homozygous inactivation of *EXT1/EXT2* confers to the osteochondroma cap a scattered distribution of proteoglycans across the ECM [20].

Areas with a growth plate-like distribution of proteoglycans in gradients possibly contain chondrocytes with functional *EXT1/EXT2*. Areas with reduced amount of proteoglycans with no gradient formation have probably chondrocytes with homozygous inactivation of EXT1/*EXT2*. It has been shown that cell polarity is lost in osteochondroma, which is reflected either by the random orientation of primary cilia in the tumour or the lack of these organelles in some osteochondroma cells [34]. Interestingly, the columns of stacked cells in osteochondroma retained the growth plate's cell polarity, in which primary cilia are aligned in a common axis, indicating the presence of wild-type chondrocytes in the tumour [34].

Most likely, the formation of an osteochondroma takes place when epiphyseal growth plate chondrocytes with homozygous inactivation of *EXT1/EXT2* disrupt the diffusion gradients and signal transduction. Cells with homozygous inactivation of *EXT1/EXT2* lose their ability to respond to polarity signals [34]. Hypothetically, shorter heparan sulphate chains disrupt the polarity function of primary cilia in osteochondroma cells, which leads to loss of cell/tissue polarity. If cells with homozygous inactivation of *EXT1/EXT2* are located immediately adjacent to the perichondrium, they are able to escape the proteoglycan gradient generated by neighbouring wild-type chondrocytes and form outgrowths (Figure 2).

A similar mosaic of cells with functional and dysfunctional *EXT1/EXT2* might be present in the epiphyseal growth plate of patient with multiple osteochondromas. In such a scenario, the orientation of primary cilia in the epiphyseal growth plate of patients with osteochondromas and in the osteochondromas themselves might be similar: polarized in the subset of cells that are organized into columns (wild-type chondrocytes) and non-polarized in the subset of cells that are haphazardly organized (cells with homozygous inactivation of *EXT1/EXT2*). Speculatively, the epiphyseal growth plate of a subset of patients with multiple osteochondromas does not show the typical columns of stacked chondrocytes, which might explain the short stature and the bowed bones often seen in those patients. The lack of availability of epiphyseal growth plate material from those patients does not allow to verify the hypothesis. Interestingly, mice with mutations in genes related to cell polarity processes display epiphyseal growth plates with loss of columnar organization, which decrease longitudinal growth and increase lateral expansion of the bone [9].

In mouse model of hereditary human osteochondromas based on stochastic, tissue-specific inactivation of *Ext1*, it has been demonstrated that osteochondromas develop quickly during the early post-natal period, corresponding to rapid bone growth [62]. Additionally, wild-type cells constitute the major population of cells in the tumour [62]. It indicates that homozygous inactivation of *Ext1* in a small fraction of chondrocytes is required and sufficient for the initiation of osteochondromas in this model. In human osteochondromas, it has been shown by fluorescence *in situ* hybridization (FISH) with an EXT1 probe that cells with homozygous deletion of *EXT1* constitute the major population of cells in the tumour [67].

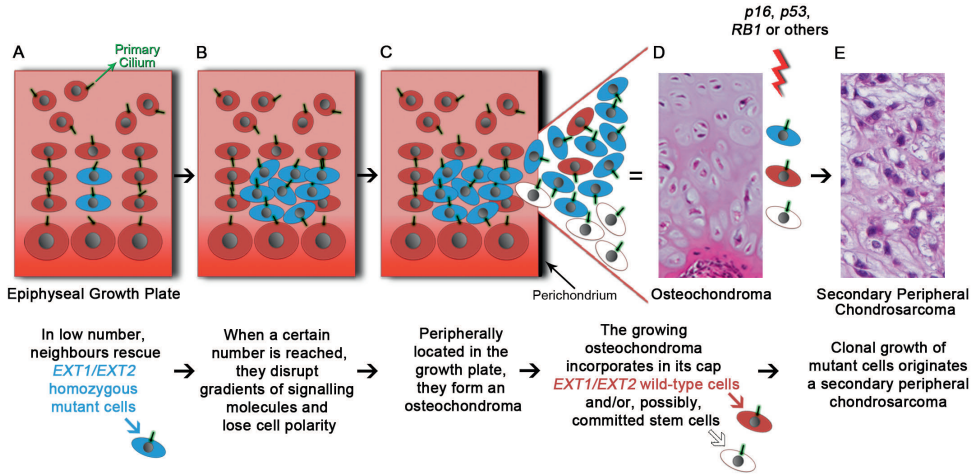


Figure 2. Osteochondroma- and secondary peripheral chondrosarcomagenesis. (A) The secretion of heparan sulphate from the neighbouring wild-type growth plate chondrocytes is able to rescue the cells with homozygous inactivation of *EXT1/EXT2* (blue cells). (B) A pool of cells with homozygous inactivation of *EXT1/EXT2* disrupts the diffusion gradients and signal transduction in the epiphyseal growth plate. These cells do not respond to polarity signals, leading to loss of cell/tissue polarity. (C) When located adjacent to the perichondrium (arrow), cells with homozygous inactivation of *EXT1/EXT2* form outgrowths (osteochondroma). (D) The osteochondroma cap is then shaped by wild-type cells (red cells) and/or committed stem cells (white cells) and homozygous mutant cells. (E) Secondary peripheral chondrosarcoma originates from *EXT1/EXT2* homozygous mutant cells or wild-type cells or committed stem cells that acquire genetic(s) alteration(s).

It is plausible to foresee that number of wild-type cells in the osteochondroma cap varies depending on the patient's age, decreasing upon osteochondroma maturation. However, the lack of tumour samples from infants with osteochondromas do not allow further verification whether wild-type cells constitute the major population of cells in more immature osteochondromas. It is unlikely that wild-type cells in the osteochondroma cap are just an incidental component [62]. Hypothetically, variable ratio between wild-type chondrocytes and cells with homozygous inactivation of *EXT1/EXT2* may explain why osteochondromas cease to grow at the time of sexual maturation and eventually are resorbed [68]. This indicates that the epiphyseal growth plate and osteochondroma may share, to some extent, similar hormonal regulation. The resorbed osteochondromas, which are in general small lesions [68], might be composed mainly by wild-type cells intermingled by few cells with homozygous inactivation of *EXT1/EXT2*. Once the fusion of the epiphyseal growth plate begins, the growth of an osteochondroma composed predominantly by wild-type cells decreases. As in the epiphyseal growth plate, the cartilaginous matrix of osteochondroma might be replaced by bone and, in the absence of a conducive environment produced by the wild-type cells, cells with homozygous inactivation of *EXT1/EXT2* may die and the osteochondroma cap could be finally resorbed.

This indicates that the epiphyseal growth plate and osteochondroma may share, to some extent, similar hormonal regulation. The resorbed osteochondromas, which are in general small lesions [68], might be composed mainly by wild-type cells intermingled by few cells with homozygous inactivation of *EXT1/EXT2*. Once the fusion of the epiphyseal growth plate begins, the growth of an osteochondroma composed predominantly by wild-type cells decreases. As in the epiphyseal growth plate, the cartilaginous matrix of osteochondroma might be replaced by bone and, in the absence of a conducive environment produced by the wild-type cells, cells with homozygous inactivation of *EXT1/EXT2* may die and the osteochondroma cap could be finally resorbed. In contrast, the unresorbed osteochondromas might be formed predominately by cells with homozygous inactivation of *EXT1/EXT2*. It is possible to foresee that the high ratio of mutated cells over the non-mutated cells may create an environment that shield osteochondroma from the mechanisms that regulate the epiphyseal growth plate, preventing the wild-type cells that could lead the resorption of the osteochondroma cap from dying.

Micro-environment promoting and inducing secondary peripheral chondrosarcoma formation

The 'double-edged sword' role of the micro-environment has become more and more prominent in either suppressing or promoting tumour formation [69]. The micro-environment provides signalling to mediate cell proliferation, differentiation and death, regulating tissue architecture and remodelling [70]. The micro-environment is also able to suppress and revert processes that ultimately lead to cancer. Conversely, the micro-environment has also been described to modulate tumour formation, growth and spread. It means that the micro environment can disrupt tissue homeostasis and promote cancer development. The destabilization of tissue homeostasis has a variety of causes, including the production of toxic substances by the stromal cells and/or other cell types, ie leading to impairment of signalling molecules [70,71].

Recently, it has been described that either benign or malignant tumour cells can create a special microenvironment that might lead to the formation of a new and different tumour type [72]. This model of tumour formation has been called a 'niche-based' model of of oncogenesis, in which a change in a specific niche/micro-environmental cell can serve as the primary moment in a multi-step process towards malignancy of a supported, but distinct, cell type. Evidences for niche-induced oncogenesis come from Shwachman–Bodian–Diamond syndrome and secondary peripheral chondrosarcoma.

Shwachman–Diamond syndrome is an autosomal recessive disorder characterized by bone marrow dysfunction, neurocognitive impairment, pancreatic insufficiency and hepatopathy [73]. It is caused by mutations in the Shwachman–Bodian Diamond syndrome, the haematopoietic progenitor cells with an *SBDS* gene mutation create a permissive

micro-environment that may poise wildtype haematopoietic cells for genetic events initiating malignant transformation [74]. This syndrome illustrates the ability of primary alterations in the bone marrow micro-environment to initiate specific events that lead to secondary genetic alterations in other cells.

The role of the micro-environment in secondary peripheral chondrosarcoma formation has been recently described (Figure 2) [67]. Secondary peripheral chondrosarcoma is a malignant cartilage-producing tumour that arises from the cartilage cap of an osteochondroma [75]. It has been shown that, while homozygous mutations in *EXT1/EXT2* are crucial for the formation of an osteochondroma, genetic alteration(s) in other gene(s) than *EXT1/EXT2* is(are) the causing event(s) of a subset of secondary peripheral chondrosarcoma [67]. Additionally, *IDH1/IDH2* mutations are shown not to be involved in secondary peripheral chondrosarcomas formation [76]. Malignant progression of secondary peripheral chondrosarcomas is characterized by a high percentage of loss of heterozygosity (ie *CDKN2A/p16*, *TP53*, *RB1*) and ploidy ranging from half to twice the normal DNA content [77–79]. It suggests that *p16*, *p53* and RB1 are involved in neoplastic transformation of an osteochondroma.

The osteochondroma cells with homozygous inactivation of *EXT1/EXT*2 are thought to create a permissive micro-environment that facilitates the *EXT* wild-type cells to acquire secondary genetic changes. The *EXT* wild-type cells may be committed stem cells or wild type chondrocytes. Such a scenario also points to a niche-based model of oncogenesis. It means that a pool of committed stem cells/wild-type chondrocytes might be found in the osteochondroma cap. The stem cells are committed to differentiate into chondrocytes and, once acquiring genetic alterations in other genes than *EXT1/EXT2* and *IDH1/IDH2*, originate chondrosarcomas and not other type of bone tumours. It has been proposed that sarcoma in general is a differentiation disease, caused by mutations hampering terminal differentiation of mesenchymal stem cells [80]. Depending on the lineage and the stage of differentiation at the time of the mutation, sarcomas with variable phenotype and histological grade could be initiated [80]. Gene expression profiles of differentiated chondrosarcoma (ie low-grade chondrosarcomas) share similarities with fully differentiated chondrocytes (ie growth plate chondrocytes and osteochondroma cells), whereas less differentiated chondrosarcomas (ie high-grade chondrosarcomas) show overlap with pre-chondrogenic stages of mesenchymal stem cells [81]. This means that clonal selection occurs during malignant progression from low-grade to high-grade chondrosarcoma and favours expansion of cell clones with gene expression profile similar to those of mesenchymal stem cells. These cell clones with a stem cell-like genotype suggest that the committed stem cells found in the osteochondroma cap or neighbouring tissue are the cells of origin of secondary peripheral chondrosarcomas. These cells then acquire genetic alteration(s) (ie *p16* or *p53* or *RB1* or others) that give them a proliferative advantage, allowing them to overgrow the osteochondroma cells with

homozygous inactivation of *EXT1/EXT2*. Consequently, secondary peripheral chondrosarcomas are presumably a clonal growth of neoplastic cells, while osteochondromas are clonal growth of different cell types (ie committed stem cells/wild-type chondrocytes and cells with homozygous inactivation of *EXT1/EXT2*). Hypothetically, secondary peripheral chondrosarcomas may arise from clonal growth of committed stem cells/ wild-type chondrocytes or cells with homozygous inactivation of *EXT1/EXT2* (Figure 2). Osteochondromas cells originating chondrosarcoma is a rare event, base on the fact that very few secondary peripheral chondrosarcomas display homozygous deletion of *EXT1/EXT2* [67].

Neoplastic transformation of an osteochondroma occurs in <1% of patients with sporadic osteochondromas and 1–3% of patients with multiple osteochondromas [75]. Neoplastic transformation usually occurs 20–60 years after the cessation of osteochondroma growth that happens at the time of the fusion of the epiphyseal growth plate at puberty [41]. It is difficult and challenging to address how the osteochondroma cells with homozygous inactivation of *EXT1/EXT2* facilitate secondary genetic changes in *EXT* wild-type cells. Considering that osteochondromas are cartilagecapped bony projections arising on the external surface of bones, it can be speculated that an osteochondroma is constantly exposed to risk of injury and micro-trauma that might lead the committed stem cells/wild type chondrocytes, either in the tumour or in the neighbouring tissue, to become more prone to acquire genetic alterations. The question why committed stem cells/wild-type chondrocytes and not *EXT*-mutated cells predominantly acquire genetic changes that lead to malignancy is answered by the fact that *EXT1* mutation gives the cells a proliferative disadvantage. The hypothesis that alterations in *EXT* give the cells a proliferative disadvantage comes from a study in multiple myeloma showing that mutation in *EXT1* leads to decreased tumour growth [82], and from the fact that *EXT*-null chondrocytes do not grow in vitro [56].

Eventually, secondary peripheral chondrosarcoma can transform into dedifferentiated chondrosarcoma, which consists of two components, a well-differentiated chondrosarcoma juxtaposed to a high-grade undifferentiated (non-cartilaginous) sarcoma [83]. Dedifferentiation might occur through environmental factors and/or when subsequent mutations drive the differentiated chondrosarcoma cells to undergo to an earlier developmental stage. Alternatively, mutated undifferentiated cells located in the chondrosarcoma through asymmetric cell division might give rise to chondrosarcoma cells and to equivalent undifferentiated cells. Genetic alterations in the undifferentiated cells may confer a proliferative advantage, which leads to an undifferentiated sarcoma.

Conclusion and future perspectives

In the epiphyseal growth plate, in osteochondroma and in secondary peripheral chondrosarcoma, the way that chondrocytes interact with each other and to their micro environment has gradually been unveiled. In the epiphyseal growth plate, these interactions lead to the formation of a polarized tissue. Cells in the epiphyseal growth plate harbouring homozygous mutations in *EXT1/EXT2* disrupt the diffusion gradients and signal transduction, leading to the loss of cell polarity and contributing to the formation of an osteochondroma. Osteochondroma acts as a niche (a permissive environment), which facilitates the committed stem cells/wild-type chondrocytes located in its cap to acquire secondary genetic changes to form a secondary peripheral chondrosarcoma.

The identification of a committed stem cell pool in the osteochondroma cap and the isolation of these cells might unveil their potential to originate a malignant tumour. Massive sequencing is expected to identify the driving mutation in secondary peripheral chondrosarcoma formation.

Acknowledgment

This work was supported by the European Network of Excellence EuroBoNeT [http://www eurobonet.eu; Grant No. 018814 (LSHC-CT-2006-018814)].

Author contributions

CEdeA and PCWH were both involved in writing the paper and had final approval of the submitted and published versions.

References

1. Campbell JT, Kaplan FS. The role of morphogens in endochondral ossification. Calcif Tissue Int 1992; 50: 283–289.
2. Mariani FV, Martin GR. Deciphering skeletal patterning: clues from the limb. Nature 2003; 423: 319–325.
3. DeLise AM, Fischer L, Tuan RS. Cellular interactions and signaling in cartilage development. Osteoarthr Cartilage 2000; 8: 309–334.
4. Hacker U, Nybakken K, Perrimon N. Heparan sulphate proteoglycans: the sweet side of development. Nat Rev Mol Cell Biol 2005; 6: 530–541.
5. Willems SM, Wiweger M, et al. Running GAGs: myxoid matrix revisited. What's in it for the pathologist? Virchows Arch 2009; 456: 181–192.
6. Kronenberg HM. Developmental regulation of the growth plate. Nature 2003; 423: 332–336.
7. Dodds GS. Row formation and other types of arrangement of cartilage cells in endochondral ossification. Anat Rec 1930; 46: 385–399.

8. Song B, Haycraft CJ, Seo H, et al. Development of the post-natal growth plate requires intraflagellar transport proteins. Dev Biol 2007; 305: 202–216.
9. Li Y, Dudley AT. Noncanonical frizzled signaling regulates cell polarity of growth plate chondrocytes. Development 2009; 136: 1083–1092.
10. Grashoff C, Aszodi A, Sakai T, et al. Integrin-linked kinase regulates chondrocyte shape and proliferation. EMBO Rep 2003; 4: 432–438.
11. Reverte CG, Benware A, Jones CW, et al. Perturbing integrin function inhibits microtubule growth from centrosomes, spindle assembly, and cytokinesis. J Cell Biol 2006; 174: 491–497.
12. Aszodi A, Hunziker EB, Brakebusch C, et al. β1 integrins regulate chondrocyte rotation, G1 progression, and cytokinesis. Genes Dev 2003; 17: 2465–2479.
13. Wolpert L. Positional information and pattern formation in development. Dev Genet 1994; 15: 485–490.
14. Wolpert L. Positional information revisited. Development 1989; 107(suppl): 3–12.
15. Tickle C. Making digit patterns in the vertebrate limb. Nat Rev Mol Cell Biol 2006; 7: 45–53.
16. Salinas PC. Signaling at the vertebrate synapse: new roles for embryonic morphogens? J Neurobiol 2005; 64: 435–445.
17. Yan D, Lin X. Shaping morphogen gradients by proteoglycans. Cold Spring Harb Perspect Biol 2009; 1: a002493.
18. Wu Y, Belenkaya TY, Lin X. Dual roles of Drosophila glypican Dally-like in Wingless/Wnt signaling and distribution. Methods Enzymol 2010; 480: 33–50.
19. Cortes M, Baria AT, Schwartz NB. Sulfation of chondroitin sulfate proteoglycans is necessary for proper Indian hedgehog signaling in the developing growth plate. Development 2009; 136: 1697–1706.
20. de Andrea CE, Prins FA, Wiweger MI, et al. Growth plate regulation and osteochondroma formation: insights from tracing proteoglycans in zebrafish models and human cartilage. J Pathol 2011; 224: 160–168.
21. Minina E, Wenzel HM, Kreschel C, et al. BMP and Ihh/PTHrP signaling interact to coordinate chondrocyte proliferation and differentiation. Development 2001; 128: 4523–4534.
22. Vortkamp A, Lee K, Lanske B, et al. Regulation of rate of cartilage differentiation by Indian hedgehog and PTH-related protein. Science 1996; 273: 613–622.
23. Zhang D, Schwarz EM, Rosier RN, et al. ALK2 functions as a BMP type I receptor and induces Indian hedgehog in chondrocytes during skeletal development. J Bone Miner Res 2003; 18: 1593–1604.
24. Bornens M. Organelle positioning and cell polarity. Nat Rev Mol Cell Biol 2008; 9: 874–886.

25. Jones C, Chen P. Planar cell polarity signaling in vertebrates. BioEssays 2007; 29: 120–132.
26. Fuerer C, Habib SJ, Nusse R. A study on the interactions between heparan sulfate proteoglycans and Wnt proteins. Dev Dyn 2010; 239: 184–190.
27. Zallen JA. Planar polarity and tissue morphogenesis. Cell 2007; 129: 1051–1063.
28. Andersson ER, Prakash N, Cajanek L, et al. Wnt5a regulates ventral midbrain morphogenesis and the development of A9–A10 dopaminergic cells in vivo. PLoS ONE 2008; 3: e3517.
29. Wheatley DN, Feilen EM, Yin Z, et al. Primary cilia in cultured mammalian cells: detection with an antibody against detyrosinated α-tubulin (ID5) and by electron microscopy. J Submicrosc Cytol Pathol 1994; 26: 91–102.
30. Poole CA, Flint MH, Beaumont BW. Analysis of the morphology and function of primary cilia in connective tissues: a cellular cybernetic probe? Cell Motil 1995; 5: 175–193.
31. Singla V, Reiter JF. The primary cilium as the cell's antenna: signaling at a sensory organelle. Science 2006; 313: 629–633.
32. Denman-Johnson K, Forge A. Establishment of hair bundle polarity and orientation in the developing vestibular system of the mouse. J Neurocytol 1999; 28: 821–835.
33. Tilney LG, Cotanche DA, Tilney MS. Actin filaments, stereocilia and hair cells of the bird cochlea. VI. How the number and arrangement of stereocilia are determined. Development 1992; 116: 213–226.
34. de Andrea CE, Wiweger M, Prins F, et al. Primary cilia organization reflects polarity in the growth plate and implies loss of polarity and mosaicism in osteochondroma. Lab Invest 2010; 90: 1091–1101.
35. Park TJ, Mitchell BJ, Abitua PB, et al. Dishevelled controls apical docking and planar polarization of basal bodies in ciliated epithelial cells. Nat Genet 2008; 40: 871–879.
36. Eggenschwiler JT, Anderson KV. Cilia and developmental signaling. Annu Rev Cell Dev Biol 2007; 23: 345–373.
37. Weise M, De Levi S, Barnes KM, et al. Effects of estrogen on growth plate senescence and epiphyseal fusion. Proc Natl Acad Sci USA 2001; 98: 6871–6876.
38. Faustini-Fustini M, Rochira V, Carani C. Oestrogen deficiency in men: where are we today? Eur J Endocrinol 1999; 140: 111–129.
39. Baron J, Klein KO, Colli MJ, et al. Catch-up growth after glucocorticoid excess: a mechanism intrinsic to the growth plate. Endocrinology 1994; 135: 1367–1371.
40. Warman ML, Cormier-Daire V, Hall C, et al. Nosology and classification of genetic skeletal disorders: 2010 revision. Am J Med Genet A 2011; 155A: 943–968.

41. Bovee JVMG, Hogendoorn PCW, Wunder JS, et al. Cartilage tumours and bone development: molecular pathology and possible therapeutic targets. Nat Rev Cancer 2010; 10: 481–488.
42. Hameetman L, Szuhai K, Yavas A, et al. The Role of EXT1 in non hereditary osteochondroma: identification of homozygous deletions. J Natl Cancer Inst 2007; 99: 396–406.
43. Wuyts W, Van Hul W. Molecular basis of multiple exostoses: mutations in the EXT1 and EXT2 genes. Hum Mutat 2000; 15: 220–227.
44. Bovee JVMG, Cleton-Jansen AM, Wuyts W, et al . EXT-mutation analysis and loss of heterozygosity in sporadic and hereditary osteochondromas and secondary chondrosarcomas. Am J Hum Genet 1999; 65: 689–698.
45. Stickens D, Clines G, Burbee D, et al. The EXT2 multiple exostoses gene defines a family of putative tumour suppressor genes. Nat Genet 1996; 14: 25–32.
46. Ahn J, Ludecke H-J, Lindow S, et al. Cloning of the putative tumour suppressor gene for hereditary multiple exostoses (EXT1). Nat Genet 1995; 11: 137–143.
47. McCormick C, Duncan G, Goutsos KT, et al. The putative tumor suppressors EXT1 and EXT2 form a stable complex that accumulates in the Golgi apparatus and catalyzes the synthesis of heparan sulfate. Proc Natl Acad Sci USA 2000; 97: 668–673.
48. Busse M, Feta A, Presto J, et al. Contribution of EXT1, EXT2, and EXTL3 to heparan sulfate chain elongation. J Biol Chem 2007; 282: 32802–32810.
49. Bernfield M, Gotte M, Park PW, et al. Functions of cell surface heparan sulfate proteoglycans. Annu Rev Biochem 1999; 68: 729–777.
50. van den Berg H, Kroon HM, Slaar A, et al. Incidence of biopsyproven bone tumors in children: a report based on the Dutch pathology registration 'PALGA'. J Pediatr Orthop 2008; 28: 29–35.
51. Khurana J, Abdul-Karim F, Bovee JVMG. Osteochondroma. In World Health Organization Classification of Tumours. Pathology and Genetics of Tumours of Soft Tissue and Bone, Fletcher CDM, Unni KK, Mertens F (eds). IARC Press: Lyons, France, 2002; 234–236.
52. Stieber JR, Dormans JP. Manifestations of hereditary multiple exostoses. J Am Acad Orthop Surg 2005; 13: 110–120.
53. Romeo S, Hogendoorn PC, Dei Tos AP. Benign cartilaginous tumors of bone: from morphology to somatic and germ-line genetics. Adv Anat Pathol 2009; 16: 307–315.
54. Jennes I, de JD, Mees K, et al. Breakpoint characterization of large deletions in EXT1 or EXT2 in 10 multiple osteochondromas families. BMC Med Genet 2011; 12: 85.

55. Hameetman L, David G, Yavas A, et al. Decreased EXT expression and intracellular accumulation of HSPG in osteochondromas and peripheral chondrosarcomas. J Pathol 2007; 211: 399–409.
56. Reijnders CM, Waaijer CJ, Hamilton A, et al. No haploinsufficiency but loss of heterozygosity for EXT in multiple osteochondromas. Am J Pathol 2010; 177: 1946–1957.
57. Zuntini M, Pedrini E, Parra A, et al. Genetic models of osteochondroma onset and neoplastic progression: evidence for mechanisms alternative to EXT genes inactivation. Oncogene 2010; 29: 3827–3834.
58. Szuhai K, Jennes I, De Jong D, et al. Tiling resolution array-CGH shows that somatic mosaic deletion of the EXT gene is causative in EXT gene mutation negative multiple osteochondromas patients. Hum Mutat 2011; 32: 2036–2049.
59. Wiweger MI, Avramut CM, de Andrea CE, et al. Cartilage ultrastructure in proteoglycan deficient zebrafish mutants brings to light new candidate genes for human skeletal disorders. J Pathol 2011; 223: 531–542.
60. Clement A, Wiweger M, von der Hardt S, et al. Regulation of zebrafish skeletogenesis by ext2/dackel and papst1/pinscher. PLoS Genet 2008; 4: e1000136.
61. Jones KB, Piombo V, Searby C, et al. A mouse model of osteochondromagenesis from clonal inactivation of Ext1 in chondrocytes. Proc Natl Acad Sci USA 2010; 107: 2054–2059.
62. Matsumoto K, Irie F, Mackem S, et al. A mouse model of chondrocyte-specific somatic mutation reveals a role for Ext1 loss of heterozygosity in multiple hereditary exostoses. Proc Natl Acad Sci USA 2010; 107: 10932–10937.
63. Du K, Peng Y, Zhang L, et al. Expression of the stem cell marker nestin in pre/hypertrophic chondrocytes in osteochondroma. J Int Med Res 2011; 39: 348–357.
64. Faraci M, Bagnasco F, Corti P, et al. Osteochondroma after hematopoietic stem cell transplantation in childhood. An Italian study on behalf of the AIEOP–HSCT group. Biol Blood Marrow Transpl 2009; 15: 1271–1276.
65. Bordigoni P, Turello R, Clement L, et al. Osteochondroma after pediatric hematopoietic stem cell transplantation: report of eight cases. Bone Marrow Transpl 2002; 29: 611–614.
66. Hilton MJ, Gutierrez L, Martinez DA, et al. EXT1 regulates chondrocyte proliferation and differentiation during endochondral bone development. Bone 2005; 36: 379–386.
67. de Andrea CE, Reijnders CM, Kroon HM, et al. Secondary peripheral chondrosarcoma evolving from osteochondroma as a result of outgrowth of cells with functional EXT. Oncogene 2012; 31: 1095-1104.

68. Passanise AM, Mehlman CT, Wall EJ, et al. Radiographic evidence of regression of a solitary osteochondroma: a report of 4 cases and a literature review. J Pediatr Orthop 2011; 31: 312–316.
69. Bissell MJ, Hines WC. Why don't we get more cancer? A proposed role of the microenvironment in restraining cancer progression. Nat Med 2011; 17: 320–329.
70. Allen M, Louise JJ. Jekyll and Hyde: the role of the microenvironment on the progression of cancer. J Pathol 2011; 223: 162–176.
71. Yen KE, Bittinger MA, Su SM, et al. Cancer-associated IDH mutations: biomarker and therapeutic opportunities. Oncogene 2010; 29: 6409–6417.
72. Raaijmakers MH, Mukherjee S, Guo S, et al. Bone progenitor dysfunction induces myelodysplasia and secondary leukaemia. Nature 2010; 464: 852–857.
73. Huang JN, Shimamura A. Clinical spectrum and molecular pathophysiology of Shwachman–Diamond syndrome. Curr Opin Hematol 2011; 18: 30–35.
74. Raaijmakers M. Niche contributions to oncogenesis: emerging concepts and implications for the hematopoietic system. Haematologica 2011; 96: 1041–1048.
75. Bertoni F, Bacchini P, Hogendoorn PCW. Chondrosarcoma. In World Health Organization Classification of Tumours. Pathology and Genetics of Tumours of Soft Tissue and Bone, Fletcher CDM, Unni KK, Mertens F (eds). IARC Press: Lyons, France, 2002; 247–251.
76. Amary MF, Bacsi K, Maggiani F, et al. IDH1 and IDH2 mutations are frequent events in central chondrosarcoma and central and periosteal chondromas but not in other mesenchymal tumours. J Pathol 2011; 224: 334–343.
77. Hallor KH, Staaf J, Bovee JVMG, et al. Genomic profiling of chondrosarcoma: chromosomal patterns in central and peripheral tumors. Clin Cancer Res 2009; 15: 2685–2694.
78. Bovee JVMG, Royen Mv, Bardoel AFJ, et al. Near-haploidy and subsequent polyploidization characterize the progression of peripheral chondrosarcoma. Am J Pathol 2000; 157: 1587–1595.
79. Bovee JVMG, Sciot R, Dal Cin P, et al. Chromosome 9 alterations and trisomy 22 in central chondrosarcoma: a cytogenetic and DNA flow cytometric analysis of chondrosarcoma subtypes. Diagn Mol Pathol 2001; 10: 228–236.
80. Mohseny AB, Hogendoorn PCW. Concise review: mesenchymal tumors: when stem cells go mad. Stem Cells 2011; 29: 397–403.
81. Boeuf S, Kunz P, Hennig T, et al . A chondrogenic gene expression signature in mesenchymal stem cells is a classifier of conventional central chondrosarcoma. J Pathol 2008; 216: 158–166.

82. Reijmers RM, Groen RW, Rozemuller H, et al. Targeting EXT1 reveals a crucial role for heparan sulfate in the growth of multiple myeloma. Blood 2010; 115: 601–604.
83. Rozeman LB, de Bruijn IH, Bacchini P, et al. Dedifferentiated peripheral chondrosarcomas: regulation of EXT-downstream molecules and differentiation-related genes. Mod Pathol 2009; 22: 1489–1498.

Chapter 3

Cartilage ultrastructure in proteoglycan-deficient zebrafish mutants brings to light new candidate genes for human skeletal disorders

Malgorzata I Wiweger, Cristina M Avramut,
Carlos E de Andrea, Frans A Prins,
Abraham J Koster, Raimond BG Ravelli,
Pancras CW Hogendoorn
Journal of Pathology 2011;223: 531-42

Abstract

Proteoglycans are molecules consisting of protein cores onto which sugar chains, i.e., glycosaminoglycans (GAGs) such as heparan or chondroitin sulphates, are attached. Proteoglycans are produced by nearly all cells, and once secreted they become a major component of the extracellular matrix. Cartilage is particularly rich in proteoglycans, and changes in the structure and composition of GAGs have been found in osteochondromas and osteoarthritis. The zebrafish (*Danio rerio*) exhibits fast development, a growth plate-like organization of its craniofacial skeleton and an availability of various mutants, making it a powerful model for the study of human skeletal disorders with unknown aetiology. We analysed skeletons from five zebrafish lines with known mutations in genes involved in proteoglycan synthesis: *dackel* (*dak/ext2*), lacking heparan sulphate; *hi307* (β*3gat3*), deficient for most GAGs; *pinscher* (*pic/slc35b2*), presenting defective sulphation of GAGs and other molecules; *hi954* (*uxs1*), lacking Notch and most GAGs due to impaired protein xylosylation; and *knypek* (*kny/gpc4*), missing the protein core of the Glypican-4 proteoglycan. Here we show that each mutant displays different phenotypes related to: (a) cartilage morphology; (b) composition of the extracellular matrix; (c) ultrastructure of the extracellular matrix; and (d) the intracellular ultrastructure of chondrocytes, proving that sulphated GAGs orchestrate the cartilage intra- and extracellular ultrastructures. The mild phenotype of the *hi307* mutant suggests that proteoglycans consisting of a protein core and a short sugar linker might suffice for proper chondrocyte stacking. Finally, *knypek* supports the involvement of Glypican-4 in the craniofacial phenotype of Simpson–Golabi–Behmel syndrome and suggests GPC4 as a modulator of the overgrowth phenotype that is associated with this syndrome and is primarily caused by a mutation in *GPC3*. Moreover, we speculate on the potential involvement of *SLC35B2*, β*3GAT3* and *UXS1* in skeletal dysplasias. This work promotes the use of zebrafish as a model of human skeletal development and associated pathologies.

Keywords: bone; cartilage; electron microscopy; glycans; osteochondroma; skeletal dysplasia; zebrafish

Introduction

The development, growth and functionality of living organisms require the presence of poly- and oligosaccharides known as glycans. Unbranched polysaccharides such as heparan sulphate (HS), chondroitin sulphate (CS), dermatan sulphate (DS) and keratan sulphate (KS) constitute a group of glycosaminoglycans (GAGs) and, when attached to a protein, form proteoglycans. GAGs/proteoglycans are produced by nearly all types of cells, but they are especially abundant in the cartilage extracellular matrix, where, together with other components of the extracellular matrix, they control many cellular events, such as adhesion, migration and differentiation [1]. This regulatory function is attributed to the various binding properties of GAGs. GAGs not only bind proteins but, also retain water molecules, thereby maintaining cartilage elasticity. Hence, it is not surprising that changes in GAG/proteoglycan structure and composition have physiological and pathological implications. For example, mutations in *EXT1* or *EXT2*, two genes that are crucial for the biosynthesis of HS, cause the development of osteochondroma, a benign cartilage-capped bone tumour [2]. Mutations in other HS-related genes have also been linked to skeletal conditions; e.g. mutation in *PERLECAN* leads to dyssegmental dysplasia [3], disruption of *GLYPICAN 3* causes Simpson–Golabi–Behmel syndrome [4], mutation in *GLYPICAN 6* results in recessive omodysplasia [5], and CS deficiency related to a mutation in the *CHST3* gene is found in spondylo-epi(meta) physeal dysplasia Omani type 6, 7. Mutations in the genes involved in the sulphation of proteoglycans are also known to cause several dysplasias (for a review, see Superti-Furga and Unger, 2007).

Different approaches and models are available for studies on diseases/disorders caused by GAG/proteoglycan dysfunction. Zebrafish (*Danio rerio*) is a popular model due to its fast development, the transparency of its embryos, its ease of manipulation at the molecular level and the availability of various mutants. The simple organization of the zebrafish skeleton and a similar developmental pattern to that of mammals makes zebrafish particularly useful for studies on skeletal development and disease. The craniofacial cartilage is one of the first to be formed during fish development. The first elements develop as early as 2 days post-fertilization (dpf) to give a fully functional cartilaginous skeleton by 5 dpf [8].

To learn more about the function of different glycans in human skeletal development and disease, we characterized the cartilage of wild-type (AB) zebrafish and five homozygous mutant lines with different defects in glycan synthesis. The mutants used in this study were identified by different groups: *dackel* (*dak/ext2*) and *pinscher* (*pic/slc35b2*, previously named *papst1*) [9], as well as *hi307* (β*3gat3*) and *hi954* (*uxs1*) [10] were selected based on their cartilage phenotypes, while *knypek* (*kny/gpc4*) was first recognized as a mutant with defective gastrulation movements [11]. Based on the functions of *ext2*, *gpc4*, *slc35b2*, β*3gat3* and *uxs1*, the biosynthesis of GAGs/proteoglycans should be affected at different steps: *dak* should lack HS only, *kny* should lack only a small population of HS, pic

should have reduced levels of sulphated CS, DS, HS, KS and non-GAG molecules, *hi307* should be deficient in CS, DS and HS, and *hi954* (*uxs1*) should lacks CS, DS, HS and other molecules requiring xylosylation (Table 1). Using light microscopy and transmission electron microscopy, we characterised the skeletons of proteoglycans-deficient zebrafish mutants and addressed the functions of different glycans in cartilage development, allowing us to speculate on the potential homology with human skeletal dysplasias.

Materials and methods

Animals

Zebrafish (*Danìo rerio H.*) embryos were obtained in natural crosses and staged in accordance with Kimmel et al [12]. Wild-type (AB) and five null mutants {*dackel* (*dak*), *exostoses (multiple) 2 allele ext2A*^{0739}; *pinscher* (*pic*), *solute carrier family 35*, *member B2 allele slc35b2*^{14MX} (previously named *PAPS transporter 1*, *papst1*) [9]; hi307, *ß1,3-glucuronyltransferase 3 allele* β*3gat3*^{hi307} [10]; *hi954*, *UDP–glucuronic acid decarboxylase 1 allele uxs1hi95410; and knypek (kny), and glypican 4 allele gpc4*^{V348} [11]} were raised to 5 dpf. Prior to fixation or freezing (GAG assay), the fish were anaesthetized in Tricane, and homozygous mutants were sorted by phenotype.

Human cartilage

Postnatal growth plates and osteochondromas were sampled at the Leiden University Medical Centre. Growth plates were from orthopaedic resections for pathological conditions not related to osteochondroma. All samples were obtained and handled according to ethical guidelines as described in the *Code for Proper Secondary Use of Human Tissue in The Netherlands* of the Dutch Federation of Medical Scientific Societies.

GAG assay

At 5 dpf, homozygous mutants were sorted by phenotype, and pools of 10 WT and sorted homozygote mutants were frozen for at least 1 h at − 20 °C prior to GAG extraction. GAG extraction and quantification was performed according to the Blyscan sulphated glycan assay manual (Biocolor, UK). GAG assays were performed three times in duplicate.

Light microscopy and immunohistology

Unless stated otherwise, all experimental procedures were performed as described previously 13. Fish were embedded in paraffin and cut into 4 µm sections. For glycogen detection only, after deparaffinization and rehydration, samples were incubated for 30 min at 60 °C in periodic acid, rinsed in water and stained with Schiff reagent for 30 min at room temperature. After a 15 min wash in water, the slides were dehydrated, mounted in micromount (Surgipath) and analysed under a light microscope.

Table 1. Theoretical changes in the biosynthesis of biologically active molecules predicted based on the known functions of the *exostosin 2* (*ext2*), *Glypican 4* (*gpc4*), *solute carrier family 35*, *member B2* (*slc35b2*); β*1,3-glucuronyltransferase 3* (β*3gat3*) and *UDP-glucuronic acid decarboxylase 1* (*uxs1*) genes.

Gene Mutant	*ext2 dackel*	*gpc4 knypek*	*slc 35b2 pinscher*	*b3gat3 hi307*	*uxs1 hi954*
Chondroitin sulphate	na	na	Reduction	Loss	Loss
Dermatan sulphate	na	na	Reduction	Loss	Loss
Heparan sulphate	Loss	Reduction	Reduction	Loss	Loss
Hyaluronan	na	na	na	na	na
Keratan sulphate	na	na	Reduction	na	na
Other molecules	na	na	Loss of all sulphated molecules	na	Loss of Notch, blood coagulation factor VII and IX

Loss, full inhibition of biosynthesis; reduction, only some molecules are affected, eg the loss of sulphated epitopes in the pic mutant; na, not affected.

Sections predigested for 30 min at 37 °C in α-amylase (0.5% w/v in PBS; Sigma) were included as negative controls. For immunostaining of the extracellular matrix, anti-CS (CS-56, Sigma) at 1:800, anti-collagen type II (II-II6B3, Developmental Studies Hybridoma Bank) at 1:200, anti-collagen I (Rockland) at 1:800 and anti-collagen VI at 1:50 (Abcam) were used as primary antibodies. The poly-HRP-Gam/R/R IgG system (ImmunoLogic), followed by DAB detection (Dako) or anti-mouse AP (Sigma) at 1:500, followed by BCIP/NBT (Sigma), was used to detect the signal. Each experiment was repeated at least three times with the same results.

Transmission electron microscopy

Fish were fixed in either: (a) 1.5% glutaraldehyde; (b) a mixture of 1.5% glutaraldehyde and 1% PFA; or (c) a mixture of 1.5% glutaraldehyde and 4% PFA; all were in 0.1 m sodium cacodylate for 1 h, followed by incubation in 1% osmium tetroxide (OsO4) in 0.1 m sodium cacodylate for 1 h. After each step of the fixation, the fish were rinsed twice with 0.1 m sodium cacodylate and finally dehydrated in a series of 70%, 80%, 90% and 3× 100% ethanol, prior to immersion in a 1:1 epon:propylene oxide solution for 1 h. The samples were washed afterwards with pure epon, embedded in pure epon LX112 and polymerized at 60 °C for 2 days. Cross-sections (800 nm thick) from five homozygous mutant fish from each line were stained with toluidine blue and analysed for general morphological figures under a light microscope. The pilot experiment revealed that WT fish fixed in 1.5% glutaraldehyde with and without addition of PFA had similar morphologies, and for further analysis all fish were fixed in 1.5% glutaraldehyde, omitting the PFA. The cartilage ultrastructures were analysed by transmission electron microscopy in the WT and two homozygous mutants from each line. For this purpose, transverse sections of 100 nm thickness were transferred to slot grids for transmission electron microscopy and post-stained with 7% uranyl acetate and Reynolds' lead citrate. The percentage of the extracellular matrix space that was filled with fibres was analysed on the electron micrographs.

Results

Concentration of total sulphated GAGs

Although the Blyscan assay does not give any indication of the concentration of single CS, KS, DS or HS, it allows for the quantification of the total level of sulphated GAGs (free and as a part of proteoglycans) present in a sample. Compared to WT, significantly decreased levels of total sulphated GAGs were detected in *pic*, *hi307* and *hi954* homozygous mutants (Figure 1), which was in line with the theoretical predictions based on what is known about the functions of *slc35b2*, β*3gat3* and *uxs1*, respectively (Table 1). A normal level of total sulphated GAGs was detected in the *kny* mutant, which lacks Glypican 4 (Figure 1). Intriguingly, the level of total sulphated GAGs in the dak mutant was elevated (Figure 1), even though a mutation in *ext2* should inhibit HS synthesis (Table 1).

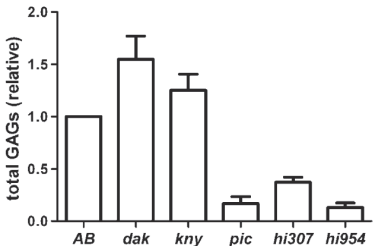


Figure 1. Relative levels of total sulphated GAGs at 5 dpf in WT and homozygote mutants: *dackel* (*dak/ext2*), *knypek* (*kny/gpc4*), *pinscher* (*pic/slc35b2*), *hi307* (β*3gat3*) and *hi954* (*uxs1*). The level of sulphated GAGs in *kny* is similar to that in WT. The *dak* mutant has a significantly higher content of sulphated GAGs than WT, whereas *pic*, *hi307* and *hi954* contain significantly lower levels of sulphated GAGs than WT.

Cartilage morphology

At 5 dpf, wild-type chondrocytes in pharyngeal arches were organized into neat stacks of cells flattened along the longitudinal axis, thus resembling chondrocytes from the proliferating zone of the mammalian growth plate (Figure 2C',D). From the analysed mutants, the morphologies of *hi307* (which in theory should lack most of proteoglycans) and *kny* (which should lack Glypican 4 only) were the most similar to WT. Although the chondrocytes in Meckel's and ceratohyal cartilages did not stack well (Figure 3A), *hi307*- and *kny*-derived chondrocytes were properly stacked and flattened in other craniofacial cartilage elements (Figure 3B). *dak*, which should lack HS only, and *pic*, which has impaired sulphation, had very severe cartilage phenotypes (Figure 3A, B). In both mutants, all chondrocytes were similar to those from human OCs, ie they were rounded and did not intercalate into stacks but remained as a disorganized cluster of cells (Figures 2E, 3A, B). In the *hi954* mutant, which should lack most GAGs and other xylated molecules, chondrocytes had an atypical appearance, often failed to intercalate and were deficient in the extracellular matrix (Figures 3B, 5B).

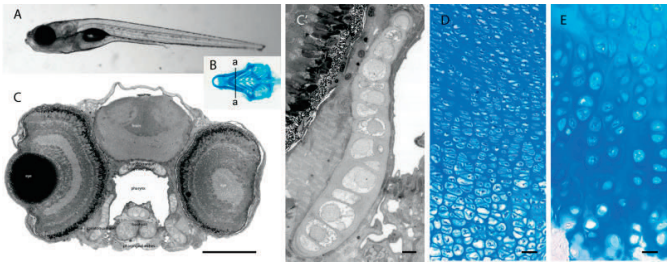


Figure 2. The organization of the cartilaginous skeleton in zebrafish at 5 dpf. WT chondrocytes in pharyngeal arches are organized into neat stacks of chondrocytes flattened along the longitudinal axis, thus resembling chondrocytes from the proliferating zone of the mammalian growth plate. Lateral view of 4 mm zebrafish WT larvae (A); craniofacial skeleton visualized by whole-mount staining with alcian blue (B); transverse section at the level indicated by aa (C); magnification of the area with palatoquadrate (C'); growth plate from a human fetus (D); cartilage cap from an osteochondroma (E). Scale bar = 5 µm (C) and 100 µm (D, E)

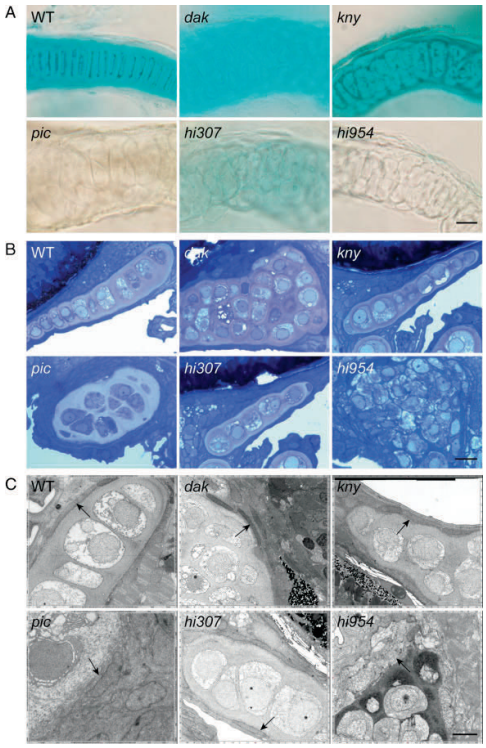


Figure 3. Defects in cartilage organization and extracellular matrix composition in proteoglycan-deficient homozygote mutants: *dackel* (*dak/ext2*), *knypek* (*kny/gpc4*), *pinscher* (*pic/slc35b2*), *hi307* (*β3gat3*) and *hi954* (*uxs1*). Neat stacks of chondrocytes flattened along the longitudinal axis are present in WT (A, B). In *kny* and *hi307*, mild chondrocyte clustering can be observed only in Meckel's and ceratohyal cartilages (A), whereas other cartilage elements appear normal (B). A loss of stacking similar to that in human OCs is especially apparent in the dak and pic mutants (A, B). *hi954* chondrocytes have an atypical appearance, with severely reduced extracellular matrix and often failure to intercalate (A). The lack of blue staining (A) and purple staining (B) in cartilage from *pic*, *hi307* and *hi954* mutants confirms the absence of sulphated proteoglycan in the extracellular matrix. The severely reduced extracellular matrix in the *hi954* mutant should be noted. Normally, cartilage elements are surrounded with a perichondrium made up of one to two layers of small, elongated cells, with little cytoplasm and extracellular matrix but rich in electron-dense material. *dak*, *kny* and *hi307* show normal perichondrium; the pic perichondrium is thicker; no perichondrium can be identified in *hi954*. The whole-mount Meckels' cartilage was stained by alcian blue (A). Sections at the level of the palatoquadrate were stained with toluidine blue (B). The perichondriums in WT and homozygous mutant fish are shown at 5 dpf (C). Scale bar = 5 µm (A), 10 µm (B) and 5 µm (C)

The spacing between WT fish chondrocytes was less pronounced than in human cartilage, but it was similarly filled with a glycan-rich extracellular matrix (Figures 2C',3). The *hi954* mutant was the only mutant that showed a severely reduced extracellular matrix deposition. None of the other mutants showed any sign of reductions or increases in the extracellular matrix accumulation (Figure 3B). In contrast to what is known from higher vertebrates, numerous lacunae enclosing small groups of chondrocytes are not present in zebrafish. However, lacunae-like borders were observed at the periphery of each cartilage element (Figure 3B, C). Therefore, we concentrated on the areas between chondrocytes where the extracellular matrix was homogeneous and looked like typical immature hyaline cartilage.

Perichondrium

In WT fish, chondrocyte elements were surrounded with a thin layer of perichondrium made up of one or two layers of small, elongated cells, with little cytoplasm and extracellular matrix but rich in electron-dense material (Figure 3C). Similar perichondria were also observed in *dak*, *kny* and *hi307* mutants (Figure 3C). The *pic* perichondrium was thickened, showing enlarged cells and a rough surface (Figure 3C). In the case of *hi954*, typical perichon-drium-like cells were not present; however, chondrocytes were neighboured by slightly elongated cells that had variable sizes, rough surfaces and were rich in cytoplasm but were poor in electron-dense material (Figure 3C).

Bone ossification

As cartilage prefigures the development of cartilage bones in fish (analogous to endochondral bones in mammals), we were interested to determine whether bone development was affected in our mutants. By 5 dpf, most of the bones stained by alizarin red were of intramembranous origin (i.e. bones that do not form upon a cartilage template; see supporting information, Table S1). Of those, the cleithrum and opercle, the first bones to develop, were found in WT and all mutant fish; however, in *dak*, *pic* and *hi307* mutants they were small and malformed (data not shown). Other dermal bones were unaffected in *kny*, *hi307* and *hi954* but were severely reduced/lost in *dak* and *pic* mutants (see supporting information, Table S1). When it comes to the cartilage bones (fish) that correspond to endochondral bones in mammals, by 5 dpf WT ossification was seen only in the 5th ceratobranchial. No alterations in bone development, including bone malformations and changes in the timing of ossification, were observed in the *kny*, *hi307* and *hi954* mutants. However, at later time-points, delays in the development of other cartilage bones were observed in *hi307* and *hi954* mutants (data not shown). The 5th arch from dak ossified normally despite severe malformations of its cartilaginous template, whereas pic ossification was reduced (see supporting information, Table S1). The blockage of cartilage bone formation in dak and pic mutants was more severe than in *hi* mutants and it persisted until at least 9 dpf (data not shown).

Secretion and composition of the extracellular matrix

The zebrafish extracellular matrix, like any other cartilage matrix from vertebrates, consists mostly of water, collagens and proteoglycans. In WT cartilage, proteoglycans stain blue with alcian blue (Figure 3A) and purple with toluidine blue (Figure 3B). Cartilage from WT, *dak* and *kny* were stained with both dyes. *hi954* remained unstained (Figure 3A, B), whereas the skeletons of *pic* and *hi307* showed pale staining (Figure 3A, B). Those observations are in line with previous reports on alcian blue stains in *dak* and *pic* [13], *hi307* [14] and *hi954* [14, 15] and also correlate well with the results from the GAG assay (Figure 1). We also examined the deposition of Collagen II and found that this protein was absent in the *hi954* mutant and significantly reduced in *hi307*, whereas other mutants did not show any abnormalities in the production of this extracellular matrix component (Figure 4B, Table 2). Collagen I and VI were normally expressed in *dak* and *kny* mutants but were reduced/absent in the *hi307* and *hi954* mutants (Figure 4B, Table 2).

Ultrastructure of the extracellular matrix

The collagen network, consisting of a net of long and thin collagen fibres associated with proteoglycan granules (electron-dense particles), was clearly visible in the extracellular matrix of WT chondrocytes (Figure 4A). The fibrils present between well-stacked chondrocytes were mostly orientated perpendicular to the longitudinal axis of cartilage elements (aligned fibres), whereas presumptively intercalating chondro-cytes were surrounded with a radially running collagen network (radial fibres) (see supporting information, Figure S1). In WT, aligned fibres were observed in 47% and radial fibres in 37% of extracellular spaces. No apparent fibrils were observed in the remaining 16% of cases. A WT-like collagen network and proteoglycan granules were also observed in the *kny* mutant (Figure 4A). *kny* had aligned and radial fibres observed in 24% and 52% of extracellular spaces, respectively. In the *dak* mutant, collagen fibres were also arranged in a similar manner as in WT cells (21% aligned and 74% radial fibres), but the number of proteoglycan granules present in the extracellular matrix was clearly reduced (Figure 4A). In the *hi307* extracellular matrix, the collagen fibres were present (Figure 4A) but, despite relatively normal stacking of chondrocytes (Figure 3A), only 8% of fibrils were aligned and 59% were radial, while 33% lacked a distinct fibre orientation. Although a mutation in β*3gat3* should block the biosynthesis of most GAGs (Table 1), many electron-dense particles (similar to those in WT proteoglycan granules) were observed in the *hi307* mutant (Figure 4A). In the *hi954* mutant, the extracellular matrix was drastically reduced and was limited to a very thin layer between chondrocytes and a slightly thicker layer at the edge of each cartilage element (Figure 4A).

In comparison to other mutants and WT fish, the extracellular matrix from *hi954* appeared richer in electron-dense material and had numerous focal condensations (Figure 5B). Occasionally, short and thick bundles of fibrous material were observed, especially at

the periphery of cartilage elements, but they were not composed of Collagen II, as indicated by the lack of immunostaining [15]. The collagen network was also disrupted in the pic mutant. Normal collagen fibres were occasionally present, whereas short and thick filaments arranged into bundles were found scattered throughout the extracellular matrix in 93% of gaps between *pic* chondrocytes (Figure 4A). The presence of proteoglycan granules in *pic* mutants was common, and they were found unbound as well as associated with collagen fibrils.

Cell membranes and junctions

Cell membranes surrounding WT chondrocytes had many short protrusions that were in contact with the collagen network (Figure 5A). Evagination of the membrane was especially pronounced between chondrocytes that were not in line with the longitudinal axis but were most likely still moving into the final position (intercalating/stacking). A WT-like appearance of the cell membranes was observed in *dak*, *kny* and *hi307* mutants (Figure 5A). Cell membranes from the *pic* mutant were considerably undulated and also had pronounced protrusions (Figure 5A). In contrast, cell membranes from the *hi954* mutant chondrocytes were smooth and free from any protrusions (Figure 5).

Cell junctions were not commonly observed in chondrocytes from WT, *dak*, *pic*, *kny* and *hi307* mutants (data not shown). This is probably because, similarly to the development of mammalian cartilage, soon after cell division, zebrafish chondrocytes become separated from each other by a layer of extracellular matrix. Interestingly, in the *hi954* mutant, minimal extracellular matrix secretion coincided with impaired cell separation. Cell junctions were maintained and often spanned relatively long fragments of cell membranes (Figure 5B). In consequence, the cells failed to separate, creating clusters of interconnected cells.

Intracellular ultrastructure of chondrocytes

The nuclei of the chondrocytes were well preserved in all fish strains. WT nuclei had regular shapes. Similar appearances of the nuclei were also observed in *dak*, *kny* and *hi307* mutants (Figure 5A). The shape of *hi954* nuclei reflected the shape of the cell, as less regular but still relatively normal. The *pic* mutant was the only one to show nuclei with irregular shapes (Figure 5A). Moreover, pic chondrocytes had mixed populations of normal- and dark-stained cells, with the latter resembling paraptotic T9-C2 cells [16]. An occasional margination of chromatin was observed in the *hi954* mutant only (data not shown). The mitochondria, ER and Golgi apparatus were confirmed in WT and all mutants but, as they showed signs of osmotic stress, they were not subjected to further analysis. This apparently damaged appearance was restricted to chondrocytes only and was observed regardless of the type of fixative. Despite the poor preservation of Golgi, in their close proximity, well-preserved centrioles/basal bodies of primary cilia having typical (9 + 0) microtubule arrangements

were found in WT and all mutant lines (data not shown).

Cytoplasmic inclusions

The presence of glycogen deposits in the cytoplasm has been reported in osteochondroma [17]. We expected to see similar deposits, at least in the *dak* mutant. To our surprise, the transmission electron microscopy images revealed that the cartilage cytoplasms of all six fish lines were devoid of an electron-dense material resembling glycogen. Furthermore, PAS staining for glycogen was negative in the zebrafish cytoplasm (data not shown). Black speckles looking like lipid droplets were found in all fish but only in a small population of chondrocytes, of which all had dark and irregular nuclei resembling cells undergoing cell death (data not shown). Large empty-looking areas devoid of electron-dense material were found in the cytoplasms of all analysed fish (Figure 5A). The content and function of those vacuoles remain unknown.

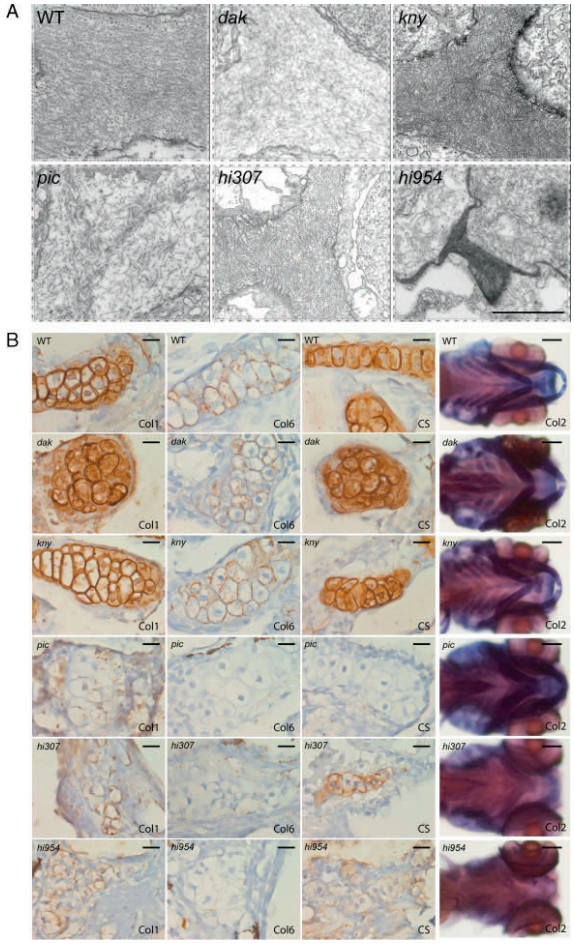


Figure 4. The organization of the extracellular matrix, unequally affected in different mutants. knypek (kny/gpc4) and dackel (dak/ext2) have WT-like collagen networks, whereas pincher (pic/slc35b2) shows a very severe disorganization of the collagen network (bundles of short fibres) (A). Only the remains of the extracellular matrix and no collagen fibres are observed in the hi954 (uxs1) mutant. Surprisingly, hi307 (β3gat3) shows only slight abnormalities in the length and orientation of the collagen network. Electron-dense particles of proteoglycans are observed in all mutants; however, their number is clearly reduced in the dak and hi954 mutants and is surprisingly unaffected in the hi307 mutant. Collagen I, Collagen II, Collagen VI and CS were immunodetected in WT and homozygote mutants at 5 dpf (B). Scale bar = 1 µm (A, B; Col1, Col2, CS) and 10 µm (B; Col2)

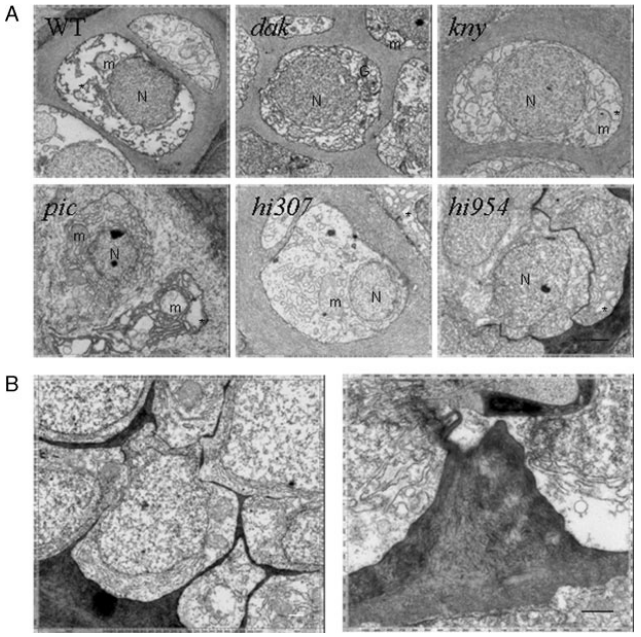


Figure 5. The ultrastructure of chondrocytes in the dackel (dak/ext2), knypek (kny/gpc4), pinscher (pic/slc35b2), hi307 (β3gat3) and hi954 (uxs1) mutants. No apparent ultrastructural changes can be observed in dak, kny and hi307. pic has two types of cells (dark and pale), severe membrane undulation and frequent cell junctions; hi954 has smooth membranes that often fail to separate. Electron micrographs show the chondrocyte ultrastructure (A). Abnormal cell junctions and extracellular matrix are seen in the hi954 homozygote mutant (B). N, nucleus; G, Golgi apparatus; m, mitochondria; *, areas devoid of electron-dense material. Scale bar = 1 μm.

Discussion

The zebrafish skeleton is composed of cartilage and bones, for which the organization and development is underlined by molecular mechanisms similar to those in mammals [18]. Here, we characterized the phenotypic changes caused by proteoglycan deficiencies in zebrafish, with the goal of shedding light on the function of proteoglycans in human skeletogenesis as well as on skeletal disorders for which mutations are still unknown [19].

A summary of the defects found in each mutant is presented in Table 2. In short, *dak* (which is mutated in the *ext2* gene) displays severe cartilage malformation and bone impairment, mild ultrastructural defects and a mild reduction of the body length; *kny* (which is mutated in *gpc4*) has very mild cartilage and bone phenotypes and no obvious ultrastructural defects, but it displays severe dwarfism; *pic*, which is mutated in *slc35b2* (*papst1*), has severe cartilage and bone defects, shows pronounced ultrastructural abnormalities (abnormal collagen filaments, enhanced cell death, frequent cell junctions), displays dwarfism and does not stain with basic dyes; *hi307* (which is mutated in β*3gat3*) has a very mild cartilage and bone phenotype, shows ultrastructural abnormalities restricted to slightly abnormal collagen fibrils, displays dwarfism and does not stain with basic dyes; lastly, *hi954* (which is mutated in *uxs1*) has a severe cartilage and bone phenotype, shows severe ultrastructural defects (reduced extracellular matrix, lack of Collagen II, fused cells, abnormal fibrils), displays dwarfism and does not stain with alcian or toluidine blue.

Table 2. Overview of the defects found in each analysed mutant and information on the human correlates.

name affected gene	WT	*dak ext2*	*pic slc35b2*	*kny gpc4*	*hi307 b3gat3*	*hi954 uxs1*
function		Glycosyltransferase involved in the elongation of the heparan sulphate, chain, forms complexes with EXT1	Adenosine 3′-phospho 5′-phosphosulphate (PAPS) transporter, required for transport of sulphate donors into Golgi	Protein core of Glypican 4 membrane-associated proteoglycan that plays a role in the control of cell division and growth regulation	Glucuronyltransferase involved in the final step of the biosynthesis of the linkage region of proteoglycans	UDP-glucuronate decarboxylase needed for the formation of UDP-xylose and latter initiation of GAG biosynthesis on the protein core of proteoglycans
zebrafish chromosome		7	20	14	7	13, 9
human homologue		*EXT2*	*SLC35B2*	*GPC4*	*β3GAT3*	*UXS1*
human chromosome		11 (p12-p11)	6 (p12.1-p11.2)	X (q26.1)	11 (q12.3)	2 (q12.2)
human disorder		Solitary and multiple osteochondromas		One case with deletion of GPC4 in addition to GPC3 in Simpson–Golabi–Behmel syndrome		
chondrocyte stacking	Normal	Severely impaired	Severely impaired	Partially impaired	Partially impaired	Impaired
ossification	Normal	Lost in some dermal and in all cartilage bones	Lost in most bones	Normal	Delay in cartilage bones	Delay in cartilage bones
perichondrium	Normal	Normal	Thicker	Normal	Normal	Missing
Alcian blue	Blue stain	Blue stain	Unstained	Blue stain	Unstained	Unstained
Toluidin blue	Purple stain	Purple stain	Unstained	Purple stain	Unstained	Unstained
collagen I	+	+	±	+	±	±
collagen II	+	+	+	+	±	−
collagen VI	+	+	−	+	−	−
CSPG	+	+	−	+	±	−
ECM fibers	Normal	Normal	Bundles	Normal	Less frequent	Absent
ECM granules	Normal	Reduced	Reduced	Normal	Normal	Absent
nucleus	Normal	Normal	Dark and pale cells	Normal	Normal	Normal
undulation of cell membranes	Mild	Mild	Severe	Mild	Mild	Absent
cell death	Occasional	Occasional	Common	Occasional	Occasional	Occasional
cell fusion	Absent	Absent	Absent	Absent	Absent	Partial
cell junctions	Seldom present	Seldom present	Often present	Seldom present	Seldomly present	Often present
body length	Normal	Slightly shorter	Dwarfism	Severe dwarfism	Dwarfism	Dwarfism
craniofacial skeleton	Normal	Severely deformed	Deformed	Deformed	Deformed	Deformed
references		9, 13, 26	9, 13	11, 32	10, 14	10, 14, 15

Staining intensity: +, strong; ± , weak; −, absent. More information on zebrafish mutants can be found at ZFIN, the zebrafish model organism database (http://zfin.org/cgi-bin/webdriver?MIval = aa-fishselect.apg).

The similarities in the cartilage phenotype and its severity in *dak* (*ext2*; lacking HS), *pic* (*slc35b2*; lacking sulphation of various molecules, e.g., HS, CS, DS and KS) and *hi954* (*uxs1*; lacking Notch and most proteoglycans) strengthen the importance of HS in cartilage morphology and ultrastructure [this report and 13, 15]. We anticipated that the lack of β*3gat3* in the *hi307* mutant would result in a total inhibition of the biosynthesis of HS, CS and DS and would consequently cause a severe phenotype but, to our surprise, it showed a relatively normal cartilage morphology. The presence of a mutation was confirmed by PCR in all phenotyped *hi307* homozygote mutants (data not shown). However, the presence of other copies or splice variants of β*3gat3* or the involvement of other genes having rescuing effects on the cartilage morphology cannot be excluded. Two other possibilities should be mentioned. First of all, GAGs have been described as the active part of proteoglycans, although it is possible that the protein cores might also be biologically active. Secondly, even if the mutation in β*3gat3* totally inhibited HS, CS and DC, proteoglycans consisting of a protein core and a very short linker (a chain of up to four sugars) could be synthesized; indeed, we found electron-dense particles in the *hi307* mutant. It is possible that these incomplete proteoglycans are sufficient to maintain the cartilage morphology, although a more detailed analysis of the GAGs in *hi307* might yield other explanations of this unexpectedly mild phenotype.

There is no doubt that proteoglycans are important for cartilage development; however, questions have been raised as to whether proteoglycans are necessary, sufficient or non-essential for the induction of bone calcification [20]. Our findings imply that GAGs are not needed for intramembranous ossification (*hi307* and *hi954*); however, reduced sulphation (*pic*) had a strong negative impact on both intramembranous and endochondral bone formation. At 5 dpf, zebrafish are just starting the ossification of cartilage bones, so conclusions about the influence of proteoglycans on endochondral ossification are premature. Carey [21] suggested that proteoglycans are not needed for cell viability or proliferation but that they are necessary for stable extracellular matrix assembly and extracellular matrix–cell interaction. Our data support this hypothesis, as severe defects in cartilage organization, including ultrastructural changes in the extracellular matrix, were observed in zebrafish with mutations in *uxs1* (*hi954*), β*3gat3* (*hi307*) and *slc35b2* (*pic*).

Transmission electron microscopy fixation is known to have an impact on the morphology of cartilage. Chemical fixation of mammal cartilage in the absence of a cationic dye results in chondrocytes having a shrunken appearance and seeming to be surrounded by haloes. This is because many components of the surrounding matrix are lost by aqueous extraction, plasma membrane–extracellular matrix connections are lost, and a pericellular lacuna free of fibrillar collagen and proteoglycans, referred to as a rim, is formed. Similar fixation methods seem to work well for the extracellular matrix in zebrafish craniofacial cartilage, but internal structures such as the mitochondria, ER and Golgi apparatus show compromised preservation. However, as different fixatives resulted in similar chondrocyte

morphologies, it might be possible that this chondrocyte appearance is actually not an artefact but reflects changes occurring with time. Even if fine ultrastructural details might be affected and if topological relationships are sometimes difficult to interpret, potential fixation artefacts are expected to be identical for all the embryos, allowing conclusions to be drawn on the differences between WT and mutant cartilage. It is not clear why similar glycogen deposits were not observed in zebrafish cytoplasm. However, as glycogen deposition seems to increase upon cartilage differentiation [22], it is possible that zebrafish chondrocytes at 5 dpf behaved like resting chondrocytes and had not yet started to accumulate glycogen.

To date, several human disorders have been found to share phenotypical similarities with corresponding zebrafish models [13, 23–25]. The dak zebrafish mutant used in this study has a human correlate: solitary and multiple osteochondromas caused by mutation in the *EXT1* or *EXT2* genes [13, 26–28]. A deletion of *GLYPICAN 4* was described in one patient with Simpson–Golabi–Behmel syndrome [29]. However, this deletion coincided with a mutation in the neighbouring gene, *GLYPICAN 3*, which on its own is a sufficient causative of Simpson–Golabi–Behmel syndrome. It is rather unlikely that *GLYPICAN 4* is involved in the patient overgrowth phenotype, but it could contribute to the craniofacial phenotype and hydrocephalus [30, 31]. These conclusions are supported by the *kny* mutant zebrafish, where a mutation of the fish *glypican 4* results in a short body length and craniofacial phenotype at the larvae stage; additionally, when Gpc4 function is rescued by an injection of WT-mRNA, some embryos survive and grow to be adults with normal overall body lengths [32]. However, those rescued mutants have smaller heads with short and thick jaw bones, forming domed skulls. Interestingly, even though they often miss some facial bones, their jaws remain functional [32]. Hence, it is quite likely that a mutation in *GLYPICAN 4* only might cause a condition that sometime coincides with Simpson–Golabi–Behmel syndrome, influencing its phenotypic variability. Judging by the severity of the cartilage phenotypes found in homozygous fish mutants, putative mutations in human *GPC4* or β*3GAT3* should not cause skeletal problems in early life, whereas mutations in *SLC35b2* or *UXS1* might be involved in the more symptomatic changes already seen prenatally or in toddlers. At present, *pic*, *hi307* and *hi954* zebrafish models cannot be linked with any human disorders, but mutations in related genes are known to cause several skeletal dysplasias. For example, a mutation in *GLYPICAN 6* causes recessive omodysplasia [5], a loss of function of NST (which is encoded by *SLC35D1*) causes Schneckenbecken dysplasia [33], and mutations in *DTDST* (*SLC26A2* sulphate transporter) result in achondrogenesis type 1B, atelosteogenesis type 2 and diastrophic dysplasia [34]. There are many more dysplasias for which the causative mutations are not known [19]. Some of them have been mapped and, interestingly, a few match the locations of the genes we modelled in zebrafish. For instance, split-hand/foot malformation 2 was linked to Xq26, where *GLYPICAN 4* has its locus [35]. However, one has to keep in mind that Xq26 contains other genes besides *GPC4*, including *SLC25A6*, *SLC26A5*

and *HS6ST2*, which might be involved in disorders caused by proteoglycan deficiencies. For those diseases that are not mapped, phenotype matching might be useful. In Table 2, we present a summary of the defects found in each mutant, which can be used as a guideline to help link human diseases with the genes. With this work, we also aim to promote zebrafish as a model for studying human skeletal development and associated pathologies.

Acknowledgements

This work was supported by the European Network of Excellence (EuroBoNeT: http://www.eurobonet.eu), Grant No. 018814 (LSHC-CT-2006-018814), to PCWH. RBGR and MCA acknowledge financial support from NWO under Project No. 016.072.321. The hybridoma collagen II (II-II6B3) antibody developed by T. Linsenmayer was obtained from the Developmental Studies Hybridoma Bank.

Statement of author contributions

MIW and PCWH were involved in the study design; MIW, CMA, FAP and RBGR collected the data; MIW, CMA, CEdeA and RBGR analysed the data; MIW, CEdeA, AJK and PCWH interpreted the data; MIW, CMA and PCWH did literature searches; MIW, CMA, CEdeA, FAP and RBGR generated figures. All authors were involved in writing the paper and had final approval of the submitted and published versions.

References

1. Willems SM, Wiweger M, Frans Graadt van Roggen J, et al. Running GAGs: myxoid matrix revisited. What's in it for the pathologist? Virchow Arch 2009; 456: 181–192.
2. Bovée JVMG, Hogendoorn PCW. Multiple osteochondromas. In World Health Organization Classification of Tumours. Pathology and Genetics of Tumours of Soft Tissue and Bone, FletcherCDM, UnniKK, MertensF (eds). IARC Press: Lyon, 2002; 360–362.
3. Arikawa-Hirasawa E, Wilcox WR, Le AH, et al. Dyssegmental dysplasia, Silverman–Handmaker type, is caused by functional null mutations of the perlecan gene. Nat Genet 2001; 27: 431–434.
4. Pilia G, Hughes-Benzie RM, MacKenzie A, et al. Mutations in GPC3, a glypican gene, cause the Simpson–Golabi–Behmel overgrowth syndrome. Nat Genet 1996; 12: 241–247.
5. Campos-Xavier AB, Martinet D, Bateman J, et al. Mutations in the heparan-sulfate proteoglycan glypican 6 (GPC6) impair endochondral ossification and cause recessive omodysplasia. Am J Hum Genet 2009; 84: 760–770.
6. Thiele H, Sakano M, Kitagawa H, et al. Loss of chondroitin 6-O-sulfotransferase-1 function results in severe human chondrodysplasia with progressive spinal involvement. Proc Natl Acad Sci USA 2004; 101: 10155–10160.

7. Hermanns P, Unger S, Rossi A, et al. Congenital joint dislocations caused by carbohydrate sulfotransferase 3 deficiency in recessive Larsen syndrome and humero-spinal dysostosis. Am J Hum Genet 2008; 82: 1368–1374.
8. Schilling TF, Kimmel CB. Musculoskeletal patterning in the pharyngeal segments of the zebrafish embryo. Development 1997; 124: 2945–2960.
9. Schilling TF, Piotrowski T, Grandel H, et al. Jaw and branchial arch mutants in zebrafish I: branchial arches. Development 1996; 123: 329–344.
10. Golling G, Amsterdam A, Sun Z, et al. Insertional mutagenesis in zebrafish rapidly identifies genes essential for early vertebrate development. Nat Genet 2002; 31: 135–140.
11. Solnica-Krezel L, Stemple DL, Mountcastle-Shah E, et al. Mutations affecting cell fates and cellular rearrangements during gastrulation in zebrafish. Development 1996; 123: 67–80.
12. Kimmel CB, Ballard WW, Kimmel SR, et al. Stages of embryonic development of the zebrafish. Dev Dyn 1995; 203: 253–310.
13. Clément A, Wiweger M, von der Hardt S, et al. Regulation of zebrafish skeletogenesis by ext2/dackel and papst1/pinscher. PLoS Genet 2008; 4: e1000136.
14. Nissen RM, Amsterdam A, Hopkins N. A zebrafish screen for craniofacial mutants identifies wdr68 as a highly conserved gene required for endothelin-1 expression. BMC Dev Biol 2006; 6: 28.
15. Eames BF, Singer A, Smith GA, et al. UDP xylose synthase 1 is required for morphogenesis and histogenesis of the craniofacial skeleton. Dev Biol 2010; 341: 400–415.
16. Hoa N, Myers MP, Douglass TG, et al. Molecular mechanisms of paraptosis induction: implications for a non-genetically modified tumor vaccine. PLoS ONE 2009; 4: e4631.
17. de Andrea CE, Wiweger M, Prins F, et al. Primary cilia organization reflects polarity in the growth plate and implies loss of polarity and mosaicism in osteochondroma. Lab Invest 2010; 90: 1091–1101.
18. Yelick PC, Schilling TF. Molecular dissection of craniofacial development using zebrafish. Crit Rev Oral Biol Med 2002; 13: 308–322.
19. Superti-Furga A, Unger S. Nosology and classification of genetic skeletal disorders: 2006 revision. Am J Med Genet A 2007; 143: 1–18.
20. Hunter GK. Role of proteoglycan in the provisional calcification of cartilage. A review and reinterpretation. Clin Orthop Relat Res 1991; 262: 256–280.
21. Carey DJ. Biological functions of proteoglycans: use of specific inhibitors of proteoglycan synthesis. Mol Cell Biochem 1991; 104: 21–28.

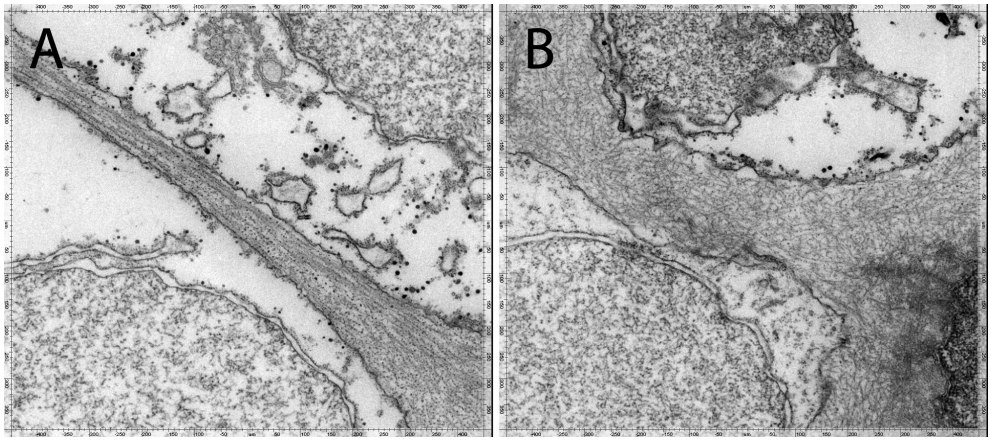
22. Mitchell NS, Shepard NL. Electron microscopic evaluation of the occurrence of matrix vesicles in cartilage. Anat Rec 1990; 227: 397–404.
23. Bassett DI, Currie PD. The zebrafish as a model for muscular dystrophy and congenital myopathy. Hum Mol Genet 2003; 12(2):(spec No): R265–270.
24. Telfer WR, Busta AS, Bonnemann CG, et al. Zebrafish models of collagen VI-related myopathies. Hum Mol Genet 2010; 19: 2433–2444.
25. Venkatasubramani N, Mayer AN. A zebrafish model for the Shwachman–Diamond syndrome (SDS). Pediatr Res 2008; 63: 348–352.
26. Lee J-S, von der HS, Rusch MA, et al. Axon sorting in the optic tract requires HSPG synthesis by ext2 (dackel) and extl3 (boxer). Neuron 2004; 44: 947–960.
27. Hameetman L, Szuhai K, Yavas A, et al. The Role of EXT1 in non-hereditary osteochondroma:identification of homozygous deletions. J Natl Cancer Inst 2007; 99: 396–406.
28. Bovée JVMG. Multiple osteochondromas. Orphanet J Rare Dis 2008; 3: 3.
29. Veugelers M, Vermeesch J, Watanabe K, et al. GPC4, the gene for human K-glypican, flanks GPC3 on Xq26: deletion of the GPC3–GPC4 gene cluster in one family with Simpson–Golabi–Behmel syndrome. Genomics 1998; 53: 1–11.
30. Veugelers M, Cat BD, Muyldermans SY, et al. Mutational analysis of the GPC3/GPC4 glypican gene cluster on Xq26 in patients with Simpson–Golabi–Behmel syndrome: identification of loss-of-function mutations in the GPC3 gene. Hum Mol Genet 2000; 9: 1321–1328.
31. Lindsay S, Ireland M, O'Brien O, et al. Large scale deletions in the GPC3 gene may account for a minority of cases of Simpson–Golabi–Behmel syndrome. J Med Genet 1997; 34: 480–483.
32. LeClair EE, Mui SR, Huang A, et al. Craniofacial skeletal defects of adult zebrafish gypican 4 (knypek) mutants. Dev Dyn 2009; 238: 2550–2563.
33. Hiraoka S, Furuichi T, Nishimura G, et al. Nucleotide–sugar transporter SLC35D1 is critical to chondroitin sulfate synthesis in cartilage and skeletal development in mouse and human. Nat Med 2007; 13: 1363–1367.
34. Rossi A, Superti-Furga A. Mutations in the diastrophic dysplasia sulfate transporter (DTDST) gene (SLC26A2): 22 novel mutations, mutation review, associated skeletal phenotypes, and diagnostic relevance. Hum Mutat 2001; 17: 159–171.
35. Faiyaz-Ul-Haque M, Zaidi SHE, King LM, et al. Fine mapping of the X-linked split-hand/split-foot malformation (SHFM2) locus to a 5.1-Mb region on Xq26.3 and analysis of candidate genes. Clin Genet 2005; 67: 93–97.

Supporting Information

Supporting Information: Table S1. Summary of bone ossification in WT and homozygous mutant fish at 5 days post-fertilization.

name	AB	*dak*	*pic*	*kny*	*hi307*	*hi954*
affected gene	WT	*ext2*	*papst1*	*gpc4*	*b3gat3*	*uxs1*
Maxilla	nd	nd	nd	nd	nd	nd
Dentary	nd	nd	nd	nd	nd	nd
Entopterygoid	nd	nd	nd	nd	+	nd
Parasphenoid	+	nd	+/-	+	+	+
Branchiostegal rays	+	nd	nd	+	+	+
Opercle	+	+	+	+	+	+
Cleithrum	+	+	+	+	+	+
Retroarticular	nd	nd	nd	nd	nd	nd
Quadrate	nd	nd	nd	nd	nd	nd
Ceratohyal	nd	nd	nd	nd	nd	nd
Hyomandibula	nd	nd	nd	nd	+	nd
5th ceratobranchial	+	+	nd	+	+	+
Pharyngeal teeth	+	+	+/-	+	+	+
Notochord	+	+/-	nd	+	+/-	+/-

+, calcification detected by staining with alizarin red; +/-, reduced ossification in comparison to WT and siblings; nd, staining not detected; light grey, dermal bones; medium grey, cartilage bones; dark grey, other bones.



Supporting Information: Figure S1. Examples of the fibrillar organization found in the extracellular matrix of WT zebrafish at 5 days post-fertilization. Between the well-stacked chondrocytes, the fibres are mostly orientated parallel to the longitudinal axis of the cartilage elements (aligned fibres) (A), whereas presumptively intercalating chondrocytes are surrounded by a radially running collagen network (radial fibres) (B).

Chapter 4

Heparan sulphate upholds osteoblastic lineage

Malgorzata I. Wiweger, Carlos E. de Andrea,
Karel Scheepstra, Zhe Zhao and
Pancras C.W. Hogendoorn

Abstract

Zebrafish (*Danio rerio*) *dackel* (*dak*) mutant has cartilage defects that strongly resemble those seen in patients with multiple osteochondromas. Osteochondromas are the most common benign cartilage-capped bone tumours caused by mutations in the *EXT1* or *EXT2*. Mutations in the *EXT* genes prohibit polymerisation of heparan sulphate, molecules that are crucial control receptor-ligand binding of many growth factors. In the zebrafish *dackel* (*dak*) mutant, heparan sulphate deficiency caused by a mutation in the *ext2* gene, affects cartilage organization and bone development. Interestingly, dermal bones (intra-membranous bones in mammals) that do not require a cartilage template are also malformed and often lost in the homozygote mutant. Normal expression of *runx2* and impaired expression of *osterix* indicate that heparan sulphate is required by osteoblast precursors for further differentiation towards mature osteoblasts. Here, we showed that loss of bones in *ext2*$^{-/-}$ coincided with abnormally high lipid deposition. The presence of one functional copy of the *ext2* gene is sufficient for the maintenance of normal osteoblast and adipocyte differentiation. Our findings indicate that heparan sulphate possibly controls mesenchymal differentiation towards osteoblastic lineage.

Keywords: Zebrafish, exostosin, heparan sulphate, bone, fat, mesenchymal precursor, osteoblastic lineage, osteochondroma, exostosis

Introduction

Heparan sulphates are glycosaminoglycans, linear heavily sulphated polysaccharides that are present in all type of cells [1]. Heparan sulphate glycosaminoglycans once attached onto a protein form heparan sulphate proteoglycans. The biosynthesis of heparan sulphate takes place in Golgi apparatus and in the endoplasmic reticulum and the elongation of glycosaminoglycans chain is maintained by type II glycosyltransferases encoded by *EXOSTOSIN* genes, *EXT1* and *EXT2* genes [2;3]. Heparan sulphates affect receptor-ligand binding and shape gradients of various signalling molecules [1]. In this way heparan sulphate alone or as a part of proteoglycans regulates various signalling pathways and controlled by them cellular and developmental processes, such as endochondral bone formation and hepatocyte clearance.

During endochondral bone development, terminally differentiated chondrocytes secrete a specialized cartilaginous extracellular matrix rich in type X collagen, which is used by osteoblasts to build a new bone [4]. Osteoblasts originate from mesenchymal stem cells. Mesenchymal stem cells can also differentiate into a variety of other cell types, including e.g. chondrocytes, myocytes and adipocytes. Differentiation into osteoblast lineage is under a strict control of *RUNX2* and *OSTERIX*. Additionally, Wingless (Wnt), bone morphogenic protein (BMP), peroxisome proliferator-activated receptor (PPAR-γ) and hedgehog (HH) signalling that are known to affect bones by triggering a switch between bone and other lineages.

Loss of osterix-expressing domain in all cartilage bones (endochondral bones in mammals) and in some dermal bones (intramembranous bones in mammals) were observed in the zebrafish *ext2*$^{-/-}$ mutant [5;6]. In this study we investigated whether the loss of bones in the *ext2*$^{-/-}$ mutant can be explained by a change in the fate of osteoblastic precursors. We found abnormally high lipid deposition in the *ext2*$^{-/-}$ mutant indicating that *ext2* gene and thereby heparan sulphate is involved in bone-to-fat switch during mesenchymal differentiation. Inhibition of PPAR-γ or stimulation of HH was reducing lipid deposition in the *ext2*$^{-/-}$ fish and partially rescued ossification.

Materials and methods

Animals and histology

Zebrafish (*Danio rerio H.*) golden and AB strains were used as wild type (WT). Homozygote *dackel* (*dak*, *ext2*^{to273b}), *knypek* (*kny*, *gpc*^{V348}), *pinscher* (*pic*, *slc35b2*^{14MX}), *hi307* (β*3gat3*^{hi307}), *hi954* (*uxs1*^{hi954}) and *hi1002* (*csnk1α1*^{hi1002}) mutants were obtain in obtained in natural crosses and staged according to Kimmel et al. [7]. The *dak* mutant was also maintained in *Tg* (*osterix:nuGFP*) background (8). Unless stated otherwise, embryos were anesthetized in tricane, fixed in 4% paraformaldehyde, dehydrated in a series of Methanol dilutions and stored at -20C.

Cartilage and bones were stained with Alcian blue and alizarin red respectively as described previously [5]. Lipid deposits were visualized with Oil Red O as described by Li and co-authors [9].

In situ hybridization and immunohistochemistry

Whole mount mRNA in situ was done accordingly to Thiesse 2008 [10] using: *collagen 10* [11], *osterix* [5], *cebpa* and *ppar-γ* rybo-probes. Whole mount immunostaining on zebrafish embryos was performed as described previously [5] using as a primary antibodies from the Developmental Studies Hybridoma Bank: anti-MF-20 for muscles and collagen II for cartilage, both in dilution of 1:250. For light microscopy, the anti-Digoxigenin-AP, Fab fragments (Roche) at 1:4000 or anti-mouse AP (Sigma) at 1:500 followed by BCIP/NBT (Sigma) were used to detect the signal. For confocal microscopy, Alexa 488 and 546 were used as the secondary antibody in dilution 1:200. Each experiment was repeated at least three times with the same results.

Quantitative RT-PCR

The expression level of chosen bone-specific and adipocyte-specific marker was determined by quantitative RT-PCR. Quantitative PCR was performed as previously described [12] using on-column DNase I digestion. The absence of genomic contamination in cDNAs was confirmed by PCR. The sequence of the qPCR primers are listed in Table 1. Unless stated otherwise, the primers were designed as such that the amplicons were 100-150 bp, spanning at least one intron to avoid amplification from possible genomic DNA contaminant in the template. All the samples were examined in triplicate, and the expression of each marker was normalized to *slc25a5* level.

Results

The importance of the heparan sulphate for preosteoblast differentiation

The presence of defects in the development of bones in the *ext2*$^{-/-}$ larvae was describe by Clément et al in 2008 (Figure 1A) [5]. In order to pinpoint at which step bone formation is affected and by which mechanism, we examined the expression of various bone molecular markers in the *ext2*$^{-/-}$ and compare it with WT fish. During bone development in zebrafish, the sequence of molecular events is similar to this seen in mammals i.e. the expression of *runx2* precedes *osterix* and it is finally followed by *osteocalcin* and *osteopontin*. Real time PCR revealed that in the homozygote *ext2* mutants, the expression level of early osteoblasts markers such as *runx2a* and *runx2b* was similar to the wild type levels (Figure 1B). However, the reduced expression of *osterix*, *collagen1a1*, *osteopontin* and *osteocalcin* in the *ext2*$^{-/-}$ fish (Figure 1B) indicated that heparan sulphate is needed by osteochondroprogenitors/ preosteoblasts to follow their commitment toward osteoblastic lineage.

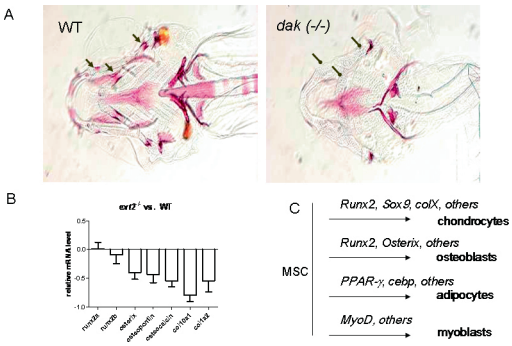


Figure 1. Bone development is impaired in *ext2*$^{-/-}$ fish. A, Alizarin red stain for ossification in the craniofacial skeleton at 6 dpf. B, Expression levels of bone markers in the homozygote *ext2* mutants vs. WT at 5 dpf. The results represent an average from four single embryos. Expression was normalized against *slc25a5*. C, Schematic representation of lineages into which mesenchymal stem cells can differentiate. Scale = 0.1 mm.

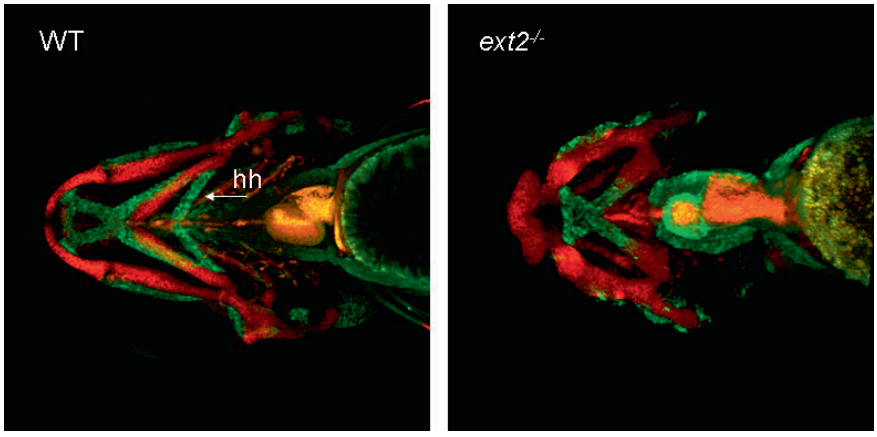


Figure 2. Lack of bones is not compensated by the development of ectopic craniofacial muscles. A, Musco-skeletal phenotype in fish at 4 dpf; whole mount immunolocalisation using MF-20 antibody for muscles (green) and collagen II for cartilage (red) indicates that the overall musculature of mutant fish resembled this from WT, with exception for hh muscle that seems to be misplaced around the heart area in *ext2*$^{-/-}$ fish.

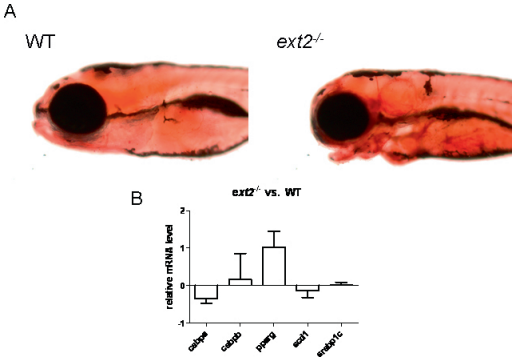


Figure 3. The expression levels lipogenic/adipogenic markers confirms that decreased bone formation coincided with increased lipid metabolism in the *ext2*$^{-/-}$ fish. A, Oil red O stain for ossification in the craniofacial skeleton at 6 dpf. B, the amount of transcripts was determined by quantitative PCR and normalised to *slc25a5* level. Primer sequences are given in Table 1. Means from five single fish are shown.

Bone loss coincides with the elevated levels of lipids in the ext2$^{-/-}$ fish

From mammal systems it is known that osteoblasts originate from mesenchymal precursors, but mesenchymal precursors can also differentiate toward other lineages such as: i) chondroblasts, ii) myoblasts and/or iii) adipocytes (Figure 1C). There why, we checked if diminished bone development in *ext2*$^{-/-}$ coincides with gain of other lineage(s).

Early differentiation of chondrocytes is known to be unaffected in the *ext2*$^{-/-}$ craniofacial cartilage [5]. However, the terminal differentiation is clearly impaired in the *ext2*$^{-/-}$ chondrocytes as indicated by reduced expression of collagen X [5].

The whole mount immunohistology with MF-20, showed that muscles in *ext2*$^{-/-}$ fish were shorter and more spaced out as they fitted the misshapen cartilaginous skeleton, but the overall musculature of mutant fish resembled this from WT (Figure 2) with exception for hh muscle that was apparently absent in *ext2*$^{-/-}$ fish (Figure 2, Table 2). Possibly, this muscle is misplaced all around the heart area.

Oil red O, a stain for neutral triglycerides, lipids and some lipoproteins, highlighted blood vessels, heart, tectum, guts, swim bladder and the remains of yolk in wild type and the *ext2* mutant fish (Figure 3A). However, in the *ext2*$^{-/-}$ fish, the staining was more intense and additional patches of lipid deposits were visible (Figure 3A). Abnormally high lipid accumulation was observed especially in the head, partially but not explicitly at the position of missing bones (Figure 3A). The expression was not restricted to any cell, but first adipocytes are known to develop in zebrafish only by 8 dpf [23]. Stronger Oil Red O stain in the *ext2*$^{-/-}$ fish coincided with over two fold over-expression on *ppar-γ* and normal level of *cebp* (Figure 3B) suggesting that general lipid metabolism is up-regulated in the *dak* homozygote mutant.

Abnormal lipid deposition is specific to the ext2-/- fish

The loss of bones coinciding with enhanced lipid deposition that we observed in the *dak* mutant was specific to the *ext2*$^{-/-}$ fish. For example, *pinscher* (*pic*) which in the result of mutation in a PAPS transporter fails to sulphate different molecules (including heparan sulphate) has even more strong bone phenotype then *dak* [5;6] but loss of bones in *pic* did not coincided with abnormal lipid deposition (data not shown). Oil Red O staining also did not show any alteration in the lipid deposition in *hi307* and *hi954*, two proteoglycan-deficient mutants with mild bone phenotype [6]. Those *hi*-mutants are mutated in β*3gat3* and *uxs1* respectively, and lack various proteoglycans including heparan sulphate. Also mutant without defects in proteoglycans such as *hi1002* which has a mutation in *casein kinase 1 alpha1a* having severely reduced bones did not deposit more lipids (data not shown). The specificity the phenotype in the dak mutant may suggests new function of the *ext2* in controlling lipid metabolism.

Table 1. Sequences of primers used for quantitative PCR. Unless stated otherwise, the primers were designed to construct amplicons of 100-150 bp, spanning at least one exon-exon junction to avoid errors due to possible genomic DNA contamination in the template. A, adipocyte-specific gene; B, bone specific gene; C, cartilage specific gene; HK, house keeping gene; #, gene with one exon, gDNA contamination in the template was checked with col1a2 primers.

Primer name	Sequence 5`→3`	
adopql qPCR F1	AACCTGGAAGAGATGGCAGA	A
adopql qPCR R1	CAGGAAAGCCTCTTGGTCCT	A
cebpa qPCR F1	CACAACAGCTCCAAGCAAGA	A#
cebpa qPCR R1	AATCCATGTAGCCGTTCAGG	A#
cebpb qPCR F1	TGTTCAGCCCGGACTTTATG	A#
cebpb qPCR R1	AGTCTGGTACGGCAGGTACG	A#
col1a2 qPCR F2	CTGGCATGAAGGGACACAG	B
col1a2 qPCR R2	GGGGTTCCATTTGATCCAG	B
col10a1 qPCR F2	CCTGTCTGGCTCATACCACA	B
col10a1 qPCR R2	AAGGCCACCAGGAGAAGAAG	B
osteocalcin qPCR F1	TGAGTGCTGCAGAATCTCCTAA	B
osteocalcin qPCR R1	GTCAGGTCTCCAGGTGCAGT	B
osteopontin qPCR F1	TGAAACAGATGAGAAGGAAGAGG	B
osteopontin qPCR R1	GGGTAGCCCAAACTGTCTCC	B
osterix qPCR F2	GCGTCGATTCTGGAGGAG	B
osterix qPCR R2	AATCTCGGACTGGACTGGTG	B
ppar-γ qPCR F1	GGTTTCATTACGGCGTTCAC	A
ppar-γ qPCR R1	TGCGGCTCTTCTTGTGTATG	A
runx2a qPCR F1	AACTTTCTGTGCTCGGTGCT	B, C
runx2a qPCR R1	GTCATTTCCAGCCATTACCG	B, C
runx2b qPCR F2	CAAACACCCAGACCCTCACT	B, C
runx2b qPCR R2	GTATGACCATGGTGGGGAAG	B, C
scd1 qPCR F1	GTGGCGAAATGTCATTCTGA	A
scd1 qPCR R1	CCATACACGAAACACGCAAA	A
slc25a5 qPCR F1	CCCCCATTGAGAGAGTCAAA	HK
slc25a5 qPCR R1	CCTCTCCAGAACGACAGGAA	HK
sox9a qPCR F1	GGAGCTCAGCAAAACTCTGG	C
sox9a qPCR R1	AGTCGGGGTGATCTTTCTTG	C
srebp1c qPCR F1	CCCCCAGCAGACTCTCTACA	A
srebp1c qPCR R1	CGACAGACTCTGGATCGTCA	A

Discussion

Impairment in chondrocyte terminal differentiation in *Ext* mutants suggests that a defect in the replacement of cartilage template by bone can be expected in the cartilaginous cap of multiple osteochondromas. Indeed, osteopontin has been shown to be down-regulated in osteochondromas [13]. Furthermore, the loss of osterix-expressing domain in all cartilage bones (endochondral bones in mammals) and in some dermal bones (intramembranous bones in mammals) have been reported in zebrafish *ext2*$^{-/-}$ mutant [5].

The *ext2*$^{-/-}$ larvae at 5 dpf have 90% reduction in the level of heparan sulphate and that deficiency affects cartilage organization and bone development [5;14]. The presence of one functional copy of the *ext2* gene seems to be sufficient for the maintenance of normal differentiation of chondrocytes and osteoblasts. Also the *Ext2* heterozygote mice were shown to have normal ColX expression as indicated by the intensity and localisation of the mRNA transcript after *in situ* hybridisation [15]. However, the *Ext1* heterozygote mice had reduced ColX expression in the growth plate as measured by quantitative RT-PCR [16]. It is not known if different methods used for evaluation of the terminal hypertrophy in mice account for the different results. However, it is more likely that a mutation in *EXT1* might cause more severe reduction of the heparan sulphate level then mutation in *EXT2*.

Table 2. Cranial muscles in the zebrafish head at 4 dpf. Muscles were scored based on the MF-20 immuno staining of myosin. Muscles were analysed under stereomicroscope as descrived in (26) and scores as present (x) or absent (a). Asterixs indicate muscles that were reduced to a small dot. Minimum seven fish were analysed in each group. B, Branchail arches; D, Dorsal posterior; E, extraocular; H, Hyoid arch; and M, Manibular arch.

Region	Muscle		wild type	*ext2* $^{(-/-)}$
M	intermandibularis anterior	ima	**x**	**x**
H	interhyoideus	ih	**x**	**x**
B	tranversus ventralis	tv	**x**	**x**
M	intermandibularis posterior	imp	**x**	**x**
H	hyohyoideus	hh	**x**	**a**
B	rectus ventralis	rv	**x**	**x**
B	rectus communis	rc	**x**	**x**
M	adductor mandibulae	am	**x**	**x**
M	levator arcus palatini	lap	**x**	**x**
M	dilator operculi	do	**x**	**x***
H	adductor hyoideus	ah	**x**	**x**

We have previously shown that there is a total loss of cartilage bones and partial loss of dermal bones in the ext2-/- fish [5;6]. The reduced expression of osterix and collagen X in the *ext2*$^{-/-}$ fish can be observed from 96 hpf. As this defect is getting more pronounced with time, it is highly unlikely that the impaired expression of bone markers could be only caused by the developmental delay in the *ext2*$^{-/-}$ fish. *Osterix* mRNA expression is restricted to the immature chondro/osteoprogenitor cells and mature osteoblasts, excluding hypertrophic chondrocytes [18]. Similarly to the *ext2*$^{-/-}$ fish, *Osterix*-null mice do not form bones as they are unable to differentiate preosteoblasts to osteoblasts [19]. Moreover, it was shown that cells treated with dexamethasone, an *Osterix* inhibitor, choose adipogenic instead of osteoblast lineage, whereas PPAR-γ -null mice have increased osteoblast number [20] Importantly, fat in bone marrow might not only suppress osteoblastogenesis, but might promote bone resorption because marrow adipocytes, much like fat cells elsewhere, secrete inflammatory cytokines capable of recruiting osteoclasts. Unfortunately, we were not able to test this hypothesis as, in zebrafish, first osteoclasts develop by 16 dpf, hence after the time of premature death of *ext2*$^{-/-}$ fish.

Normal expression of *runx2* and impaired expression of *osterix* that was observed in the *ext2*$^{-/-}$ fish indicates that heparan sulphate is required by osteoblast precursors for further differentiation towards osteoblastic lineage. Mesenchymal precursors can differentiate towards osteoblasts, but they also can become chondrocytes, adipocytes, myoblasts, fibroblasts and epithelial cells. Heparan sulphate deficiency does not affect early chondrocyte differentiation [5], but it affects differentiation of other lineages. Recently, it has been shown that embryonic stem cells derived from the *Ext1*$^{-/-}$ mice are unable to differentiate into hematopoietic lineages [21]. Our study shows that heparan sulphate maintains osteoblast differentiation by inhibiting adipocyte lineage in the *ext2*$^{-/-}$ fish.

In five-days-old zebrafish lipids can be observed in the remains of yolk as well as in the brain, heart, vasculature, liver, pancreas, gall and swim bladders [22]. Abnormal accumulation of lipids in the *ext2*$^{-/-}$ fish was not related to any cell/adipocytes, but filled spaces taken by fluids. Zebrafish adipocytes start to be formed by 8 dpf and only upon feeding [23]. Fatty acids, when not stored in adipocytes they accumulate into the circulation [24]. *ppar-γ* and *fabp1la* are being used as pre-adipocyte markers, however since they have more broad expression (*ppar-γ* is also present in the liver, intestines, kidney, skin, gills and skeletal muscles of juvenile zebrafish) [25]; whereas the *fabp1la* gene can be found in caudal hematopoietic tissue [23] they rather can be used as readout of lipid metabolism.

Our data indicate that heparan sulphate act as regulator of osteoblastogenesis by inhibiting PPAR-γ signalling and show that heparan sulphate has multiple functions during endochondral bone development. First of all, heparan sulphate is required for the terminal differentiation of the cartilaginous template and consecutive formation of a scaffold that needed for further bone development. Secondly, heparan sulphate maintains osteoblast

differentiation in a *runx2* independent process. It still remains to be established how exactly heparan sulphate controls the "bone-to-fat" switch and if *PPAR-γ* signalling targeted for therapy for osteochondroma.

Acknowledgments

We thank Marcel Winter the assistance with RT-PCR and and Prof. Schulte-Merker from Hubrecht Institute, Utrecht, the Netherlands for the Tg(osterix:nuGFP) zebrafish line. This work was supported by the European network of excellence EuroBoNeT (http://www.eurobonet.eu) [grant number 018814 (LSHC-CT-2006-018814)].

References

1. Hacker U, Nybakken K, Perrimon N. Heparan sulphate proteoglycans: the sweet side of development. Nat Rev Mol Cell Biol 2005;6:530-41.
2. McCormick C, Duncan G, Goutsos KT, Tufaro F. The putative tumor suppressors EXT1 and EXT2 form a stable complex that accumulates in the golgi apparatus and catalyzes the synthesis of heparan sulfate. Proc Natl Acad Sci USA 2000;97:668-73.
3. Busse M, Feta A, Presto J, Wilen M, Gronning M, Kjellen L, et al. Contribution of EXT1, EXT2, and EXTL3 to heparan sulfate chain elongation. J Biol Chem 2007 9;282:32802-10.
4. Kronenberg HM. Developmental regulation of the growth plate. Nature 2003 May 15;423:332-6.
5. Clément A, Wiweger M, von der Hardt S., Rusch MA, Selleck SB, Chien CB, et al. Regulation of zebrafish skeletogenesis by ext2/dackel and papst1/pinscher. PLoS Genet 2008;4:e1000136.
6. Wiweger MI, Avramut C, de Andrea CE, Prins FA, Koster JG, Ravellli R., et al. Cartilage ultrastructure in proteoglycan-deficient zebrafish mutants brings to light new candidate genes for human skeletal disorders. J Pathol 2011;223:531-42.
7. Kimmel CB, Ballard WW, Kimmel SR, Ullmann B, Schilling TF. Stages of embryonic development of the zebrafish. Dev Dyn 1995 Jul;203:253-310.
8. Spoorendonk KM, Peterson-Maduro J, Renn J, Trowe T, Kranenbarg S, Winkler C, et al. Retinoic acid and Cyp26b1 are critical regulators of osteogenesis in the axial skeleton. Development 2008;135:3765-74.
9. Li N, Felber K, Elks P, Croucher P, Roehl HH. Tracking gene expression during zebrafish osteoblast differentiation. Dev Dyn 2009;238:459-66.
10. Thisse C, Thisse B. High-resolution in situ hybridization to whole-mount zebrafish embryos. Nat Protoc 2008;3:59-69.

11. Avaron F, Hoffman L, Guay D, Akimenko MA. Characterization of two new zebrafish members of the hedgehog family: atypical expression of a zebrafish indian hedgehog gene in skeletal elements of both endochondral and dermal origins. Dev Dyn 2006;2352:478-89.
12. de Jong M, Rauwerda H, Bruning O, Verkooijen J, Spaink HP, Breit TM. RNA isolation method for single embryo transcriptome analysis in zebrafish. BMC Res Notes 2010;3:73.
13. Hameetman L, Rozeman LB, Lombaerts M, Oosting J, Taminiau AHM, Cleton-Jansen AM, et al. Peripheral chondrosarcoma progression is accompanied by decreased Indian Hedgehog (IHH) signalling. J Pathol 2006;209:501-11.
14. Lee J-S, von der HS, Rusch MA, Stringer SE, Stickney HL, Talbot WS, et al. Axon sorting in the optic tract requires HSPG synthesis by ext2 (dackel) and extl3 (boxer). Neuron 2004;44:947-60.
15. Stickens D, Zak BM, Rougier N, Esko JD, Werb Z. Mice deficient in Ext2 lack heparan sulfate and develop exostoses. Development 2005;132:5055-68.
16. Hilton MJ, Gutierrez L, Martinez DA, Wells DE. EXT1 regulates chondrocyte proliferation and differentiation during endochondral bone development. Bone 2005;36:379-86.
17. de Andrea CE, Prins FA, Wiweger MI, Hogendoorn PCW. Growth Plate Regulation and Osteochondroma Formation: Insights from Tracing Proteoglycans in Zebrafish Models and Human Cartilage. J Pathol 2011;224:160-8.
18. Kaback LA, Soung dY, Naik A, Smith N, Schwarz EM, O'Keefe RJ, et al. Osterix/Sp7 regulates mesenchymal stem cell mediated endochondral ossification. J Cell Physiol 2008;214:173-82.
19. Akiyama H, Kim JE, Nakashima K, Balmes G, Iwai N, Deng JM, et al. Osteo-chondroprogenitor cells are derived from Sox9 expressing precursors. Proc Natl Acad Sci U S A 2005;102:14665-70.
20. Mikami Y, Lee M, Irie S, Honda MJ. Dexamethasone modulates osteogenesis and adipogenesis with regulation of osterix expression in rat calvaria-derived cells. J Cell Physiol 2011;226:739-48.
21. Holley RJ, Pickford CE, Rushton G, Lacaud G, Gallagher JT, Kouskoff V, et al. Influencing Hematopoietic Differentiation of Mouse Embryonic Stem Cells using Soluble Heparin and Heparan Sulfate Saccharides. J Biol Chem 2011;286:6241-52.
22. Holtta-Vuori M, Salo VT, Nyberg L, Brackmann C, Enejder A, Panula P, et al. Zebrafish: gaining popularity in lipid research. Biochem J 201015;429:235-42.
23. Flynn EJ, III, Trent CM, Rawls JF. Ontogeny and nutritional control of adipogenesis in zebrafish (Danio rerio). J Lipid Res 2009;50:1641-52.

24. Cousin W, Fontaine C, Dani C, Peraldi P. Hedgehog and adipogenesis: fat and fiction. Biochimie 2007;89:1447-53.
25. Ibabe A, Herrero A, Cajaraville MP. Modulation of peroxisome proliferator-activated receptors (PPARs) by PPAR(alpha)- and PPAR(gamma)-specific ligands and by 17beta-estradiol in isolated zebrafish hepatocytes.
Toxicol In Vitro 2005;19(6):725-35.
26. Schilling TF, Kimmel CB. Musculoskeletal patterning in the pharyngeal segments of the zebrafish embryo. Development 1997;124:2945-60.

Chapter 5

Growth plate regulation and osteochondroma formation: insights from tracing proteoglycans in zebrafish models and human cartilage

Carlos E de Andrea, Frans A Prins,
Malgorzata I Wiweger and Pancras CW Hogendoorn
Journal of Pathology 2011; 224:160-168

Abstract

Proteoglycans are secreted into the extracellular matrix of virtually all cell types and function in several cellular processes. They consist of a core protein onto which glycosaminoglycans (e.g., heparan or chondroitin sulphates), are attached. Proteoglycans are important modulators of gradient formation and signal transduction. Impaired biosynthesis of heparan sulphate glycosaminoglycans causes osteochondroma, the most common bone tumour to occur during adolescence. Cytochemical staining with positively charged dyes (e.g., polyethyleneimine—PEI) allows, visualisation of proteoglycans and provides a detailed description of how proteoglycans are distributed throughout the cartilage matrix. PEI staining was studied by electron and reflection contrast microscopy in human growth plates, osteochondromas and five different proteoglycan-deficient zebrafish mutants displaying one of the following skeletal phenotypes: *dackel* (*dak/ext2*), lacking heparan sulphate and identified as a model for human multiple osteochondromas; *hi307* (β*3gat3*), deficient for most glycosaminoglycans; *pinscher* (*pic/slc35b2*), presenting with defective sulphation of glycosaminoglycans; *hi954* (*uxs1*), lacking most glycosaminoglycans; and *knypek* (*kny/gpc4*), missing the protein core of the glypican-4 proteoglycan. The panel of genetically well-characterized proteoglycan-deficient zebrafish mutants serves as a convincing and comprehensive study model to investigate proteoglycan distribution and the relation of this distribution to the model mutation status. They also provide insight into the distributions and gradients that can be expected in the human homologue. Human growth plate, wild-type zebrafish and fish mutants with mild proteoglycan defects (*hi307* and *kny*) displayed proteoglycans distributed in a gradient throughout the matrix. Although the mutants *pic* and *hi954*, which had severely impaired proteoglycan biosynthesis, showed no PEI staining, *dak* mutants demonstrated reduced PEI staining and no gradient formation. Most chondrocytes from human osteochondromas showed normal PEI staining. However, approximately 10% of tumour chondrocytes were similar to those found in the *dak* mutant (e.g., lack of PEI gradients). The cells in the reduced PEI-stained areas are likely associated with loss-of-function mutations in the *EXT* genes, and they might contribute to tumour initiation by disrupting the gradients.

Keywords: growth plate; osteochondroma; proteoglycans; heparan sulphate; gradients; exostosis; zebrafish; bone tumours

Introduction

Bone formation and development are governed by gradients of signalling molecules, which trigger specific cell responses. Proteoglycans are important modulators of gradient formation and signal transduction [1,2]. They are found in the extracellular matrix and attached to the cell membrane in virtually all types of tissue [2]. Proteoglycans are composed of highly diverse core proteins to which one or more glycosaminoglycans chains are covalently linked at specific sites (Figure 1). Glycosaminoglycans are unbranched polysaccharides that consist of a backbone of repeating disaccharide units, often containing negatively charged sulphate groups [3]. Some proteoglycans have only one glycosaminoglycan chain (e.g., decorin), whereas others have more than one hundred chains (e.g., aggrecan). For example, heparan sulphate proteoglycans are composed of diverse core proteins onto which two or three heparan sulphate glycosaminoglycan chains are attached.

Bone lengthening occurs in the epiphyseal growth plate, a specialised cartilage structure found at the ends of long bones. Bone elongation is achieved through successive rounds of growth plate chondrocyte divisions, matrix secretion, hypertrophy, apoptosis, calcification and replacement with mineralised. Growth plate regulation requires signalling molecules, such as members of the Wingless (Wnt/Wg), Hedgehog (Hh), Transforming growth factor-β (TGFβ), Bone morphogenetic protein (BMP) and fibroblast growth factor (FGF) families [4]. Many of these molecules bind proteoglycans, heparan sulphate proteoglycans in particular. Proteoglycans influence the distribution of these signalling molecules in the extracellular matrix, their receptor-binding affinity and the responses of cells to secreted protein factors [2]. Although studies have shown that several signal transduction pathways rely on gradients established by the proteoglycan distribution [5,6], it is still unclear how these gradients are formed and shaped.

Mutations affecting the biosynthesis of either proteoglycan or glycosaminoglycan are the cause of several human disorders. Loss-of-function mutations in the *EXT1* (8q24.1) and *EXT2* (11p11) tumour suppressor genes have been linked to osteochondromas [7–10]. *EXT1* and *EXT2* encode type II transmembrane glycosyltransferases 11, which localise to the endoplasmic reticulum and Golgi complex. EXT1 and EXT2 form an oligomeric complex that catalyses the elongation of heparan sulphate glycosaminoglycan chains [3, 12]. Therefore, the impairment of heparan sulphate glycosaminoglycan chain elongation is thought to be the initiating event for osteochondroma formation.

Osteochondromas are the most common benign bone tumours of adolescence [13]. They are characterised by sporadic (non-familial/solitary) or multiple (hereditary) cartilage-capped bony projections from the metaphyses of endochondral bones adjacent to the growth plate and develop during skeletal growth [14]. Multiple osteochondromas, previously called hereditary multiple exostoses, result from an autosomal dominant disorder, with a prevalence of 1 in 18 000 [15]. Patients with multiple osteochondromas are short in

stature and have bowed bones that can restrict movement and ultimately result in joint dislocation [15]. In contrast, patients with sporadic lesions may develop symptoms on the affected side. Sporadic and multiple lesions are morphologically indistinguishable [14].

Model systems have provided significant insight into osteochondroma pathogenesis and show a detailed picture of the role of heparan sulphate proteoglycans in tumour formation. Reduced EXT1 and EXT2 co-polymerase activity results in the production of short heparan sulphate chains [16]. Short chains decrease fibroblast growth factor 2 signal transduction, which may impair chondrocyte differentiation. The zebrafish *dackel* (*dak/ext2*) mutant has a cartilage phenotype that strongly resembles that of human osteochondromas. *dak* cells transplanted into wild-type zebrafish cartilage behave normally when juxtaposed with wild-type cells and abnormally when implanted at the edge of cartilage [17]; these results indicate that *ext*-null cells are not autonomous and that the secretion of heparan sulphate proteoglycans from the neighbouring wild-type cells is able to rescue the mutant cells within the chondrocyte stack. However, at the edge of the cartilage elements, where the level of heparan sulphate proteoglycans is decreased, *ext*-null chondrocytes start to form outgrowths [17]. These outgrowths suggest that a pool of mutant chondrocytes at a specific location in the growth plate is required to escape the proteoglycan gradient generated by neighbouring cells and give rise to osteochondromas. Recent studies using Cre recombinase drivers to generate *Ext1* knockouts in mouse skeletal cells show that somatic loss of the wild-type *Ext1* allele is needed for osteochondroma formation. Loss of heterozygosity has also been detected in a subset of human sporadic and multiple osteochondromas [8,10,18, 19]. Interestingly, during tumour formation in mice, wild-type chondrocytes are recruited from the growth plate or the neighbouring tissue to generate a non-clonal population of cells [20,21]. Given that cells require a certain threshold level and distribution of heparan sulphate proteoglycans to grow properly, the wild-type chondrocytes may create an environment conducive for *EXT1*$^{-/-}$ cells to proliferate and form a tumour [22]. We previously reported that growth plate-like polarity was retained in subpopulations of osteochondroma cells, which may also indicate the presence of a heterogeneous cell composition in human osteochondromas [23].

Despite all of the progress in the understanding of the pathogenesis of osteochondroma, many questions remain unanswered: (a) how do the null-*EXT1* cells give rise to an osteochondroma; and (b) what is the proteoglycan distribution in osteochondromas that are present within the cartilaginous matrix? Proteoglycans can be localised with an electron microscope using positively charged, electron-dense dyes. Polyethyleneimine (PEI) is a well-described cationic dye that binds to anionic sites, allowing visualisation and quantification of negatively charged sites of proteoglycans in cartilage and other tissues at the ultrastructural level [24–27]. Using electron and reflection contrast microscopy, we analysed the overall distribution of proteoglycan anionic sites in human growth plates,

osteochondromas and five different proteoglycan-deficient zebrafish mutants displaying a skeletal phenotype. The panel of genetically well-characterised proteoglycan-deficient zebrafish mutants served as a convincing and comprehensive study model to investigate proteoglycan distribution and provided insights into the distribution and gradients that could be expected in the human homologue. Our results provide clues to understand the biology of the growth plate and the pathogenic mechanism of osteochondroma by demonstrating the presence of the proteoglycan gradient through the cartilage matrix and its focal loss in tumours.

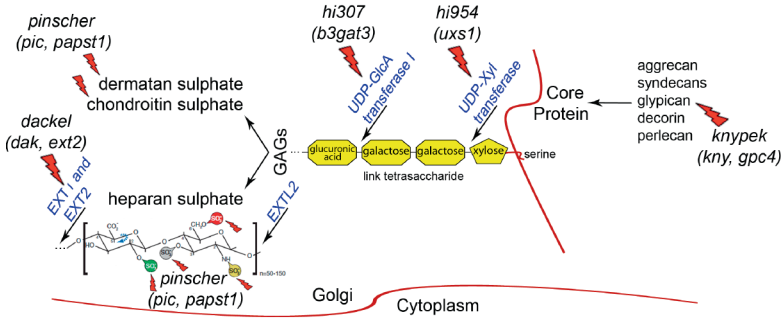


Figure 1. Schematic representation of proteoglycan biosynthesis, showing the specific steps in which the five homozygous zebrafish mutants (italics) are affected.

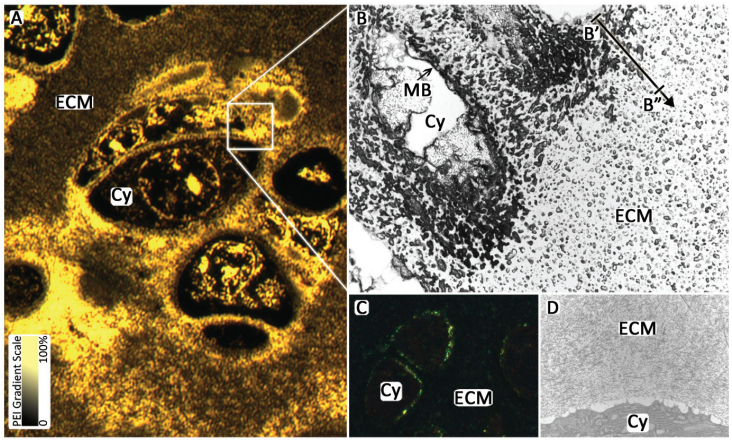


Figure 2. Spatial distribution of polyethyleneimine (PEI) in the normal human growth plate. The distribution of anionic sites by PEI was evaluated by reflection contrast (A) and electron microscopy (B). A concentration gradient of electron-dense deposits of PEI (black) is observed as a function of distance through the cartilage (B′ to B″). Negative controls show no PEI-positive structures in either the electron micrographs (C) or the reflection contrast image (D). CY, cytoplasm; MB, cell membrane; ECM, extracellular matrix. Magnifications: (A) × 110; (B) × 10 000; (C) × 100; (D) × 20 000.

Materials and methods

Animals

Zebrafish (*Danio rerio H.*) embryos were obtained by natural crosses and staged in accordance with Kimmel et al. [28]. Wild-type and five null mutants were selected: *dackel* (*dak*), *exostoses (multiple) 2*; *pinscher* (*pic/slc35b2*), *solute carrier family 35, member B2* (previously named *PAPS transporter 1*, *papst1*); *hi307*, β-*1,3-glucuronyltransferase 3*; *hi954*, *UDP-glucuronic acid decarboxylase 1*; and *knypek* (*kny*) *glypican 4*. Zebrafish were raised until 5-days post-fertilization. Each homozygous mutant line has been previously characterised [29]. Prior to these experiments, the fish were anaesthetised in Tricane, and the homozygous mutants were sorted by phenotype.

Human cartilage

Two postnatal growth plates and two osteochondromas were obtained from surgical specimens at the Leiden University Medical Centre. One osteochondroma (L-2999) was a sporadic lesion from a 16 year-old patient. The other (L-2675) was a lesion from a 32 year-old patient with multiple osteochondromas, confirmed in multidisciplinary discussions of the case by the National Bone Tumour Committee according to the Dutch guidelines. The growth plates were from orthopaedic resections for pathological conditions not related to osteochondroma. All samples were handled in a coded fashion, and all procedures were performed according to the ethical guidelines of the Code for Proper Secondary Use of Human Tissue in The Netherlands (Dutch Federation of Medical Scientific Societies).

Tissue preparation

The method of tissue preparation has been described previously [24–26,30]. Anionic sites in zebrafish cartilage, human growth plate and osteochondroma were labelled by tissue incubation in polyethyleneimine (PEI; PEI-600, Polysciences, Warrington, PA, USA), a synthetic polymer that is highly cationic and water-soluble and forms an electron-dense insoluble product upon reaction with osmic acid. Two methods were applied: (a) the PEI pre-embedding method, where PEI incubation precedes tissue fixation; and (b) the PEI post-embedding method, where PEI incubation follows fixation in 2.5% glutaraldehyde in 0.1 m sodium cacodylate buffer, pH 7.4, for 1 h. Freshly collected tissues were incubated with 1% PEI in sodium cacodylate buffer at a pH of 7.4 or 1.0, each for 6 or 12 h, with constant agitation. After incubation, the samples were washed three times in sodium cacodylate buffer and fixed and/or stained with 2% phosphotungstic acid and 1% glutaraldehyde for 1 h. Next, they were washed three times in sodium cacodylate buffer, fixed in 1% osmic acid and embedded in Epon. For the negative controls, the samples were incubated in sodium cacodylate buffer without PEI.

Morphological techniques

Ultrathin sections of zebrafish cartilage, human growth plate and osteochondroma were obtained for each experimental condition and briefly stained with phosphotungstic acid. Two fish were analysed from each line. Sequential sections were placed on glass slides for reflection contrast microscopy or on grids for electron microscopy. The preparations were examined under a Leitz Orthoplan microscope (Leitz, Wetzlar, Germany) equipped for epi-illumination, which was adapted for reflection contrast microscopy as described previously [31]. The slides were examined under a 100× objective lens. A JEOL JEM-1011 electron microscope equipped with a MegaView III digital camera was used for ultrastructural analysis.

Data analysis

For gradient analysis, the electron-dense deposits of PEI were plotted using ImageJ software, version 1.41h (National Institutes of Health, Bethesda, MD, USA). The plot profile represents the intensity of pixels along a line within a selected area in the cartilage, starting from the cell surface and moving to the periphery/neighbouring cell. The x axis shows the distance through the selection and the y axis the average pixel intensity, in which 0 is black and 255 is white.

Results

Distribution of the proteoglycan anionic sites in cartilage

PEI deposition was evaluated by electron and reflection contrast microscopy in zebrafish and human cartilage (Figure 2). Wild-type zebrafish and proteoglycan-deficient mutants were used to determine the optimal conditions for studying the distribution of anionic sites in cartilage and the specificity of binding at the given condition. PEI post-embedding methods showed a virtual absence of stained anionic sites at different pH levels (see Supporting information, Figure S1). In contrast, PEI pre-embedding methods revealed that the decrease in the number of stained anionic sites followed the reduction in the pH level, thereby reflecting the charge-dependent specificity of its binding. The PEI pre-embedding method usually affects the preservation of cell components. However, at pH 7.4, PEI staining provided good cell preservation and excellent contrast within the cartilage matrix. As a result, this condition was used for further studies. Electron-dense deposits were observed throughout the extracellular matrix, and they outlined branched, round to oval, winding structures (Figures 2,3). To confirm the binding of PEI to the anionic sites of the proteoglycans, zebrafish mutants with impaired proteoglycan synthesis were used. PEI-positive structures were found in the extracellular matrix in wild-type fish and in the cartilage of mutant fish that lacked the glypican 4-core protein (*kny/gpc4*) or some glycosaminoglycans (*hi307/b3gat3*). No PEI staining was observed, either in mutants that were unable to add negatively charged sulphate groups to glycosaminoglycans (*pic/slc35b2*) or in ones that lack most of the glycosaminoglycans (*hi954/uxs1*) (Figure 3). The same results were obtained 6 and 12 h

after incubation with PEI. Nuclear staining was present in all fish lines analysed and was most likely due to negatively charged phosphate ions present in the DNA structure [32].

Gradients of proteoglycans in cartilage

PEI-positive aggregates were identified in the cytoplasm and in the extracellular matrix of wild-type zebrafish cartilage. Large and densely packed cytoplasmic aggregates of proteoglycans were found in close contact with the plasma membrane (Figure 3). In the matrix of the wild-type, *kny* (*gpc4*) and *hi307* (β*3gat3*) zebrafish mutants, there was a broader variation in the diameter of the PEI aggregates (Figure 3). Additionally, the aggregates resembled vesicles, which enclosed electron-dense deposits of PEI and were filled in with less densely packed deposits (Figure 3, arrowheads). The plot profile of the electron micrographs shows the gradient formation (Figure 4), in which the diameter of the PEI aggregates decreased with the distance from the cell surface. Although the human growth plate has a more complex organisation compared with fish cartilage, similar PEI distribution patterns were identified (Figure 5). Contrast-reflection images showed that all analysed cells in the growth plate (n = 64) were surrounded by PEI-positive aggregates (Figure 5). Growth plate chondrocytes are classically divided into three distinct zones: resting, proliferating and hypertrophic [23]. No differences between those zones were observed. The plot profiles of the electron micrographs showed gradient formation between columns of chondrocytes in the growth plate (Figure 5, cell–matrix plot profile). However, no gradient was found between cells within a column (Figure 5, cell–cell plot profile).

Reduction in proteoglycan aggregates and no gradient formation in Ext mutant chondrocytes

The homozygous *dak* zebrafish mutant, which has a mutation in the homologue of the human *EXT2* gene, has a cartilage phenotype that resembles that of osteochondroma [17]. Reduced PEI staining was observed in this mutant. Small electron-dense deposits of PEI were found homogeneously distributed throughout the extracellular matrix (Figure 4). Reflection contrast images demonstrated a reduction in PEI staining in all cells of the cartilage elements (n = 84). PEI deposits were often observed in the nucleus of these cells and in the endoplasmic reticulum (Figure 3). The plot profile of the electron micrographs showed a prominent reduction in PEI aggregates and no gradient formation (Figure 4).

Scattered proteoglycan distribution in osteochondroma

In both sporadic and multiple osteochondromas, contrast reflection microscopy showed that the majority of cells were surrounded by PEI-positive matrix (n = 53/59) (Figure 6A,C). The plot profile of the electron micrographs demonstrated gradient formation similar to that observed in wild-type zebrafish and in the human growth plate (Figure 5).

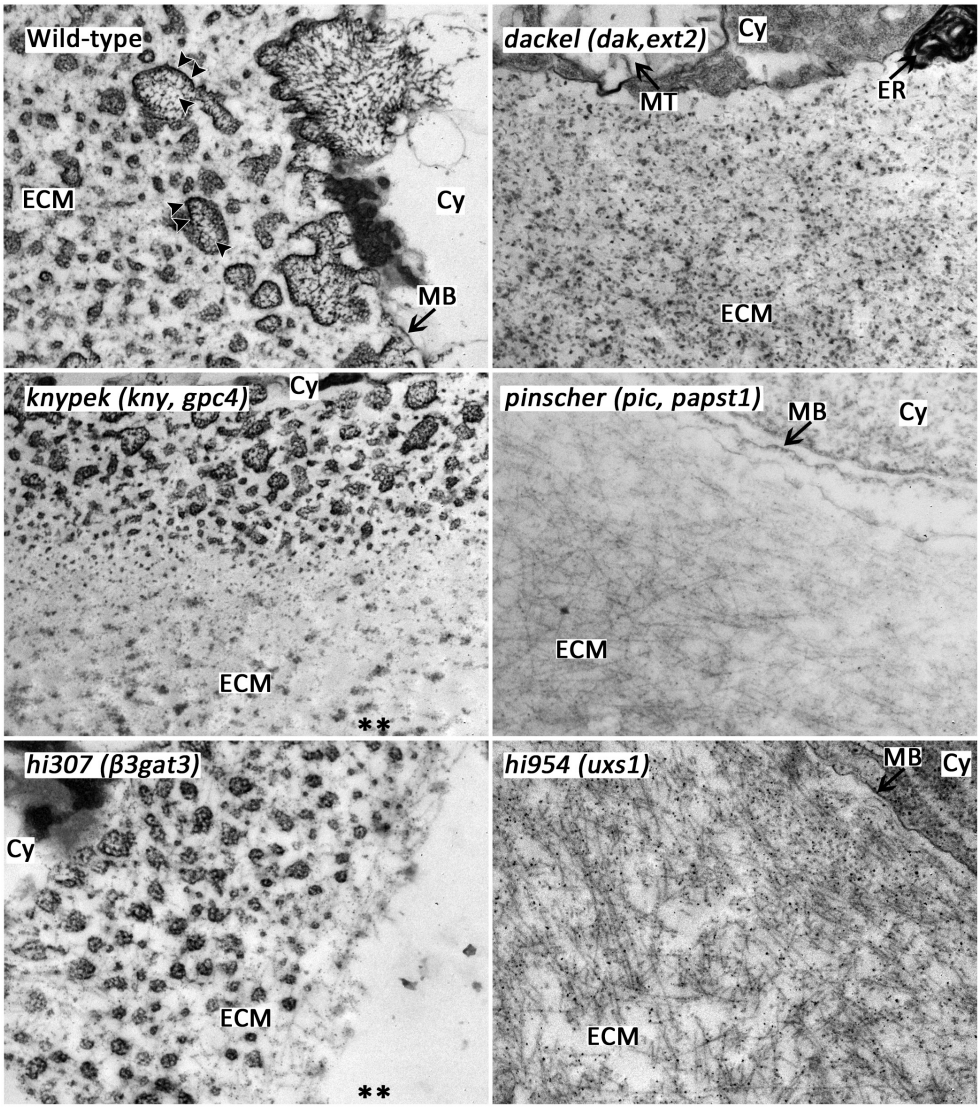


Figure 3. The distribution of proteoglycans in the zebrafish cartilage in wild-type and proteoglycan-deficient homozygous mutants. Electron-dense deposits of PEI were found in the cytoplasm (Cy) and accumulated in the endoplasmic reticulum (ER) and the extracellular matrix (ECM). In the wild-type zebrafish, *kny* and *hi307* PEI staining revealed a gradient. No PEI staining was observed in the mutants with severe impairment of proteoglycan biosynthesis, *pinscher* (*pic*) and *hi954*. Reduced PEI staining was identified in heparan sulphate–deficient *dackel* (*dak*) mutants. PEI aggregates often formed vesicle-like structures, enclosed in a line of electron-dense deposits (wild-type, two arrowheads) containing, in its interior, more loosely packed deposits (wild-type, arrowhead). MB, cell membrane; MT, mitochondria; **, edge of the cartilage. All electron micrographs are × 40 000.

However, approximately 10% of osteochondroma cells (n = 6/53) resembled dak chondrocytes (Figure 6A,B,D,E). Both contrast-reflection and electron micrographs showed a scattered distribution of proteoglycans and a prominent reduction in PEI aggregates in the matrix surrounding these cells (Figure 5). The plot profile indicated that no gradients were formed around small populations of osteochondroma cells. This finding suggests the presence of both normal and proteoglycan-deficient cells in the cartilage cap (Figure 6A,C).

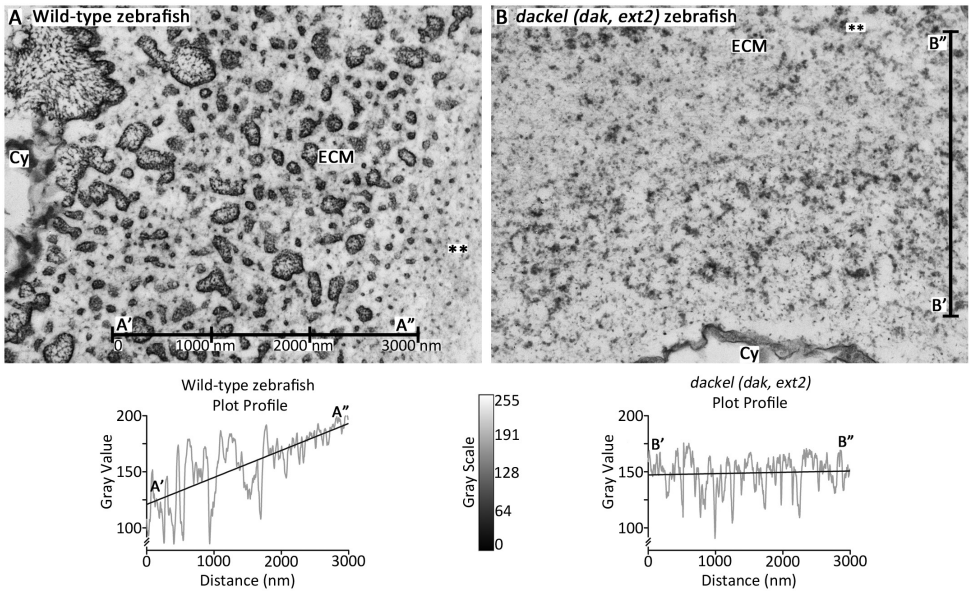


Figure 4. The distribution of proteoglycans shows gradients in the normal cartilage and a lack of gradient in *dackel* (*dak/ext2*) zebrafish mutants. The line of the plot profile in wild-type zebrafish demonstrates a decrease in PEI staining intensity from A' to A", which reflects gradient formation. The plot profile in the *dackel* (*dak/ext2*) mutant shows a prominent reduction of PEI staining intensity and an absence of gradient (from B' to B"). The PEI staining in dackel is similar to that found in the region close to the edge of the cartilage (**) of wild-type zebrafish. Cy, cytoplasm; ECM, extracellular matrix. All electron micrographs are × 30 000.

Discussion

We demonstrated a cytochemical method for the visualisation and quantification of negatively charged proteoglycan-associated sites in cartilage and confirmed this finding by observing an absence of PEI staining in zebrafish variants with severely impaired proteoglycan biosynthesis: *pic* (*slc35b2*) and *hi954* (*uxs1*). At pH 7.4, the PEI staining pattern in the cartilage matrix of the growth plate and of wild-type zebrafish was similar to that observed in epiphyseal and osteoarthritic cartilage, which has been previously reported [26,33].

Regular histochemical stains (e.g., alcian blue) notoriously demonstrate different compositions, organisation of proteoglycans [34,35] and the presence of pericellular, territorial and interterritorial matrix compartments in cartilage [36]. The pattern of PEI staining also reflects a diverse proteoglycan distribution. The overall distribution of proteoglycans in gradients, as shown by PEI staining, may be either the cause or the consequence of the formation of compartments in cartilage. In any case, proteoglycans are well known to play a role in the physiological regulation and homeostasis of cartilage.

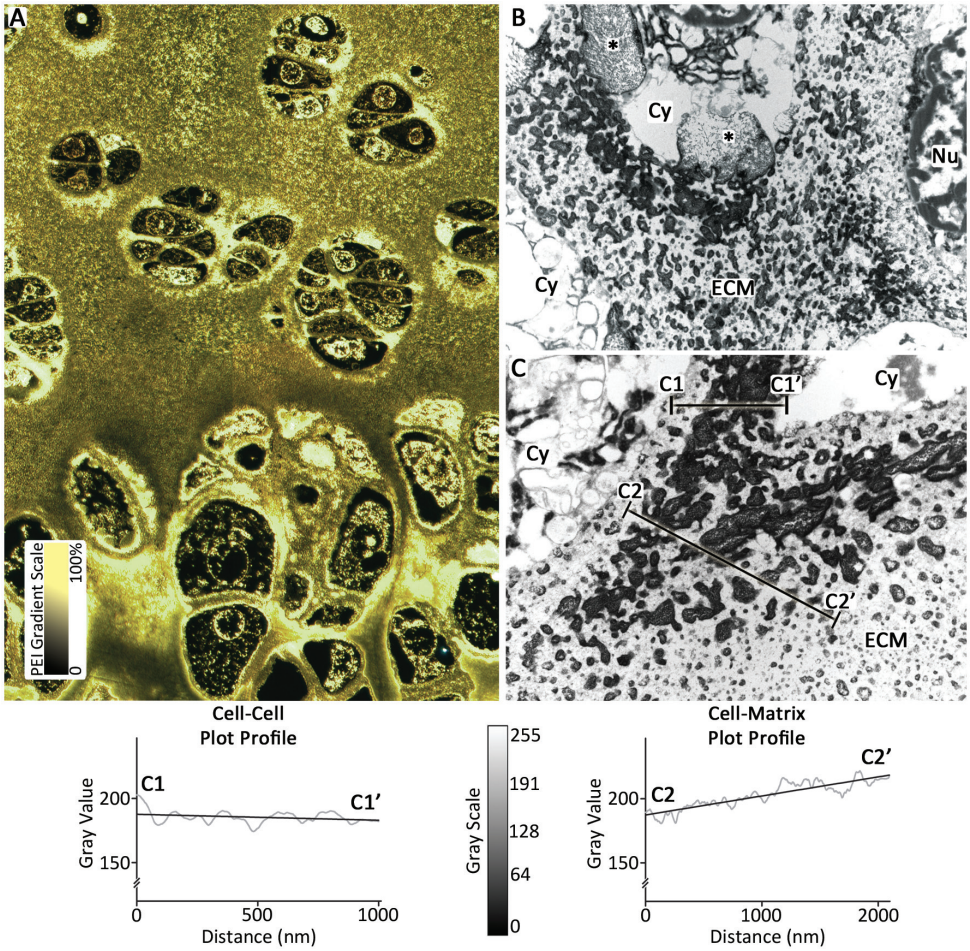


Figure 5. The distribution of proteoglycans in the growth plate. Contrast-reflection images (four pictures shown together) (A) show all cells surrounded by PEI staining. Electron-dense deposits of PEI are found in the cytoplasm (Cy) (B, *) and in the extracellular matrix (ECM) (A–C). The plot profile of the electron micrographs demonstrates a larger gradient formation from C2 to C2′ in the peripheral region (between columns of cells, cell–matrix plot profile) and a smoother gradient from C1 to C1′ in the region inside the column (between cells of the same column, cell–cell plot profile). Nu, nucleus. Magnifications: (A) × 90; (B) × 10 000; (C) × 20 000.

The distribution of proteoglycans in zebrafish cartilage is neither affected by a lack of glypican-4 (*kny* mutant), nor a GPI-anchored cell surface heparan sulphate proteoglycan, nor by the absence of UDP–Gal transferase I (*hi307* mutant). This enzyme, encoded by β*3gat3*, is involved in the construction of the tetrasaccharide linkage region required for heparan, chondroitin and dermatan sulphate biosynthesis (Figure 1).

The development of the growth plate and its regulation are controlled by morphogen gradients (reviewed in 3). Heparan sulphate proteoglycans one of the essential regulators for morphogen gradient formation [6]. In this study, the gradient formed by proteoglycans is hypothesised to be involved in such regulation. The vesicle-like aggregates visualised by PEI staining might be related to a gradient formation of signalling molecules. The concentration of a given proteoglycan-binding molecule might be associated with the size of the aggregates at a certain position across the matrix. For example, the dilution of a signalling molecule increases with the distance from the cell surface, following the decrease in size of the proteoglycan aggregates. Proteoglycans in secretory vesicles have been described as having a role in packaging granular contents, maintaining enzymes (e.g., proteases) in an active state and regulating various tissue homeostasis-related biological activities after secretion [37].

Recent studies have shown that the cartilage cap of mouse osteochondromas is a mosaic of wild-type chondrocytes and cells lacking functional *Ext1* [20,21]. Here we demonstrate, using PEI staining, that human osteochondromas have a heterogeneous composition of both normal and proteoglycan-deficient cells. Approximately 10% of osteochondroma cells showed a prominent reduction in PEI aggregates in the surrounding matrix, with no gradient formation. Similar patterns were observed in the cartilage of *dackel*, the zebrafish homologue of human multiple osteochondromas. The human osteochondroma cells in the reduced PEI staining areas are likely associated with loss-of-function mutations in the *EXT* genes. Taken together, these findings provide major insight into human osteochondromagenesis. Cells in the growth plate or in the neighbouring tissue harbouring homozygous mutations in *EXT1/2* disrupt the diffusion gradients and signal transduction, which may contribute to tumour initiation. Reflection contrast images of osteochondromas show a reduction, but not an absence, of proteoglycans in the pericellular region of the proteoglycan-deficient cells. It is well described that the *EXT1*-null mutation in mice is embryonic lethal [22], and *EXT1*-null cells are difficult to grow in culture [18]. Therefore, a certain threshold level of heparan sulphate seems to be critical for *EXT1*-null cell survival. The integration of wild-type chondrocytes into the osteochondroma cap could provide an environment conducive to tumour cell proliferation and development. The ability of mutant cells to recruit normal cells to participate in the formation of a lesion is well described in fibrous dysplasia of the bone [38].

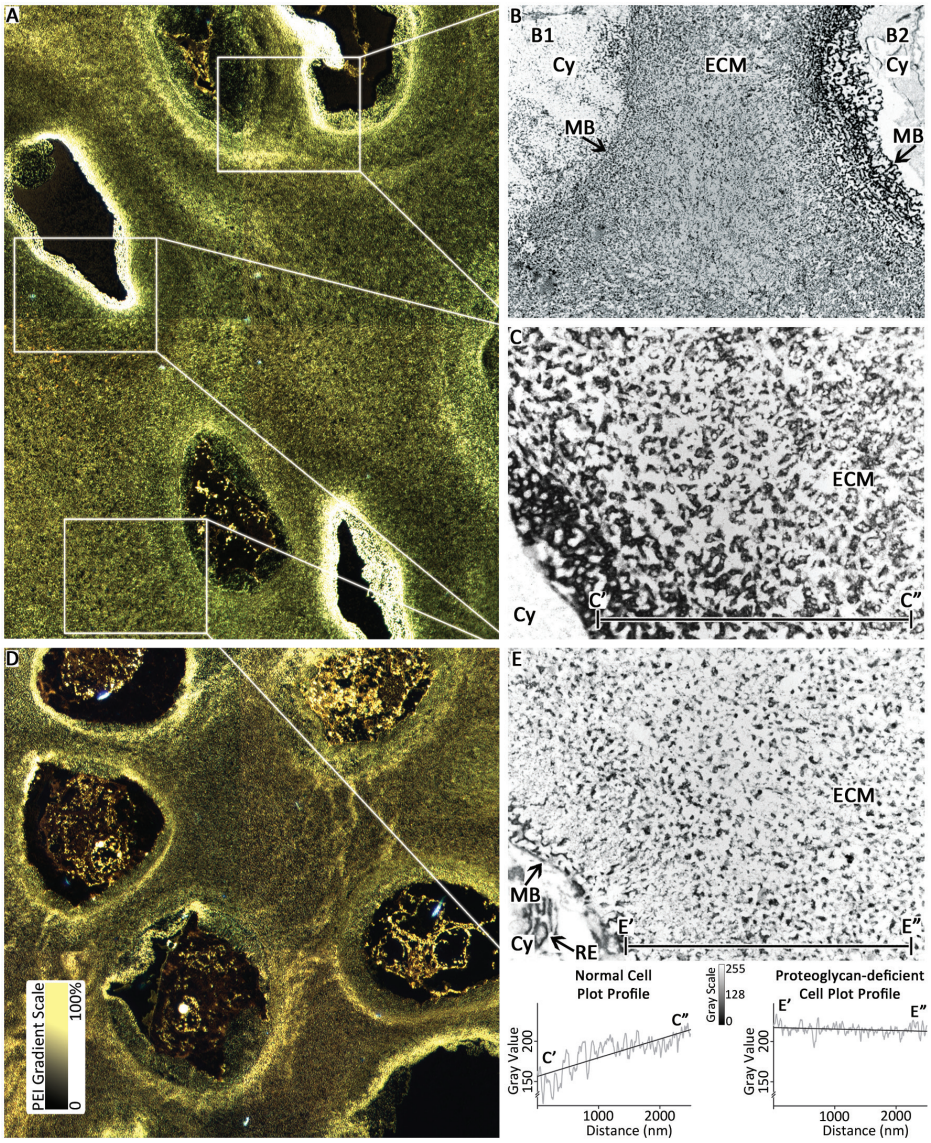


Figure 6. The scattered distribution of proteoglycans in osteochondroma. Contrast reflection images (CRI, four pictures shown together) (A, D) show cells surrounded by PEI staining and unstained cells. Electron micrographs (B, C, E) taken from similar areas of the CRI represent two neighbouring cells (B), in which one cell (B2) has a normal distribution of PEI and the other (B1) has a reduction in PEI staining. The normal cells (C) show gradient formation of electron-dense deposits of PEI from C′ to C″ as a function of distance through the cartilage (normal cell plot profile). Proteoglycan-deficient cells (E) demonstrate few PEI aggregates and no gradient formation from E to E″ (proteoglycan-deficient cell plot profile); electron-dense deposits of PEI were observed in the endoplasmic reticulum (RE) (E). Cy, cytoplasm; MB, cell membrane; ECM, extracellular matrix. Magnifications: (A, D) × 90; (B) × 6000; (C, E) × 20 000.

Although these data significantly advance our understanding of growth plate regulation and the pathogenesis of osteochondroma, a number of questions remain. For instance, how are macromolecules trafficked across the extracellular matrix of the growth plate? How does the mixture of both normal and proteoglycan-deficient cells explain the severity of the phenotype in patients with multiple osteochondromas? Is this mixture of cells homogenously present throughout the tumour? How are proteoglycans distributed in osteochondroma cases that have functional *EXT1/2*? In any event, this study clearly demonstrates the existence of proteoglycan gradients within the growth plate and an absence of this gradient around a subset of osteochondroma cells, which affects the diffusion of signalling molecules and implies a distinct role in the pathogenic mechanisms of tumour formation.

Acknowledgements

This work was supported by the European Network of Excellence EuroBoNeT (http://www.eurobonet.eu), Grant No. 018814 (LSHC-CT-2006-018814).

Author contributions

CEdeA and PCWH were involved in the study design; CEdeA, MIW and FAP collected the data; CEdeA, MIW and PCWH analysed and interpreted the data; MIW, CEdeA and PCWH carried out literature searches; CEdeA and FAP generated the figures. All authors were involved in writing the paper and had final approval of the submitted and published versions.

References

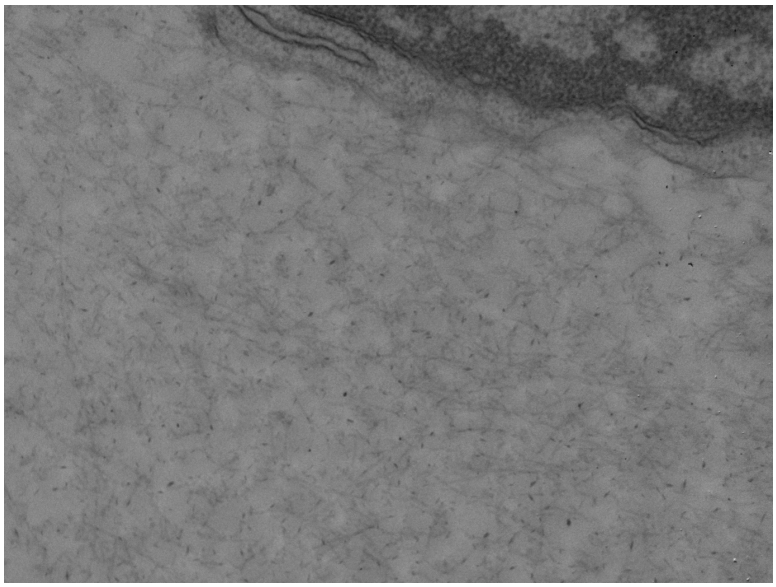
1. Yan D, Lin X. Shaping morphogen gradients by proteoglycans. Cold Spring Harbor Perspect Biol 2009; 1: a002493.
2. Hacker U, Nybakken K, Perrimon N. Heparan sulphate proteoglycans: the sweet side of development. Nat Rev Mol Cell Biol 2005; 6: 530–541.
3. Bulow HE, Hobert O. The molecular diversity of glycosaminoglycans shapes animal development. Annu Rev Cell Dev Biol 2006; 22: 375–407.
4. Kronenberg HM. Developmental regulation of the growth plate. Nature 2003; 423: 332–336.
5. Wu Y, Belenkaya TY, Lin X. Dual roles of Drosophila glypican Dally-like in Wingless/Wnt signaling and distribution. Methods Enzymol 2010; 480: 33–50.
6. Cortes M, Baria AT, Schwartz NB. Sulfation of chondroitin sulfate proteoglycans is necessary for proper Indian hedgehog signaling in the developing growth plate. Development 2009; 136: 1697–1706.
7. Bovee JVMG, Hogendoorn PCW, Wunder JS, et al. Cartilage tumours and bone development: molecular pathology and possible therapeutic targets. Nat Rev Cancer 2010; 10: 481–488.

8. Hameetman L, Szuhai K, Yavas A, et al. The role of EXT1 in non hereditary osteochondroma: identification of homozygous deletions. J Natl Cancer Inst 2007; 99: 396–406.
9. Wuyts W, Van Hul W. Molecular basis of multiple exostoses: mutations in the EXT1 and EXT2 genes. Hum Mutat 2000; 15: 220–227.
10. Bovee JVMG, Cleton-Jansen AM, Wuyts W, et al. EXT-mutation analysis and loss of heterozygosity in sporadic and hereditary osteochondromas and secondary chondrosarcomas. Am J Hum Genet 1999; 65: 689–698.
11. McCormick C, Leduc Y, Martindale D, et al. The putative tumour suppressor EXT1 alters the expression of cell-surface heparan sulfate. Nat Genet 1998; 19: 158–161.
12. Zak BM, Crawford BE, Esko JD. Hereditary multiple exostoses and heparan sulfate polymerization. Biochim Biophys Acta 2002; 1573: 346–355.
13. van den Berg H, Kroon HM, Slaar A, et al. Incidence of biopsy-proven bone tumors in children: a report based on the Dutch pathology registration 'PALGA'. J Pediatr Orthop 2008; 28: 29–35.
14. Khurana J, Abdul-Karim F, Bovée JVMG. Osteochondroma. In World Health Organization Classification of Tumours. Pathology and Genetics of Tumours of Soft Tissue and Bone, Fletcher CDM, Unni KK, Mertens F (eds). IARC Press: Lyon, France, 2002; 234–236.
15. Stieber JR, Dormans JP. Manifestations of hereditary multiple exostoses. J Am Acad Orthop Surg 2005; 13: 110–120.
16. Osterholm C, Barczyk MM, Busse M, et al. Mutation in the heparan sulfate biosynthesis enzyme EXT1 influences growth factor signaling and fibroblast interactions with the extracellular matrix. J Biol Chem 2009; 284: 34935–34943.
17. Clément A, Wiweger M, von der Hardt S, et al. Regulation of zebrafish skeletogenesis by ext2/dackel and papst1/pinscher. PLoS Genet 2008; 4: e1000136.
18. Reijnders CM, Waaijer CJ, Hamilton A, et al. No haploinsufficiency but loss of heterozygosity for EXT in multiple osteochondromas. Am J Pathol 2010; 177: 1946–1957.
19. Zuntini M, Pedrini E, Parra A, et al. Genetic models of osteochondroma onset and neoplastic progression: evidence for mechanisms alternative to EXT genes inactivation. Oncogene 2010; 29: 3827–3834.
20. Jones KB, Piombo V, Searby C, et al. A mouse model of osteochondromagenesis from clonal inactivation of Ext1 in chondrocytes. Proc Natl Acad Sci USA 2010; 107: 2054–2059.
21. Matsumoto K, Irie F, Mackem S, et al. A mouse model of chondrocyte-specific somatic mutation reveals a role for Ext1 loss of heterozygosity in multiple hereditary exostoses. Proc Natl Acad Sci USA 2010; 107: 10932–10937.

22. Hilton MJ, Gutierrez L, Martinez DA, et al. EXT1 regulates chondrocyte proliferation and differentiation during endochondral bone development. Bone 2005; 36: 379–386.
23. de Andrea CE, Wiweger M, Prins F, et al. Primary cilia organization reflects polarity in the growth plate and implies loss of polarity and mosaicism in osteochondroma. Lab Invest 2010; 90: 1091–1101.
24. Vernier RL, Klein DJ, Sisson SP, et al. Heparan sulfate-rich anionic sites in the human glomerular basement membrane. Decreased concentration in congenital nephrotic syndrome. N Engl J Med 1983; 309: 1001–1009.
25. Hogendoorn PCW, De Heer E, Weening JJ, et al. Glomerular capillary wall charge and antibody binding in passive Heymann nephritis. J Lab Clin Med 1988; 111: 150–157.
26. Sauren YM, Mieremet RH, Groot CG, et al. Polyethyleneimine as a contrast agent for ultrastructural localization and characterization of proteoglycans in the matrix of cartilage and bone. J Histochem Cytochem 1991; 39: 331–340.
27. Schurer JW, Kalicharan D, Hoedemaeker PJ, et al. The use of polyethyleneimine for demonstration of anionic sites in basement membranes and collagen fibrils. J Histochem Cytochem 1978; 26: 688–689.
28. Kimmel CB, Ballard WW, Kimmel SR, et al. Stages of embryonic development of the zebrafish. Dev Dyn 1995; 203: 253–310.
29. Wiweger MI, Avramut C, de Andrea CE, et al. Cartilage ultrastructure in proteoglycan-deficient zebrafish mutants brings to light new candidate genes for human skeletal disorders. J Pathol 2011; 223:531-42.
30. Ueda H, Toriumi H, Leng CG, et al. A histochemical study of anionic sites in the intermediate layer of rat femoral cartilage using polyethyleneimine at different pH levels. Histochem J 1997; 29: 617–624.
31. Prins FA, Diemen-Steenvoorde R, Bonnet J, et al. Reflection contrast microscopy of ultrathin sections in immunocytochemical localization studies: a versatile technique bridging electron microscopy with light microscopy. Histochem 1993; 99: 417–425.
32. Sissoeff I, Grisvard J, Guille E. Studies on metal ions–DNA interactions: specific behaviour of reiterative DNA sequences. Prog Biophys Mol Biol 1976; 31: 165–199.
33. Sauren YM, Mieremet RH, Lafeber FP, et al. Changes in proteoglycans of ageing and osteoarthritic human articular cartilage: an electron microscopic study with polyethyleneimine. Anat Rec 1994; 240: 208–216.
34. Heinegard D. Proteoglycans and more—from molecules to biology. Int J Exp Pathol 2009; 90: 575–586.
35. Willems SM, Wiweger M, Frans Graadt van Roggen J, et al. Running GAGs: myxoid matrix revisited. What's in it for the pathologist? Virchow Arch 2009; 456: 181–192.

36. Heinegard D, Saxne T. The role of the cartilage matrix in osteoarthritis. Nat Rev Rheumatol 2011; 7: 50–56.
37. Esko JD, Kimata K, Lindahl U. Proteoglycans and sulfated glycosaminoglycans. In Essentials of Glycobiology, 2nd edn, Varki A, Cummings RD, Esko JD, et al. (eds). Cold Spring Harbor Laboratory Press: Cold Spring Harbor, NY, 2009.
38. Bianco P, Kuznetsov SA, Riminucci M, et al. Reproduction of human fibrous dysplasia of bone in immunocompromised mice by transplanted mosaics of normal and Gsα-mutated skeletal progenitor cells. J Clin Invest 1998; 101: 1737–1744.

Supporting Information



Supporting Information: Figure S1. Post-embedding PEI at pH 1.0, showing a virtual absence of stained anionic sites.

Chapter 6

Primary cilia organization reflects polarity in the growth plate and implies loss of polarity and mosaicism in osteochondroma

Carlos E de Andrea, Malgorzata Wiweger,
Frans Prins, Judith VMG Bovée,
Salvatore Romeo and Pancras CW Hogendoorn
Laboratory Investigation 2010;90:1091-101

Abstract

Primary cilia are specialized cell surface projections found on most cell types. Involved in several signaling pathways, primary cilia have been reported to modulate cell and tissue organization. Although they have been implicated in regulating cartilage and bone growth, little is known about the organization of primary cilia in the growth plate cartilage and osteochondroma. Osteochondromas are bone tumors formed along the growth plate, and they are caused by mutations in *EXT1* or *EXT2* genes. In this study, we show the organization of primary cilia within and between the zones of the growth plate and osteochondroma. Using confocal and electron microscopy, we found that in both tissues, primary cilia have a similar formation but a distinct organization. The shortest ciliary length is associated with the proliferative state of the cells, as confirmed by Ki-67 immunostaining. Primary cilia organization in the growth plate showed that non-polarized chondrocytes (resting zone) are becoming polarized (proliferating and hypertrophic zones), orienting the primary cilia parallel to the longitudinal axis of the bone. The alignment of primary cilia forms one virtual axis that crosses the center of the columns of chondrocytes reflecting the polarity axis of the growth plate. We also show that primary cilia in osteochondromas are found randomly located on the cell surface. Strikingly, the growth plate-like polarity was retained in sub-populations of osteochondroma cells that were organized into small columns. Based on this, we propose the existence of a mixture ('mosaic') of normal lining ($EXT^{+/-}$ or $EXT^{wt/wt}$) and $EXT^{-/-}$ cells in the cartilaginous cap of osteochondromas.

Keywords: bone tumor; cartilage; cell polarity; growth plate; hereditary multiple exostoses; osteochondroma

Introduction

The growth plate is a highly organized, cartilaginous template needed for the longitudinal growth of long bones. Structurally, the growth plate can be divided into three distinct zones [1]. The mitotic spindles of proliferating chondrocytes are aligned perpendicular to the long axis of the growing bone. The chondrocytes have to undertake a series of cell movements/rotations and shape changes to align one on top of the other to generate the typical columns of the growth plate [2,3,4]. Once acquired, this columnar organization is maintained. On the metaphyseal side of the growth plate, the chondrocytes form the hypertrophic zone. The cells stop proliferating and change their expression profile to synthesize type X collagen and to prepare for programmed cell death and mineralization [1]. Regulation of the growth plate is tightly maintained by signaling pathways in which heparan sulfate proteoglycans have a crucial role in facilitating the transport of signaling molecules within the extracellular matrix and in modulating the receptor-ligand interactions.

Mutations in *EXT1* and *EXT2* genes, which are involved in synthesis of heparan sulfate chains, lead to hereditary multiple osteochondromas (previously known as hereditary multiple exostoses), most likely by deregulating signaling pathways. Osteochondromas are the most common benign bone tumors [5] and usually arise from the juxta-epiphyseal region of the growth plate. Although the cells seem somewhat disorganized, the histological features of osteochondromas are similar to those of the growth plate [6].

Primary cilia are specialized cell surface projections present on most eukaryotic cells [7,8]. The primary cilium can be viewed as the antenna of the cell, which receives and transduces mechanical and chemical signals from the surrounding cells and the extracellular matrix [9] Primary cilia are formed during interphase, when the centriole pair moves together to the plasma membrane. The mother centriole becomes the basal body of the cilium by generating a 9+0 microtubular doublet symmetry that represents the structural core of the axoneme [9] Construction of the axoneme requires effective intraflagellar transport, a bidirectional drive system for molecules run by motor protein complexes. Anterograde transport, from the base to the tip of the primary cilium, is driven by heteromeric kinesin-II motor proteins, which are composed of KIF3A and KIF3B motor subunits. Retrograde transport, from the tip to the base of the cilium, is mediated by dynein 1B [10].

The link between cilia function and growth plate development is described in several recent studies. Primary cilia have been implicated as recipients of some signaling pathways essential for the regulation of the growth plate, such as the non-canonical Wnt and Indian Hedgehog pathways [3,11,12,13,14]. KIF3A deficiency has been shown to cause abnormal topography of Hedgehog signaling and growth plate dysfunction [15]. In several tissues, the organization of primary cilia has been shown to reflect cell polarity [16,17,18]. In cartilage, it has been reported that primary cilia have a specific orientation pointing away from the articular surface in articular chondrocytes or located at the center of the columnar

cells in the growth plate [3,19,20]. In the extensor tendon, cilia are aligned parallel to the collagen fibers and the long axis of the tendon [8,21,22].

In this study we show the organization of primary cilia within and between the zones of the growth plate and osteochondroma. In both tissues, cilia were found to have similar forms and ultrastructures but distinct organization. In the growth plate, non-polarized chondrocytes (resting zone) are becoming polarized (proliferating and hypertrophic zones), orienting the cilia parallel to the longitudinal axis of the bone. This reflects cell polarity. In osteochondromas, primary cilia are randomly located on the cell surface. Strikingly, the growth plate-like polarity was retained in sub-populations of osteochondroma cells that were organized into small columns. We also show that the shortest ciliary length was related to the proliferative state of the cells.

Materials and methods

Growth Plate and Osteochondroma Samples

Five postnatal growth plates were sampled from orthopedic resections for pathological conditions not related to osteochondroma. Five osteochondroma cases were retrieved from the surgical pathology files. Patient data were obtained by reviewing pathological reports or clinical charts (Supplementary Table 1). All samples were obtained from the Leiden University Medical Center and handled according to ethical guidelines as described in the Code for Proper Secondary Use of Human Tissue in the Netherlands of the Dutch Federation of Medical Scientific Societies.

Histopathological and Immunohistochemistry Evaluation

All the samples were fixed in formalin, decalcified and embedded in paraffin as previously described.23 For histopathological evaluation, 4 μm-thick sections were stained with hematoxylin and eosin (H&E).

To compare osteochondromas with growth plates, three zones were identified in the cartilaginous cap of the tumor (Figure 1) according to the following morphologic features:

- Resting zone: spherical chondrocytes, single or in pairs, irregularly arranged;
- Proliferating zone: flattened chondrocytes arranged in columns or forming clusters;
- Hypertrophic zone: medium/large and rounder chondrocytes.

Pre-hypertrophic and hypertrophic zones were counted as a single zone because morphological distinction of the two is not reliable [24].

Immunohistochemistry was performed for proliferation rate analysis using a monoclonal antibody against Ki-67 (clone MIB1, 1:100; Dako, Glostrup, Germany) according to standard laboratory procedures [25].

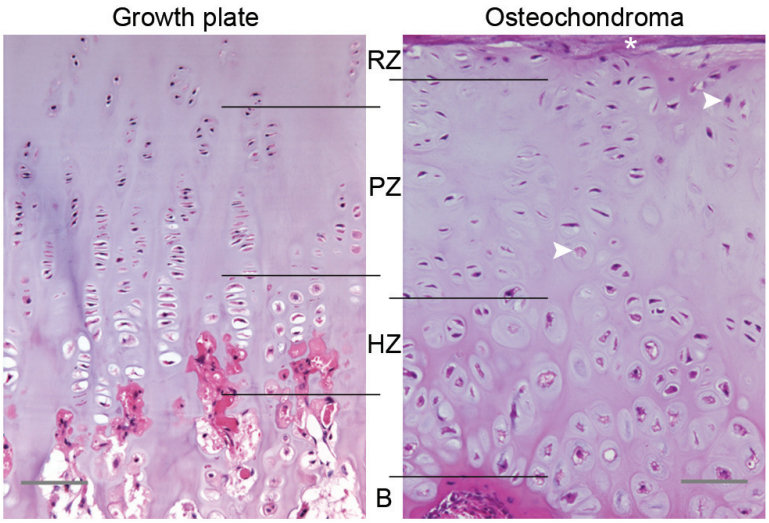


Figure 1. Histology of the growth plate and osteochondroma. The growth plate is formed by three zones: resting (RZ), proliferating (PZ) and pre/hypertrophic (HZ) that over time turn into bone (B). Along the growth plate, the chondrocytes undergo proliferation (PZ) and differentiation (HZ and B). During these processes, the cell columnar organization is maintained. Osteochondromas are formed by three layers: outer perichondrium (asterisk), cartilaginous cap and underlying bone. The histological features of osteochondromas are to some extent similar to the ones of the growth plate. The zonation is less defined (RZ, PZ and HZ), and the cells are irregularly arranged and rarely acquire columnar organization. Hypertrophic-like chondrocytes (arrowhead) are observed within the RZ and PZ. The osteochondroma cells also undergo terminal ossification (B). (RZ, resting zone; PZ, proliferating zone; HZ, hypertrophic zone; Scale bars, 100 µm).

Immunofluorescence Staining

For immunofluorescence studies, 20 µm-thick sections of growth plates and osteochondromas were cut parallel to the longitudinal axis of the bone or the tumor. The sections were incubated with testicular hyaluronidase (2 mg/ml in 0.1 M Tris saline, pH 5.0; Sigma-Aldrich, St Louis, MO, USA) at 37 °C for 2 h and with 0.5% Triton X-100 in PHEM buffer (PIPES 0.05 M, HEPES 0.025 M, EGTA 0.01 M and $MgCl_2$ 0.01 M) at room temperature for 5 min as previously described.7, 26 In addition, to increase antibody penetration, proteinase K (5 µl/ml in 0.1 M Tris-buffered saline, pH 5.0; DakoCytomation, Carpinteria, CA, USA) was applied at room temperature for 3 min. The sections were stained with primary monoclonal antibodies against acetylated α-tubulin (clone 6-11b-1, 1:1000; Sigma-Aldrich, Steinheim, Germany), γ-tubulin (clone GTU-88, 1:1000; Sigma-Aldrich, USA) and/or Ki-67 (1:100) and/or a polyclonal antibody against KIF3A (1:100; Abcam, Cambridge, UK) at 4 °C overnight. Secondary antibodies conjugated with Alexa Fluor 488 (1:200; Invitrogen Molecular Probes, Eugene, OR, USA) or Alexa Fluor 647 (1:200) were applied for 30 min to detect the primary antibody.

Finally, the sections were mounted in Vectashield with propidium iodide (Vector Laboratories, Burlingame, CA, USA). Negative controls were sections stained without adding the primary antibody.

Electron Microscopy

Electron microscopy studies were performed on two growth plates and two osteochondromas as previously described [27]. To evaluate the ultrastructure of primary cilia, ultrathin sections were examined in a JEOL JEM-1011 electron microscope equipped with a MegaView III digital camera.

Confocal Microscopy and Analysis of Primary Cilia

Fluorescently labeled primary cilia were imaged using a confocal laser scanning microscope (LSM 510; Zeiss, Jena, Germany) and a plan apochromat × 63/1.40 oil or a C-Apo × 40/1.2 water immersion objective lens (both from Zeiss). All images were acquired at a resolution of 1024 × 1024 or 512 × 512 pixels, a pinhole of 1 Airy unit, and an average of two successive scans at a speed of 6. After initial scanning to orient the section parallel to the longitudinal axis of the bone/tumor, z-series were imaged at 0.5 µm intervals to depths as great as 20 µm. A total of 10 fields of randomly selected views from each zone of the growth plate and osteochondroma were scanned in their full depth and used to evaluate (ImageJ software; NIH Image, Bethesda, MD, USA) the presence of the cilium in each z-stack series as well as its characteristics (length, location, orientation and position). Only viable cells (with cytoplasm and a nucleus stained with propidium iodide) were selected. In addition, to avoid considering centrioles or auto-fluorescence of the tissue as a cilium, only cilia that appeared on at least three consecutive images and approximately 90° to the incident light were analyzed. Colocalization of the KIF3A subunit and α-tubulin was used to correctly identify primary cilia. The γ-tubulin antibody was used to analyze the orientation of the centrioles. In addition, the cell nuclei stained with propidium iodide were ‘pseudo-colored’ in blue by changing the color of the channel in the confocal microscope settings.

Statistical Analysis

Data are expressed as mean±s.e.m. Statistical significance was computed by one-way ANOVA followed by post hoc Tukey’s HSD test using the SPSS 16.0 software package. Results were considered significant when $P<0.05$.

Results

Morphology of the Growth Plate and Osteochondroma

All three zones (resting, proliferating and hypertrophic) were identified in all analyzed samples. Although present, the 'zonation' in the osteochondromas was less defined (Figure 1) and the cells were irregularly arranged and rarely acquired columnar organization. In addition, hypertrophic-like chondrocytes were often observed within the resting and proliferating zones in osteochondromas but not in the growth plate (Figure 1).

The Presence of Primary Cilia

Primary cilia were found on cells at all stages of differentiation in both the growth plate and osteochondromas (Figure 2a and b). All the three zones of osteochondroma had a significantly higher percentage of cells with primary cilia when compared with the growth plate (resting: 94.9 vs 89.4%, P=0.044; proliferating: 93.2 vs 71.9%, P<0.001; and hypertrophic: 94 vs 71.6%, P<0.001, respectively). In the growth plate analyzed with respect to zones, the percentage of ciliated cells was significantly higher in the resting (89.4%) than in the proliferating and hypertrophic zones (71.9 and 71.6%, respectively; P<0.001). No significant differences were observed between the three zones in osteochondroma samples (P=0.532).

Proliferation Rate in the Growth Plate and Osteochondroma

A lower proliferation rate was observed in osteochondroma, as shown by Ki-67 immunostaining, a known marker of cell proliferation. Fewer Ki-67-positive cells were identified along the tumor (Supplementary Figure 1b). In contrast, a difference in proliferation was observed between the zones of the growth plate. A higher proliferation rate was found in the proliferating than in the resting and hypertrophic zones (Supplementary Figure 1a).
Double staining for Ki-67 and primary cilia could not be evaluated because of tissue detachment from the glass slides during antigen retrieval procedures.

Length of Primary Cilia

The measurement of the length of primary cilia was performed in the three zones of the growth plate and in osteochondromas. A high variability of primary cilium length within and between zones was observed (Figure 2c). In the growth plate, primary cilia of the proliferating zone (mean length 1.62 μm) were significantly shorter than those in the resting (mean length 2.39 μm) and the hypertrophic zones (mean length 2.23 μm) (in both, P<0.001; Figure 2c). In the osteochondromas, similar results were found. However, cilia were significantly shorter only in the proliferating zone (mean length 2.13 μm) than the hypertrophic zone (mean length 2.38 μm) (P<0.001; Figure 2c).

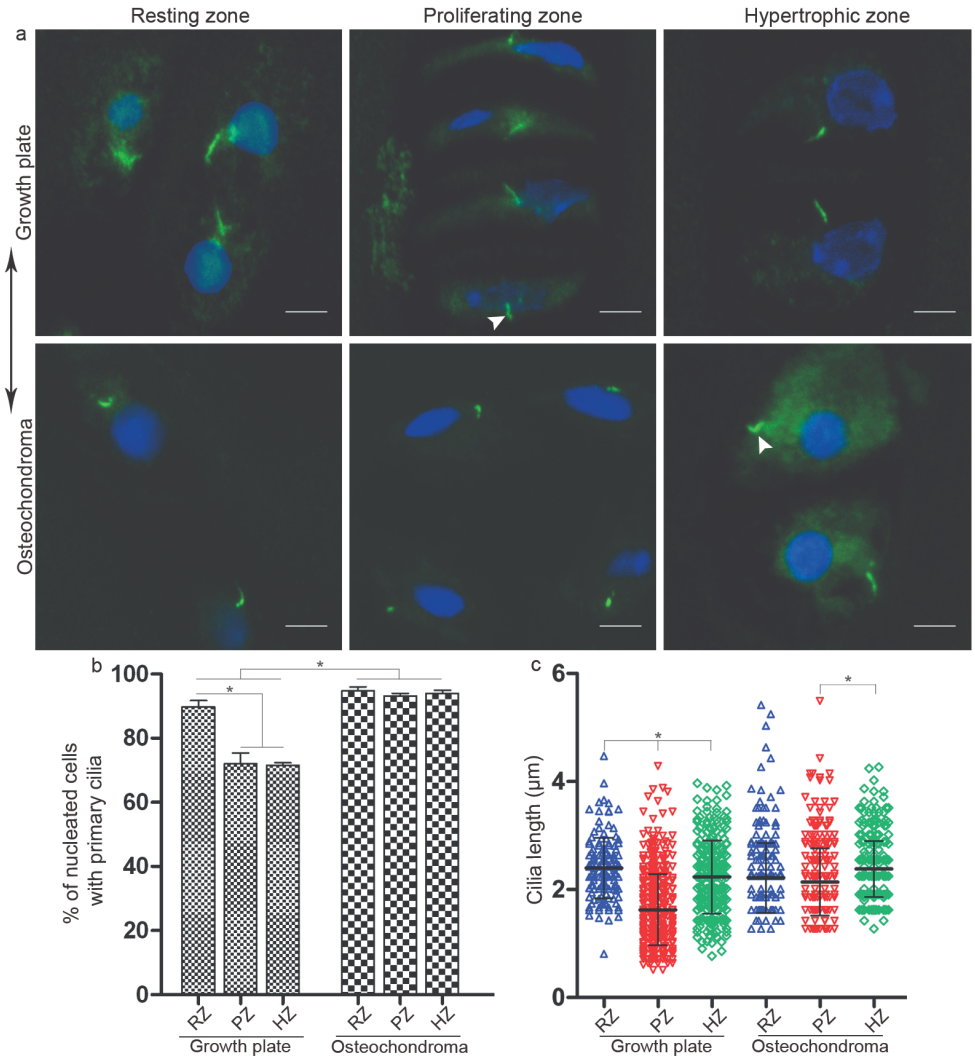


Figure 2. Primary cilia are found on cells at all stages of differentiation in both the growth plate and osteochondroma. Fluorescently labeled primary cilia (green) are found on the cell surface projecting into the extracellular matrix (a). Undulations along the axoneme length are observed (a; arrowheads). The percentage of nucleated cells with primary cilia is depicted (b). A high number of ciliated cells are observed among the proliferating cells of the growth plate. The average length of the cilium in each zone of both tissues is shown (c). High variability in length of the cilium was observed within and between the zones. Nuclei are stained with propidium iodide and pseudocolored in blue. Error bars represent s.e.m. *P<0.05, as determined by one-way ANOVA followed by post hoc Tukey's HSD test. (RZ, resting zone; PZ, proliferating zone; HZ, hypertrophic zone; Arrow-bar, longitudinal axis of the bone or tumor; Scale bars, 5 µm).

In the osteochondromas, similar results were found. However, cilia were significantly shorter only in the proliferating zone (mean length 2.13 µm) than the hypertrophic zone (mean length 2.38 µm) ($P<0.001$; Figure 2c).

The ciliary axonemes were found projecting into the extracellular matrix in both tissues. Undulations along the axoneme length were observed (Figure 2a, arrowheads), as previously described in chondrocytes [8].

The Ultrastructure of Primary Cilia

Electron microscopy revealed the presence of the centriole with a typical 9+0 microtubule doublet organization in the growth plate (Figure 3c) and osteochondromas (Figure 3f). The basal body of the cilium, which is formed by one centriole, was found supporting the axoneme (Figure 3a, b, d and e). At higher magnification, the ciliary axoneme was observed retracted within a plasma membrane invagination (Figure 3a, b and e).

Numerous small clusters of glycogen were found in large areas of the cytoplasm in osteochondroma cells (Figure 3d), but not in the growth plate.

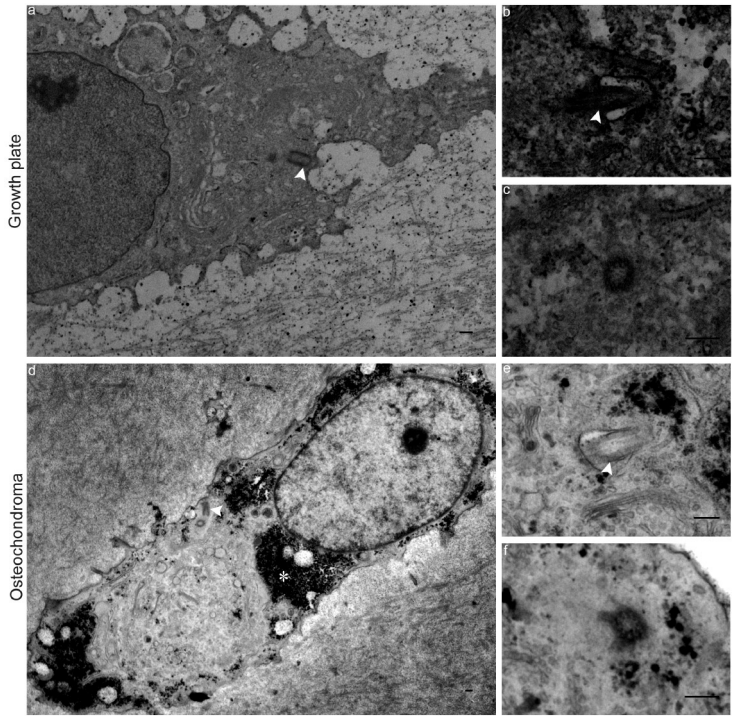


Figure 3. Electron micrographs of the primary cilium and the centrioles. The cilium is observed with a similar ultrastructure in the cells of the growth plate (a–c) and osteochondroma (d–f). The centriole with a typical 9+0 microtubule doublet organization is found in both tissues (c, f). One centriole forms the basal body of the cilium that supports the axoneme (arrowheads) (b, e). The axoneme is observed retracted within a plasma membrane invagination (a, b, e). Numerous small clusters of glycogen (asterisk) are found in large areas of the cytoplasm in osteochondroma cells but not in the growth plate (d). (Scale bars, 0.25 µm).

Localization of KIF3A Kinesin II Subunit

The KIF3A subunit has been shown to have a critical role in growth plate formation [15]. Using an antibody against the KIF3A subunit, positive cells were found in the growth plate and osteochondromas. One strongly stained spot (Figure 4) could be observed, although the staining was diffuse throughout the cytoplasm in both tissues. We next analyzed whether the strongly stained KIF3A spot was properly located in the primary cilia, and we were able to colocalize the KIF3A spot with the cilia (Figure 4).

Primary Cilia Organization in the Growth Plate and Osteochondroma

The typical architecture of the growth plate may reveal a specific location of the organelles within the chondrocytes [28]. To address this hypothesis, we studied the organization of primary cilia along the x–y axis of the growth plate and osteochondromas. In the growth plate, we found that primary cilia in the resting zone do not acquire a clear pattern of orientation (Figure 5c). However, in the proliferating and hypertrophic zones, primary cilia were oriented parallel to the longitudinal axis of the bone pointing either toward the epiphyseal side or the metaphyseal side of the growth plate (Figure 5a and d). At lower magnification, one virtual axis that is formed by the alignment of primary cilia and crosses the center of each column of chondrocytes could be identified (Figure 5a and 6a, left panel). The parallel axes seem to represent the axis of chondrocyte polarity inside the growth plate.

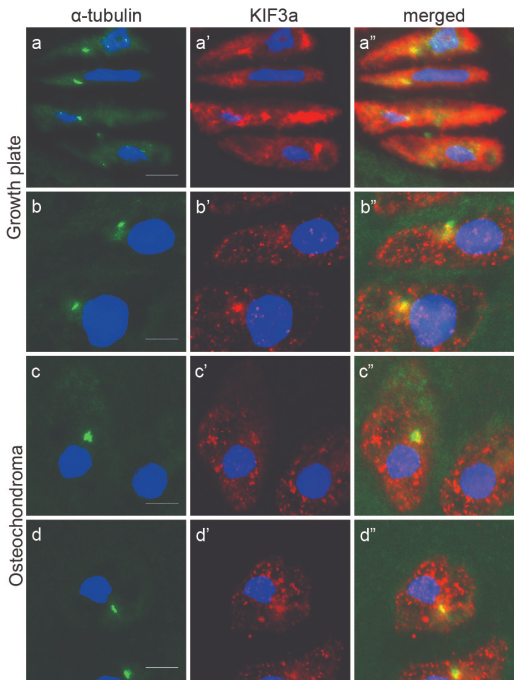


Figure 3. KIF3A subunit, which facilitates intraflagellar transport, is present in the cells of the growth plate and osteochondroma. Immunolabeling with antibodies against acetylated α-tubulin (a–d; green) and KIF3A (a'–d'; red) shows colocalization of both proteins (merged) in the primary cilium in the growth plate (a" and b") and osteochondroma (c" and d''). Nuclei are stained with propidium iodide and pseudo-colored in blue. (Scale bars, 5 μm).

To confirm this specific positioning of the cell region containing the cilium, we immunolabeled the centrioles using an antibody against γ-tubulin (Figure 5e). The centrioles are located in the centrosome of the cell next to the plasma membrane. The centrioles were found aligned inside the columns of cells, delineating one virtual axis (Figure 5e). In osteochondromas, primary cilia were randomly located along the x–y axis of the tumor either on the center or on the lateral-medial region of the cells in relation to the longitudinal axis of the tumor (Figure 5b and 6a, right panel).

In 5 osteochondromas analyzed, 12 sub-populations of cells were found organized into small columns. Interestingly, in 10 of the 12 small columns identified, the cilia were aligned in one axis parallel to the axis of tumor growth (Figure 5h).

Discussion

Primary cilia were found to reflect cell polarity in several tissues [16,17,29]. It has been shown that primary cilia have a critical role in the development of the growth plate. Disturbance of the intraflagellar transport system leads to a depletion of cells with primary cilia and defects in the growth plate such as disruption of cell shape and lack of columnar orientation, which suggests defects in cell movement/rotation [3,11,12].

In this study, we showed that, in the proliferating and hypertrophic zones of the growth plate, the organization of primary cilia forms virtual axes parallel to the longitudinal axis of the bone. The fact that this orientation pattern of the cilium was not detected in the resting zone implies that polarization gradients exist inside the growth plate, driving the cells to their specific positions and orientations. It has been suggested that the polarization gradients are generated and maintained by the cartilage itself and that the resting zone establishes the organization of the growth plate [30].

Several morphogens or signaling molecules are secreted from the two opposite poles of the growth plate, having an important role in chondrocyte proliferation and differentiation [1]. The normal diffusion and function of morphogens regulate the formation of zones in the growth plate [31]. Inside each zone of the growth plate, the chondrocytes respond in an orchestrated manner to the signaling molecules, which reflects a collective cell behavior that is typical for polarized tissues in which the cells adopt the same polarity axis and identical positioning of their organelles [32]. In conclusion, the results provide evidence that normal growth plate formation depends on the establishment and maintenance of individual and collective chondrocyte polarity.

We also showed that the osteochondroma cells have a primary cilium and its formation is similar to that of the growth plate cilia. However, no clear orientation of the cilium was observed in the osteochondromas, with primary cilia often randomly located along the x–y axis either organized on the center or on the lateral-medial region of the cells in relation to the growth axis of the tumor.

This suggests that the presence of primary cilia is not sufficient to direct proper organization of the chondrocytes. The formation of the ciliary axis seems to be a final result of several factors (eg, signaling molecules and their effective transduction) that determine the final orientation of the cells.

Primary cilia have been shown to mediate Indian Hedgehog signaling [9,15] Indian Hedgehog is secreted by pre-hypertrophic chondrocytes, and its diffusion generates a signal gradient inside the growth plate that coordinates cell proliferation and differentiation [1]. The alignment of primary cilia might be critical for transduction of this signaling molecule along the growth plate. Homogeneous expression of Indian Hedgehog has been shown in osteochondromas, which is suggestive of autonomous cell signaling [6]. Therefore, correct orientation of the cilium is no longer needed to receive and transduce the diffusion gradient of Indian Hedgehog signaling. Other deregulated signaling pathways might also contribute to the misorientation of primary cilia. Intriguingly, some sub-populations of osteochondroma cells, which were organized into small columns, appeared to keep the growth plate cell polarity. This leads us to hypothesize that a mixture ('mosaic') exists of normal lining ($EXT^{+/-}$ or $EXT^{wt/wt}$) and $EXT^{-/-}$ cells in the cartilaginous cap. In this mixture, the normal lining cells would produce heparan sulfate proteoglycans and the receptor-ligand interactions would be modulated regularly. Consequently, these cells would respond to the polarization signals and align primary cilia in one axis. Further analysis will be required to identify mosaicism in osteochondromas.

This study sheds light on the events related to primary cilia formation. For example, the smallest ciliary length was associated with the proliferative state of the cells. In addition, several proliferating cells were found to have primary cilia. Knowing that the cell turnover is increased in the proliferating zone and that primary cilia are absent in replicating cells [10], it is possible that only a subset of proliferating cells are in mitosis. This suggests that the cilia length is directly related to cell cycle duration. Further studies on cilia function are necessary. Interestingly, several hypertrophic cells with well-preserved morphology were found without cilia (Figure 5d and g, asterisks). As most of them undergo apoptosis [1], this observation might indicate that primary cilia were disassembled in the early stages of apoptosis. In addition, the osteochondroma cells were found to have a higher percentage of cells with primary cilia. The presence of primary cilia might be associated with the lower proliferation rate of the tumor, which was confirmed by Ki-67 immunostaining. Taken together, the primary cilia length observed in osteochondromas is similar to that in the growth plate, suggesting that ciliary formation is normal in these tumors. This also enforces the hypothesis that deregulation of cell–cell and/or cell–matrix signaling pathways is instrumental to the pathogenesis of osteochondromas.

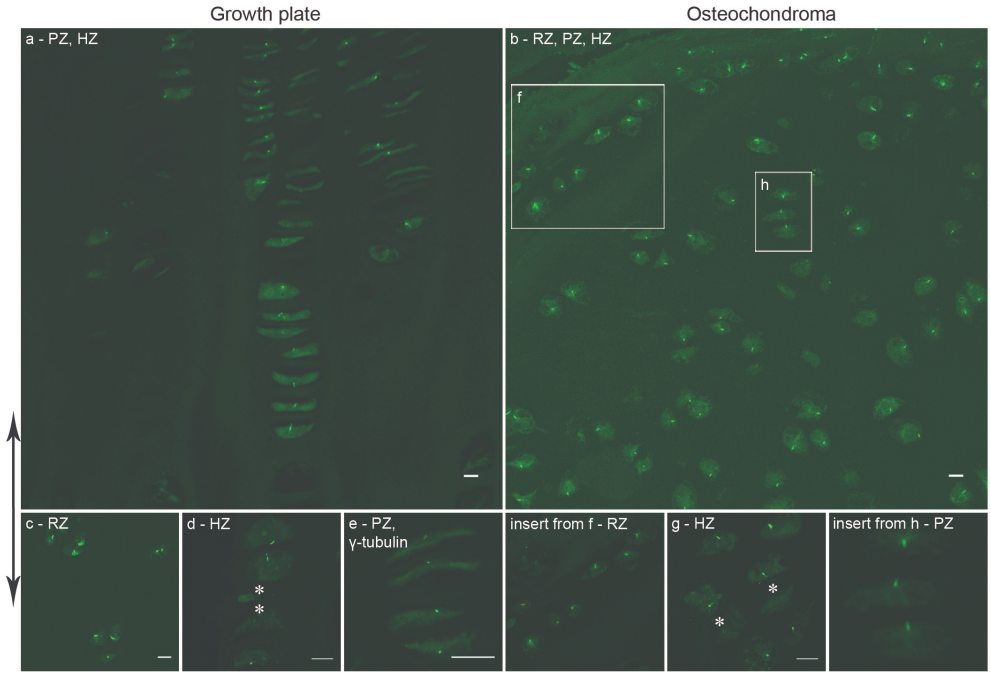


Figure 5. The organization of primary cilia in the growth plate and osteochondroma. Primary cilia (green) in the growth plate (a) are organized in such a way that they form a virtual axis crossing the center of the columns of proliferating and hypertrophic chondrocytes. The ciliary axis is always parallel to the longitudinal axis of the bone (arrow-bar). γ-Tubulin marks the location of the centrioles and confirms the existence of one virtual axis (e). Primary cilia in osteochondromas are randomly located along the x–y axis of the tumor (b). On rare occasions when osteochondroma cells are organized into small columns (h), primary cilia are aligned parallel to the longitudinal axis of the tumor (arrow-bar). In the resting zones of both tissues, primary cilia do not acquire any clear orientation (c, f). Some hypertrophic cells of the growth plate and osteochondroma with a well-preserved morphology are found without cilia (d, g). (RZ—resting zone; PZ—proliferating zone; HZ—hypertrophic zone; asterisks—cells without primary cilia; f and h, inserted from b; arrow-bar—longitudinal axis of the bone or tumor; scale bars, 10 μm).

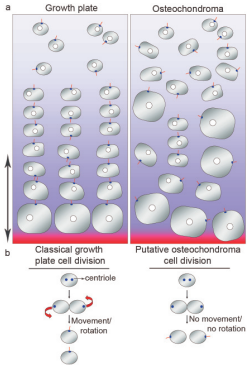


Figure 6. Primary cilia organization reflects cell polarity in the growth plate and in sub-populations of osteochondroma cells. Schematic representation shows the virtual axis that is formed by the alignment of primary cilia and crosses the center of each column of chondrocytes (a, left and right panels). Chondrocytes of the growth plate are known to divide parallel to the longitudinal axis of the bone (arrow-bar) (b, left panel). The daughter chondrocytes must undertake a series of cell movements/rotations and shape changes to generate the typical columns of the growth plate and align primary cilia on one common axis (a, b, left panel). A model is proposed in which an osteochondroma forms as a consequence of chondrocytes losing their ability to move/rotate to re-orient themselves with respect to the growth axis (arrow-bar) (b, right panel). Interestingly, some sub-populations of osteochondroma cells are able to form columns and to orient the cilium parallel to the longitudinal axis of the tumor (arrow-bar) (a, right panel).

The alignment of primary cilia along the growth plate supports the idea that the chondrocytes of the growth plate have the ability to move/rotate (Figure 6b) [2,4,33]. Integrins are the major class of cell adhesion molecules that mediate cell–matrix signaling pathways [33]. Integrins have heparan-binding domains, which indicate that heparan sulfate proteoglycans may modulate integrin signaling and cell adhesion [34]. Movement/rotation problems in the chondrocytes of the growth plate have been reported in β1-integrin-null mice [33]. The β1-integrin-null growth plates show larger and round-shaped proliferating chondrocytes arranged side by side, possibly reflecting impaired movement and inability to form columns [33]. Strikingly, β1-integrin receptors have been reported to colocalize with α-tubulin in the primary cilia of chondrocytes [35]. The loss of *EXT* expression results in disordered distribution of heparan sulfate proteoglycans. Recently, we showed that in osteochondromas, heparan sulfate proteoglycans are no longer present at the cell surface but accumulate in the cytoplasm [36]. Therefore, it is possible that the lack of heparan sulfate proteoglycans at the cell surface might influence cell adhesion and motility. The random orientation of the cilium in osteochondromas leads to the assumption that osteochondroma cells have impaired movement (Figure 6b) that may underlie the lack of orientation of the cells, which is a morphological characteristic of this tumor. The impaired movement might be caused by diminished heparan sulfate proteoglycans, which in turn could reduce integrin signaling activity and cell adhesion to the surrounding matrix.

In conclusion, we showed that the organization of primary cilia reflects cell polarity in the growth plate and in sub-populations of osteochondroma cells. We also showed that the ciliary formation in osteochondroma seems to be similar to that of the growth plate. The growth plate-like polarity retained in sub-populations of osteochondroma cells (organized into small columns) leads us to propose the existence of a mixture ('mosaic') of normal lining ($EXT^{+/-}$ or $EXT^{wt/wt}$) and $EXT^{-/-}$ cells in the cartilaginous cap of osteochondromas.

Note added in proof

Since the work described in this paper was completed and submitted for publication, the mixture ("mosaic") of normal lining ($EXT^{+/-}$ or $EXT^{wt/wt}$) and $EXT^{-/-}$ cells in the cartilaginous cap of osteochondromas has been elegantly reported by Jones et al (Proc Natl Acad Sci U S A 2010;107:2054–2059) using a conditional mouse model for *Ext1*.

Acknowledgements

We thank Annemieke M. van der Wal for the expert technical help. This study was supported by EuroBoNet, a European Commission-granted Network of Excellence for studying the pathology and genetics of bone tumors (Grant LSHC-CT-2006–018814).

References

1. Kronenberg HM. Developmental regulation of the growth plate. Nature 2003;15:332–336.
2. Dodds GS. Row formation and other types of arrangement of cartilage cells in endochondral ossification. Anat Rec 1930;46:385–399.
3. Song B, Haycraft CJ, Seo H, et al. Development of the post-natal growth plate requires intraflagellar transport proteins. Dev Biol 2007;305:202–216.
4. Li Y, Dudley AT. Noncanonical frizzled signaling regulates cell polarity of growth plate chondrocytes. Development 2009;136:1083–1092.
5. van den Berg H, Kroon HM, Slaar A, et al. Incidence of biopsy-proven bone tumors in children: a report based on the Dutch pathology registration 'PALGA'. J Pediatr Orthop 2008;28:29–35.
6. Benoist-Lasselin C, de Margerie E, Gibbs L, et al. Defective chondrocyte proliferation and differentiation in osteochondromas of MHE patients. Bone 2006;39:17–26.
7. Wheatley DN, Feilen EM, Yin Z, et al. Primary cilia in cultured mammalian cells: detection with an antibody against detyrosinated alpha-tubulin (ID5) and by electron microscopy. J Submicrosc Cytol Pathol 1994;26:91–102.
8. Poole CA, Flint MH, Beaumont BW. Analysis of the morphology and function of primary cilia in connective tissues: a cellular cybernetic probe? Cell Motil 1985;5:175–193.
9. Singla V, Reiter JF. The primary cilium as the cell's antenna: signaling at a sensory organelle. Science 2006;313:629–633.
10. Plotnikova OV, Golemis EA, Pugacheva EN. Cell cycle-dependent ciliogenesis and cancer. Cancer Res 2008;68:2058–2061.
11. Haycraft CJ, Zhang Q, Song B, et al. Intraflagellar transport is essential for endochondral bone formation. Development 2007;134:307–316.
12. McGlashan SR, Haycraft CJ, Jensen CG, et al. Articular cartilage and growth plate defects are associated with chondrocyte cytoskeletal abnormalities in Tg737orpk mice lacking the primary cilia protein polaris. Matrix Biol 2007;26:234–246.
13. Pedersen LB, Veland IR, Schroder JM, et al. Assembly of primary cilia. Dev Dyn 2008;237:1993–2006.
14. Sloboda RD, Rosenbaum JL. Making sense of cilia and flagella. J Cell Biol 2007;179:575–582.
15. Koyama E, Young B, Nagayama M, et al. Conditional Kif3a ablation causes abnormal hedgehog signaling topography, growth plate dysfunction, and excessive bone and cartilage formation during mouse skeletogenesis. Development 2007;134:2159–2169.

16. Patel V, Li L, Cobo-Stark P, et al. Acute kidney injury and aberrant planar cell polarity induce cyst formation in mice lacking renal cilia. Hum Mol Genet 2008;17:1578–1590.
17. Jones C, Roper VC, Foucher I, et al. Ciliary proteins link basal body polarization to planar cell polarity regulation. Nat Genet 2008;40:69–77.
18. Zhang Y, Wada J, Yasuhara A, et al. The role for HNF-1beta-targeted collectrin in maintenance of primary cilia and cell polarity in collecting duct cells. PLoS ONE 2007;2:e414.
19. McGlashan SR, Cluett EC, Jensen CG, et al. Primary cilia in osteoarthritic chondrocytes: from chondrons to clusters. Dev Dyn 2008;237:2013–2020.
20. Ascenzi MG, Lenox M, Farnum C. Analysis of the orientation of primary cilia in growth plate cartilage: a mathematical method based on multiphoton microscopical images. J Struct Biol 2007;158:293–306.
21. Donnelly E, Williams R, Farnum C. The primary cilium of connective tissue cells: imaging by multiphoton microscopy. Anat Rec (Hoboken) 2008;291:1062–1073.
22. Donnelly E, Ascenzi MG, Farnum C. Primary cilia are highly oriented with respect to collagen direction and long axis of extensor tendon. J Orthop Res 2010;28:77–82.
23. Romeo S, Bovée JVMG, Jadnanansing NAA, et al. Expression of cartilage growth plate signalling molecules in chondroblastoma. J Pathol 2004;202:113–120.
24. Aigner T, Frischolz S, Dertinger S, et al. Type X collagen expression and hypertrophic differentiation in chondrogenic neoplasias. Histochem Cell Biol 1997;107:435–440.
25. Bovée JVMG, Cleton-Jansen AM, Kuipers-Dijkshoorn N, et al. Loss of heterozygosity and DNA ploidy point to a diverging genetic mechanism in the origin of peripheral and central chondrosarcoma. Genes Chrom Cancer 1999;26:237–246.
26. Poole CA, Jensen CG, Snyder JA, et al. Confocal analysis of primary cilia structure and colocalization with the Golgi apparatus in chondrocytes and aortic smooth muscle cells. Cell Biol Int 1997;21:483–494.
27. Prins FA, Diemen-Steenvoorde R, Bonnet J, et al. Reflection contrast microscopy of ultrathin sections in immunocytochemical localization studies: a versatile technique bridging electron microscopy with light microscopy. Histochem 1993;99:417–425.
28. Holmes LB, Trelstad RL. Cell polarity in precartilage mouse limb mesenchyme cells. Dev Biol 1980;78:511–520.
29. Lu CJ, Du H, Wu J, et al. Non-random distribution and sensory functions of primary cilia in vascular smooth muscle cells. Kidney Blood Press Res 2008;31:171–184.
30. Abad V, Meyers JL, Weise M, et al. The role of the resting zone in growth plate chondrogenesis. Endocrinology 2002;143:1851–1857.

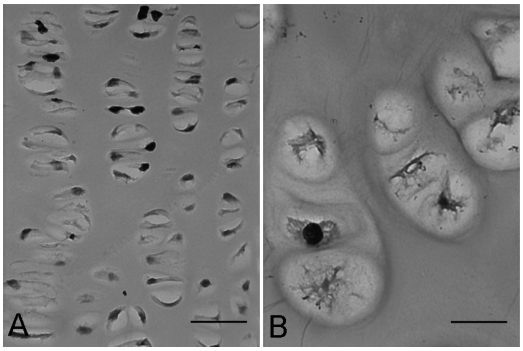
31. Campbell JT, Kaplan FS. The role of morphogens in endochondral ossification. Calcif Tissue Int 1992;50:283–289.
32. Bornens M. Organelle positioning and cell polarity. Nat Rev Mol Cell Biol 2008;9:874–886.
33. Aszodi A, Hunziker EB, Brakebusch C, et al. Beta1 integrins regulate chondrocyte rotation, G1 progression, and cytokinesis. Genes Dev 2003;17:2465–2479.
34. Beauvais DM, Burbach BJ, Rapraeger AC. The syndecan-1 ectodomain regulates alphavbeta3 integrin activity in human mammary carcinoma cells. J Cell Biol 2004;167:171–181.
35. McGlashan SR, Jensen CG, Poole CA. Localization of extracellular matrix receptors on the chondrocyte primary cilium. J Histochem Cytochem 2006;54:1005–1014.
36. Hameetman L, David G, Yavas A, et al. Decreased EXT expression and intracellular accumulation of HSPG in osteochondromas and peripheral chondrosarcomas. J Pathol 2007;211:399–409.

Supplementary Information

Supplementary Table S1. Summary of clinicopathological and tumor data.

Patient no.	Material	Age (years)	Gender	MO/solitary	Location	Thickness of Cartilage Cap (mm)
L741	GP	2	M	-	Femur	-
L996	GP	8	M	-	Femur	-
L1142	GP	12	F	-	Femur	-
L1234	GP	8	F	-	Femur	-
L2461	GP	9	F	-	Femur	-
L296	OC	24	M	Solitary	Tibia	4
L523	OC	20	F	MO	Femur	6
L726	OC	6	M	MO	Rib	4
L1591	OC	23	M	Solitary	Femur	3
L2489	OC	15	M	Solitary	Humerus	5

GP – growth plate; OC – osteochondroma; MO – multiple osteochondroma.



Supplementary Figure S1. The proliferation rate of the growth plate and osteochondroma. Immunohistochemistry with Ki-67 antibody, a known marker for cell proliferation, is used to show that the proliferation rate is higher in proliferating zone of the growth plate and lower in an osteochondroma. Positive nuclei are often present in proliferating chondrocytes from the growth plate (a; from a 2-year-old patient) and rarely present in osteochondromas (b; from a 6-year-old patient). (Scale bars, 10 µm).

Chapter 7

Secondary peripheral chondrosarcoma evolving from osteochondroma as a result of outgrowth of cells with functional *EXT*

Carlos E. de Andrea, Christianne M.A. Reijnders,
Herman M. Kroon, Daniëlle de Jong,
Pancras C. W. Hogendoorn, Karoly Szuhai
and Judith V.M.G. Bovée
Oncogene 2012;31:1095–1104

Abstract

Secondary peripheral chondrosarcoma is the result of malignant transformation of a pre-existing osteochondroma, the most common benign bone tumor. Osteochondromas are caused by genetic abnormalities in *EXT1* or *EXT2*: homozygous deletion of *EXT1* characterizes sporadic osteochondromas (non-familial/solitary), and germline mutations in *EXT1* or *EXT2* combined with loss of heterozygosity define hereditary multiple osteochondromas. While cells with homozygous inactivation of *EXT* and wild-type cells shape osteochondromas, the cellular composition of secondary peripheral chondrosarcomas and the role of *EXT* in their formation have remained unclear. We report using a targeted-tiling-resolution oligo-array-CGH (array comparative genomic hybridization) that homozygous deletions of *EXT1* or *EXT2* are much less frequently detected (2/17, 12%) in sporadic secondary peripheral chondrosarcomas than expected based on the assumption that they originate in sporadic osteochondromas, in which homozygous inactivation of *EXT1* is found in ~80% of our cases. FISH with an EXT1 probe confirmed that, unlike sporadic osteochondromas, cells from sporadic secondary peripheral chondrosarcomas predominantly retained one (hemizygous deleted loci) or both copies (wild-type) of the *EXT1* locus. By immunohistochemistry, we confirm the presence of cells with dysfunctional *EXT1* in sporadic osteochondromas and show cells with functional *EXT1* in sporadic secondary peripheral chondrosarcomas. These immuno results were verified in osteochondromas and secondary peripheral chondrosarcomas in the setting of hereditary multiple osteochondromas. Our data therefore point to a model of oncogenesis in which the osteochondroma creates a niche in which wild-type cells with functional *EXT* are predisposed to acquire other mutations giving rise to secondary peripheral chondrosarcoma, indicating that *EXT*-independent mechanisms are involved in the pathogenesis of secondary peripheral chondrosarcoma.

Keywords: chondrosarcoma; osteochondroma; *EXT1*; array-CGH; FISH; bone tumors

Introduction

Secondary peripheral chondrosarcomas arise in the cartilaginous cap of a pre-existing osteochondroma (Bertoni et al., 2002). Osteochondromas are the most common benign bone tumors of adolescence (Khurana et al., 2002; van den Berg et al., 2008). They occur as sporadic (non-familial/solitary) or multiple (hereditary) cartilage-capped bony projections from the metaphyses of endochondral bones adjacent to the growth plate (Khurana et al., 2002; Bovee et al., 2010). Osteochondromas develop during skeletal growth (13–15 years) and cease to grow when the growth plate fuses at puberty (van den Berg et al., 2008).

Sporadic and multiple osteochondromas have been linked to genetic alterations in two main loci, *EXT1* at 8q24 (65%) or *EXT2* at 11p11-13 (35%) (Bovee et al., 2010). The majority of the multiple osteochondromas (70–75%) are caused by point mutations. Deletions involving single or multiple exons are found in about 10% of all hereditary cases and no genomic alterations are detected in about 10–15%. In some of these negative cases, somatic mosaicism with large genomic deletions of *EXT1* and *EXT2* have been described as the underlying mechanism of multiple osteochondroma formation (Szuhai et al., 2011). In sporadic osteochondromas, homozygous deletions of *EXT1* are identified (Hameetman et al., 2007b; Reijnders et al., 2010; Zuntini et al., 2010; Szuhai et al., 2011). Recent experimental studies using mice and zebrafish knockdown models show that homozygous inactivation of *Ext1* or *Ext2* is required for osteochondromagenesis (Clément et al., 2008; Jones et al., 2010; Matsumoto et al., 2010). In humans, loss of the remaining wild-type allele of *EXT* has been detected in approximately 40% of sporadic and multiple osteochondromas (Hameetman et al., 2007b; Reijnders et al., 2010; Zuntini et al., 2010). In sporadic osteochondromas, we have described homozygous deletions of *EXT1* in ~80% of the cases (Hameetman et al., 2007b; Reijnders et al., 2010; Zuntini et al., 2010). It was shown recently that during the formation of osteochondromas, chondrocytes with functional *EXT* from the growth plate or the neighboring tissue are being integrated into the cartilaginous cap, generating a mosaic mixture of wild-type cells and cells with homozygous inactivation of *EXT1* or *EXT2* (de Andrea et al., 2010, 2011; Jones et al., 2010; Matsumoto et al., 2010).

Less than 1% of patients with sporadic osteochondromas and 1–3% of patients with multiple osteochondromas at the age of 30–60 years will eventually develop a secondary peripheral chondrosarcoma (Dorfman et al., 2002). Secondary peripheral chondrosarcomas are malignant cartilage-producing tumors. Contrary to what is observed in osteochondromas, homozygous inactivations of the *EXT* genes are detected in a much smaller subset (~15%) of secondary peripheral chondrosarcomas (Hecht et al., 1995; Raskind et al., 1995; Bovée et al., 1999; Hallor et al., 2009; Zuntini et al., 2010).

Although osteochondromas and secondary peripheral chondrosarcomas are associated, many aspects on the pathogenesis of this malignant bone tumor remain unestablished.

The homozygous inactivation of the *EXT* genes required for osteochondromagenesis, the mixture of cells with distinct genetic background within the osteochondroma cap and the low frequency of homozygous inactivation of the *EXT* genes in secondary peripheral chondrosarcomas lead to two central questions: (i) Are the cells with homozygous inactivation of *EXT1/2* of osteochondromas the cellular origin of secondary peripheral chondrosarcomas? (ii) Do the *EXT* genes act as tumor-suppressor genes in the formation of secondary peripheral chondrosarcomas?

To address these unsolved questions, we studied 17 clinically and radiologically well-documented secondary peripheral chondrosarcomas derived from sporadic osteochondromas. The copy-number alterations of *EXT1* or *EXT2* were assessed by targeted-tiling-resolution oligo-array-CGH and the genetic changes involving the *EXT1* locus were investigated by fluorescence in situ hybridization (FISH). Additionally, the potential function of *EXT1* was explored by immunohistochemistry. Sporadic osteochondromas were used as a reference to understand the formation of a secondary peripheral chondrosarcoma. Multiple osteochondromas and secondary peripheral chondrosarcomas derived from patients with multiple osteochondromas were used to validate the generated model.

Results

Clinical findings and imaging studies

The anatomical distribution and the cartilaginous cap thickness of the 17 sporadic peripheral chondrosarcomas are shown in Table 1. Sixteen patients showed no adverse outcome (metastases or death of disease). However, one patient with a pelvic lesion developed a large local recurrence approximately 3 years after the primary surgery and died a few months later of the disease. No germline mutations in *EXT1* or *EXT2* were detected. In the imaging studies, a pre-existing osteochondroma and/or its stalk were identified in all 17 cases (Supplementary Figure 1). All cases diagnosed as grade-I secondary peripheral chondrosarcoma fulfilled the criteria for recommending resection for malignant concerns. These criteria included histological features in accordance with the WHO classification (Khurana et al., 2002; van den Berg et al., 2008) or a cartilage cap thickness of 1.5 cm or greater, or a clinical history and/or radiographic signs of tumor growth (Supplementary Figure 1B–B4). Case L-868 was radiologically classified as a borderline lesion. The criteria used for this case included age of the patient (18-year-old man) with a growing lesion on an almost mature skeleton, in which the growth plates were nearly closed (Supplementary Figure 2).

Table 1. Clinical and radiological information. FISH and EXT-tiling array results.

Case Number	Sample	Age	Location	Cartilaginous cap thickness	Fluorescent in situ Hybridization with an EXT1 probe				EXT tiling array
					No Loss	Hemizygous Loss	Homozygous Loss	Gain*	
L-741	GP	8	-	-	86%	10%	4%	0	
L-1142	GP	12	-	-	89%	9%	2%	0	
L-2390	AC	54	-	-	93%	5%	2%	0	
L-2776	AC	60	-	-	93%	6%	1%	0	
	Cut-off values				-	15%	6%	-	
L-0657	OC	12	Distal Femur	1.5 cm	NA	NA	NA	NA	Homozygous loss *EXT1***
L-0673	OC	12	Proximal Humerus	0.2 cm	7%	2%	91%	0	Homozygous loss *EXT1***
L-1455	OC	17	Proximal Fibula	1 cm	7%	3%	90%	0	Homozygous loss *EXT1***
L-1520	OC	16	Proximal Humerus	0.5 cm	9%	2%	89%	0	Homozygous loss *EXT1***
L-1649	OC	21	Proximal Humerus	1.5 cm	5%	0	95%	0	Homozygous loss *EXT1***
L-1480	grade I PCS	16	Distal Femur	1.5 cm	NA	NA	NA	NA	Normal CGH Profile
L-2644	grade I PCS	46	Proximal Fibula	1 cm	NA	NA	NA	NA	Normal CGH Profile
L-868	Borderline lesion	18	Proximal Humerus	1 cm	24%	34%	42%	0	Hemizygous loss of *EXT1*
L-163	grade I PCS	49	Proximal Tibia	2 cm	NA	NA	NA	NA	Hemizygous loss of *EXT1*
L-626	grade I PCS	21	Proximal Femur	4 cm	60%	28%	12%	0	Hemizygous loss of *EXT1*
L-627	grade I PCS	32	Scapula	2 cm	NA	NA	NA	NA	Hemizygous loss of *EXT1*
L-724	grade I PCS	83	Pelvis	15 cm	NA	NA	NA	NA	Hemizygous loss of *EXT1*
L-739	grade I PCS	37	Pelvis	10 cm	48%	47%	5%	0	Hemizygous loss of *EXT1*
L-1655	grade I PCS	40	Proximal Femur	2 cm	NA	NA	NA	NA	Hemizygous loss of *EXT1*
L-2361	grade I PCS	25	Femur	2 cm	8%	77%	15%	0	Hemizygous loss of *EXT1*
L-11	grade II PCS	49	Pelvis	8 cm	9%	74%	11%	6%	Hemizygous loss of *EXT1*
L-76	grade II PCS	49	Pelvis	20 cm	44%	54%	2%	0	Hemizygous loss of *EXT1*
L-1165	grade II PCS	38	Pelvis	14 cm	NA	NA	NA	NA	Hemizygous loss of *EXT1*
L-1618	grade II PCS	44	Pelvis	30 cm	36%	43%	21%	0	Hemizygous loss of *EXT1*
L-224	grade II PCS	26	Pelvis	11 cm	40%	42%	16%	2%	Homozygous loss *EXT1* exon 10***
L-1245	grade I PCS	25	Proximal Fibula	0.8 cm	4%	84%	12%	0	Homozygous loss *EXT1* exon 2-11
L-123	grade II PCS	60	Distal Femur	13 cm	73%	7%	0	20%	Gain of the *EXT1*region

GP, epiphyseal growth plate; AC, articular cartilage; OC, sporadic osteochondroma; PCS, sporadic secondary peripheral chondrosarcoma; FISH, fluorescence *in situ* hybridization; NA, not available due to bad FISH; *, increased of both centromere 8 and EXT1 FISH signals; **, results previously reported (Hameetman et al. 2007b); ***, the size of the deletion is smaller the used BAC probe. Blue areas show significant retention of both copies of *EXT1*; green areas, hemizygous loss of EXT1; red areas, homozygous loss of EXT1; and gray areas gain of the *EXT1* genomic region.

Homozygous deletions of EXT1/2 are uncommon in sporadic secondary peripheral chondrosarcomas

A custom-made, oligonucleotide-based microarray with a tiling coverage of *EXT1/2* genes was used to detect deletions involving any part of *EXT1* or *EXT2* genes. At least 90% of tumor tissue was isolated and analyzed in each case. Table 1 summarizes the results of the array comparative genomic hybridization (array-CGH) analysis. In the 17 sporadic secondary peripheral chondrosarcomas, homozygous deletion of *EXT1* was found in two cases (L-1245, grade-I; and L-224, grade-II) (Figure 1). L-1245 showed deletions involving exon-2 to exon-11. Based on the array profile of L-1245, the proportion of the cell fraction containing homozygous deletion of *EXT1* was ~25% (Figure 1). L-224 showed deletions in exon-10, which is smaller than the bacterial artificial chromosome probe used for FISH analysis. Hemizygous deletion of *EXT1* was found in 12 cases (not shown). A significant gain of chromosome arm 8q was identified in one case (L-123, not shown). No alterations involving the *EXT1* gene were seen in two cases (Figure 1). Additionally, no alterations involving the *EXT2* gene were identified (not shown).

Retention of one or both copies of EXT1 in the cells of sporadic secondary peripheral chondrosarcomas

To further investigate the genetic changes in *EXT1*, FISH was performed in the setting of sporadic lesions and was successful in 10 out of 17 secondary peripheral chondrosarcomas and in 4 out of 5 sporadic osteochondromas. Failures were due to DNA damage as a result of decalcification. In sporadic osteochondromas, the majority of the cells showed loss of both copies (homozygous loss) of the *EXT1* locus (mean of all cases: 91%; Figure 2 and Table 1), as expected. Surprisingly, within the tumor, cells retaining both copies of the *EXT1* locus (wild-type alleles) were also observed (mean of all cases: 7%; Figure 2 and Table 1), which were commonly located in the hypertrophic layer of the osteochondroma cap (Supplementary Figure 3). Although hemizygous losses were detected, the number of cells with one copy of the gene was below the cut-off value based on the correction factors obtained from FISH data from growth plate and articular cartilage, indicating that these losses reflected truncation artifacts. In each analyzed sporadic peripheral chondrosarcoma, the patterns of copy-number alterations involving the *EXT1* locus compared with the chromosome-8 centromere signals varied widely (Figure 2 and Table 1). Five cases showed cells with no losses (wild-type alleles), as well as hemizygous and homozygous deletions. Two cases showed cells with wild-type and hemizygous deleted loci. One case showed cells with no loss, hemizygous deletion and gain of the *EXT1* locus. Two cases showed cells with no losses, hemizygous and homozygous deletion, as well as gain of the *EXT1* locus. Additionally, all except three cases (L-739, grade-I; L-868, borderline cases; L-2361, grade-I) showed aneuploid cells (>2 signals with a centromere-8 probe) ranging from 4 to 50% of the total amount of cells.

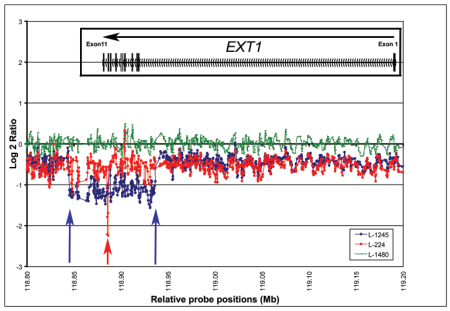


Figure 1. Array-CGH results overview of the genomic region on chromosome-8, including the *EXT1* gene area, shows the profile of samples with homozygous deletions (L-224, a grade-II secondary peripheral chondrosarcoma; and L-1245, a grade-I secondary peripheral chondrosarcoma). In both cases, loss of an area that exceeded the *EXT1* region (indicated by the values lower than 0) containing a region with additional deletion ranging from ~100 kb (blue arrows) to ~10 kb (red arrow) reflecting the homozygous deletion were detected. As reference, a sample (L-1480, a grade-I secondary peripheral chondrosarcoma) with no alteration involving *EXT1* was plotted in green.

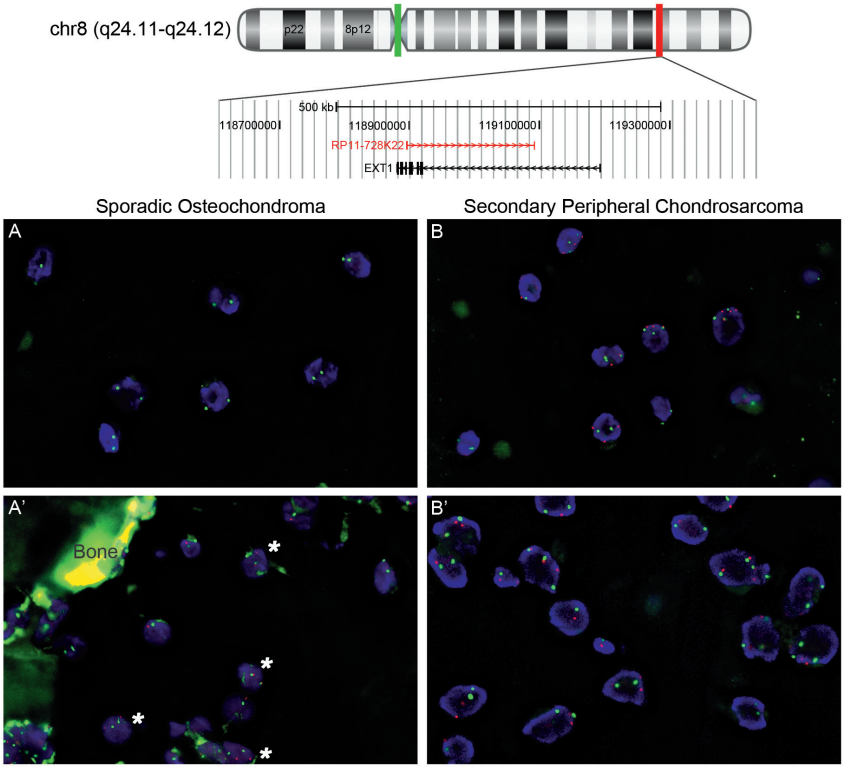


Figure 2. Genomic deletions detected by FISH using an EXT1 probe. The illustration (upper panel) is showing the exact locations and the assigned colors of the used EXT1 locus (red) and centromere-8 (green) probes. Samples were counterstained using 4',6-diamidino-2-phenylindole (DAPI), indicating the nucleus of individual cells in blue. (a) The lack of red signals with retained green signals indicates a homozygous loss of the EXT1 loci, which characterize the superficial layer of a sporadic osteochondroma (L-673). (a') Cells with retained red signals (wild-type, asterisks) and loss of both copies were observed in the hypertrophic layer of a sporadic osteochondroma (L-673), indicating the presence of two cell populations. (b, b') EXT1 wild-type cells and gain of the EXT1 genomic region were detected in secondary peripheral chondrosarcomas (L-123, grade-II).

In three remarkably large lesions (L-76, L-123 and L-739) no significant homozygous losses were identified; however, hemizygous loss was detected (Table 1). There was no correlation between the size of the lesion and the percentage of cells carrying a homozygous deletion (Spearman's coefficient=0.31).

Cells with functional EXT in sporadic and hereditary secondary peripheral chondrosarcomas

EXT1 and *EXT2* genes encode ubiquitously expressed type-II transmembrane glycosyltransferases (EXT1 and EXT2) (McCormick et al., 1998), which localize to the endoplasmic reticulum and Golgi complex, and are required for the synthesis of heparan sulfate chains on proteoglycans (Zak et al., 2002; Bulow and Hobert, 2006). To assess the potential function of *EXT1*, we evaluated the expression of the EXT1 protein, using an EXT1 antibody, and the production of heparan sulfate, using the 10E4 antibody, in the setting of sporadic and multiple lesions. The results are shown in Figures 3 and 4, and Supplementary Table 1. In both sporadic and multiple lesions, there were more EXT1- and heparan sulfate-positive chondrocytes in the hypertrophic layer than in the superficial layer. The control growth plate is shown in Supplementary Figure 4.

In the setting of sporadic lesions (Figure 3), no significant changes in the number of cells staining with EXT1 and 10E4 were seen in the hypertrophic layer when comparing osteochondromas to secondary peripheral chondrosarcomas (P=0.70). Significant changes were observed in the superficial layer of these tumors; an increasing number of cells staining with EXT1 and 10E4 were observed with increasing histological grade (Figure 3). The number of cells staining with EXT1 and 10E4 were significantly higher in the superficial layer of grade-II secondary peripheral chondrosarcomas when compared with osteochondromas and grade I secondary peripheral chondrosarcomas (P=0.035 and P=0.032, respectively). No correlation was found between age of the patient and the percentage of EXT1/10E4-positive cells (Spearman's coefficient=0.02 each), nor between size of the cartilage cap and the percentage of EXT1/10E4-positive cells (Spearman's coefficient=0.27 and 0.20, respectively).

In the setting of multiple lesions (Figure 4), the number of cells staining with EXT1 and 10E4 were significantly higher in secondary peripheral chondrosarcomas when compared to osteochondromas (for EXT1 at hypertrophic layer: P=0.006; and at superficial layer: P<0.001; and for heparan sulfate at hypertrophic layer: P=0.007; and at hypertrophic layer: P=0.008).

Discussion

Osteochondromas originate either from the chondrocytes of the growth plate or the cells of the perichondrium due to homozygous inactivation of *EXT1* or *EXT2* (Clément et al., 2008; Jones et al., 2010; Matsumoto et al., 2010).

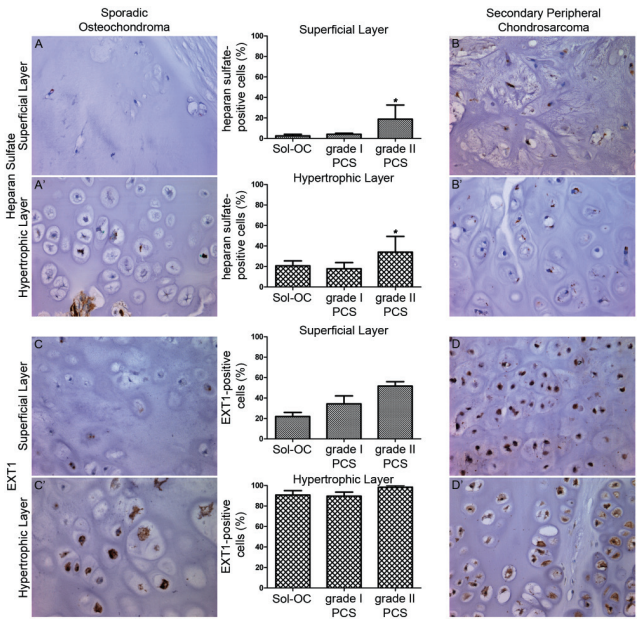


Figure 3. Immunohistochemical screening of cells with functional EXT1 in sporadic osteochondromas and peripheral chondrosarcomas. In the superficial layer of the cartilage cap, there was an increase of cells with functional *EXT1* (10E4- and EXT1-positive cells) upon neoplastic transformation from osteochondromas (a, c, respectively) to peripheral chondrosarcomas (b, d, respectively). In the hypertrophic layer, no significant changes were observed in the percentage of cells stained with EXT1 and 10E4 when comparing osteochondromas (a', c', respectively) to peripheral chondrosarcomas (b', d', respectively). The asterisks indicate P<0.05. Sol-OC, sporadic osteochondromas; PCS, sporadic secondary peripheral chondrosarcoma.

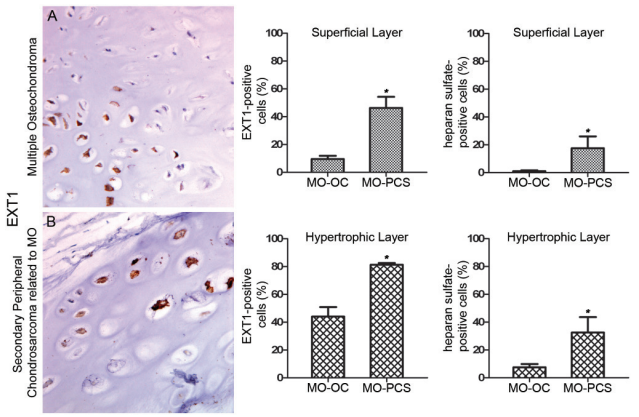


Figure 4. Immunohistochemical screening of cells with functional EXT1 in multiple osteochondromas (a) and peripheral chondrosarcomas (b) related to patients with multiple osteochondromas. In the superficial layer and in the hypertrophic layer of the cartilage cap, there was a significant increase of cells with functional *EXT1* (10E4- and EXT1-positive cells) upon neoplastic transformation from osteochondromas to peripheral chondrosarcoma. The asterisks indicate P<0.05. MO-OC, multiple osteochondromas; MO-PCS, peripheral chondrosarcoma related to patients with multiple osteochondroma.

During osteochondromagenesis, wild-type chondrocytes and cells with homozygous inactivation of EXT are shown to intermingle in the cartilaginous cap (de Andrea et al., 2010, 2011; Jones et al., 2010; Matsumoto et al., 2010). We here show that, in human osteochondromas, the wild-type chondrocytes showing both *EXT1* alleles are predominantly located in the hypertrophic layer of the osteochondroma cap.

As the chance of detecting the second hit in the *EXT1* gene depends on the ratio of wild-type versus mutated cells, our data indicate that the probability to detect a homozygous deletion in osteochondromas increases when tumor sampling is more superficial (near the perichondrium), which may explain the conflicting data that have been published by independent institutions (Hameetman et al., 2007b; Reijnders et al., 2010; Zuntini et al., 2010).

The current multistep genetic model for secondary peripheral chondrosarcoma formation assumes that osteochondroma cells with homozygous inactivation of *EXT1* or *EXT2* acquire one or more additional genetic alterations to progress into malignancy (Bovée et al., 2000). By analyzing clinically and radiologically well-documented peripheral cartilaginous tumors, we demonstrate that homozygous inactivation of the *EXT1* locus in sporadic secondary peripheral chondrosarcoma (2/17, 12%) is much less frequently detected than expected based on the assumption that it originates in a sporadic osteochondroma, in which homozygous inactivation of *EXT1* is found in ~80% of the cases reported by our institution (Hameetman et al., 2007b; Reijnders et al., 2010). *EXT* tiling array demonstrated that the most frequent event in sporadic secondary peripheral chondrosarcomas is hemizygous loss of EXT1 (12/17, 70%), followed by no alterations in *EXT1* (2/17, 12%) and gain of the EXT1 region (1/17, 6%). No deletions involving the *EXT2* gene were identified. FISH using an EXT1 probe confirmed the presence of cells with hemizygous loss and, in addition, revealed a wide intra-tumoral heterogeneity for the *EXT1* gene including homozygous losses, retentions and gains.

Immunohistochemistry against EXT1 and heparan sulfate (10E4) was used to evaluate the spatial distribution of cells with functional or dysfunctional *EXT1* in sporadic osteochondromas and sporadic secondary peripheral chondrosarcomas. The findings were further validated in multiple osteochondromas and secondary peripheral chondrosarcomas derived from patients with multiple osteochondromas. Cells with dysfunctional *EXT1* (that is, non-staining with EXT1 and heparan sulfate) are mainly populating the superficial layer of sporadic and multiple osteochondromas, which is in line with our previous results showing homozygous loss of *EXT1* in sporadic and multiple osteochondromas (Hameetman et al., 2007b; Reijnders et al., 2010). By contrast, cells with functional *EXT1* are present in the superficial layer (region near the perichondrium) of secondary peripheral chondrosarcomas related to sporadic or multiple osteochondromas, which is in line with the absence of homozygous deletions in the majority of sporadic peripheral chondrosarcomas. In addition, the amount of cells with functional *EXT1* increases with increasing tumor grade. We also observed that the percentage of EXT1-positive cells is slightly higher than the percentage of heparan sulfate-positive cells, which suggests that the cell's environment may enhance or diminish the production of heparan sulfate by modulating the activity of *EXT1* in a cell.

Taken together, whereas cells with homozygous inactivation of *EXT1* constitute an osteochondroma, cells with wild-type, functional *EXT1* compose a fully developed secondary peripheral chondrosarcoma (Figure 5). Therefore, it is possible to envision a model where secondary peripheral chondrosarcoma cells with functional *EXT1* outgrow osteochondroma cells with dysfunctional *EXT1*. This model can be demonstrated in two distinct sets of tumors: (i) In lesions with a thin cartilaginous cap thickness, cells that lost both copies of EXT1 and cells that retain one or both copies of *EXT1* are found (that is, L-868 and L-1245, both ~1 cm). In this situation, osteochondroma cells and secondary peripheral chondrosarcoma cells may be coexisting. (ii) In remarkably large lesions, cells that lost both copies of *EXT1* are absent (that is, L-76, 30 cm; L-123, 15 cm and L-739, 11 cm). In this instance, only secondary peripheral chondrosarcoma cells that retain one or both copies of EXT1 may be growing. The proposed model is reinforced by the fact that cells carrying a homozygous deletion (having no copies of the involved genomic region left at all) are not able to regain the lost alleles during neoplastic progression.

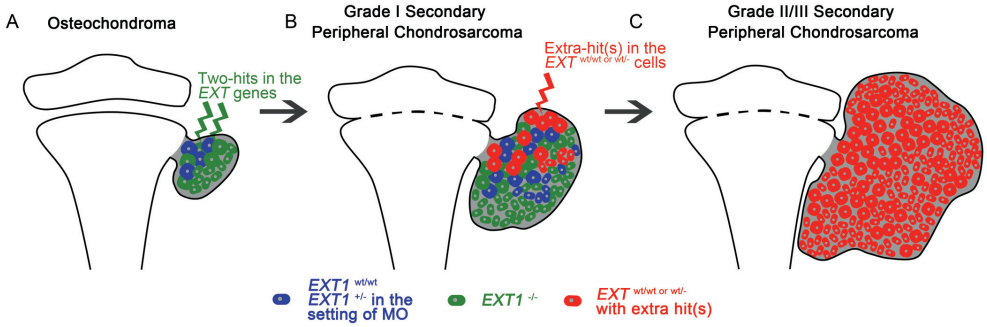


Figure 5. Secondary peripheral chondrosarcomagenesis. (a) EXT-null cells (green) and EXT wild-type cells (blue) compose the osteochondroma cap. (b) The EXT-null cells form a niche, a permissive microenvironment, which predisposes the EXT wild-type cell within the osteochondroma or from the perichondrium to acquire mutation(s) not related to EXTs to give rise to a secondary peripheral chondrosarcoma. The chondrosarcoma cells (red) get a proliferative advantage over the osteochondroma EXT-null cells. During neoplastic progression, the chondrosarcoma cells may or may not lose one copy of the EXT1 gene. (c) Only chondrosarcoma cells, which retained one or both copies of the EXT genes, form the fully developed secondary peripheral chondrosarcoma. MO, multiple osteochondromas.

In myelodysplasia and secondary leukemia, a 'niche-based' model of oncogenesis has been described, in which a change in a specific niche/microenvironmental cell can serve as the primary moment in a multi-step process toward the malignancy of a supported, but distinct, cell type (Raaijmakers et al., 2010; Raaijmakers, 2011). This model of oncogenesis seems to explain the formation of a secondary peripheral chondrosarcoma.

The osteochondroma cells with homozygous inactivation of *EXT* (loss of both copies of *EXT*) create a niche (a permissive microenvironment), which facilitates cells with functional *EXT* (retention of one or both copies of *EXTs*) located either in the osteochondroma cap or in the perichondrium that closely surrounds the lesion to acquire secondary genetic changes. Although the secondary peripheral chondrosarcoma-driving mutations are so far unknown, they differ from *EXT* mutations, indicating that *EXT*-independent mechanisms have a role in the pathogenesis of secondary peripheral chondrosarcoma. The need of functional *EXT* and heparan sulfate for cell proliferation is supported by the fact that inactivation of *EXT1* in multiple myeloma leads to decreased tumor growth (Reijmers et al., 2010) and that *EXT*-null chondrocytes do not grow in vitro (Reijnders et al., 2010). Additionally, cells with functional *EXT* in the mosaic osteochondroma cap are suggested to provide a certain threshold level and distribution of heparan sulfate, creating an environment conducive to cells with homozygous inactivation of *EXT* to proliferate and form a tumor (de Andrea et al., 2010, 2011; Jones et al., 2010; Matsumoto et al., 2010).

Osteochondromas and secondary peripheral chondrosarcomas composed by distinct cell types is strengthened by some of our previous results. First, the mRNA expression level of *EXT1* in osteochondromas is not completely absent, which suggests the presence of cells with functional *EXT1* in the tumor. Second, although not significant, the mRNA level of EXT1 seems to increase from low- to high-grade in secondary peripheral chondrosarcomas (Hameetman et al., 2007a). We have also shown that signaling pathways dependent on heparan sulfate, such as fibroblast growth factor and parathyroid hormone-related protein, are inactive in osteochondromas and active in secondary peripheral chondrosarcomas. The heparan sulfate with normal chain length synthesized by the overgrown *EXT1* wild-type cells might be related to the activation of fibroblast growth factor and parathyroid hormone-related protein in secondary peripheral chondrosarcoma.

Although we show that the vast majority of sporadic secondary peripheral chondrosarcomas do not have homozygous deletions involving *EXT1* or *EXT2*, the few reported cases with homozygous deletions of *EXT1* or *EXT2* (2/17 in the present series) suggest that malignant transformation of osteochondroma cells with homozygous inactivation of *EXT1* or *EXT2* is a rare event. Usually, these are small deletions of *EXT1* (that is, case L-224) unable to be detected by FISH.

While our data clarify the pathogenesis of secondary peripheral chondrosarcoma, a number of questions remain. For instance, which is the causative gene for peripheral chondrosarcoma formation? What factors make chondrocytes with functional *EXT1* and *EXT2* within/surrounding an osteochondroma more prone to acquire mutations that lead to malignancy?

In summary, our study shows that (i) an osteochondroma is a niche that facilitates the *EXT1* wild-type cells to acquire other mutations, distinct from mutations involving the *EXT* genes, for secondary peripheral chondrosarcoma formation; (ii) secondary peripheral chondrosarcoma is not per se originating from cells of osteochondroma with homozygous inactivation of *EXT1*, but arises predominantly and maybe even exclusively from cells with functional *EXT1* (Figure 5).

Materials and methods

Patient data and tumor samples

Based on clinical information and radiological studies, 17 sporadic secondary peripheral chondrosarcomas, in which paraffin-embedded and frozen material were available, were retrieved from the Department of Pathology at Leiden University Medical Center collected between 1991 and 2008. In addition, paraffin-embedded material from sporadic (n=10) and multiple (n=10) osteochondromas, and secondary peripheral chondrosarcomas related to patients with multiple osteochondromas (n=5), were selected for comparison in the different used techniques. For controls, epiphyseal growth plate (n=2) and articular cartilage (n=2) were obtained from orthopedic resections for pathological conditions not related to osteochondroma or chondrosarcoma. Chondrosarcoma histological grading was evaluated according to the Evans classification (Evans et al., 1977). Imaging studies (radiography, computed tomographic scans and magnetic resonance imaging scans) were reviewed in all 17 sporadic secondary peripheral chondrosarcomas and in five sporadic osteochondromas. The cartilaginous cap thickness was measured in accordance with Bernard et al. (2010). All samples were handled in a coded manner and all procedures were performed according to the ethical guidelines in Code for Proper Secondary Use of Human Tissue in The Netherlands (Dutch Federation of Medical Scientific Societies).

DNA isolation

Per sample about 60 frozen tumor sections (16-µm thick) were cut. DNA was isolated by using the Wizard Genomic DNA Purification kit (Promega, Madison, WI, USA) according to the manufacturer's manual. DNA concentration and purity were measured for each sample by using a NanoDrop spectrophotometer (Isogen, De Meern, the Netherlands) and a Bioanalyzer (Agilent, Santa Clara, CA, USA), respectively, according to the manufacturer's protocol. The percentage of tumor cells within each sample was determined on hematoxylin and eosin-stained sections and occasionally normal/reactive tissue was removed by macrodissection to achieve at least 90% of tumor tissue.

Mutation screening

The genomic DNA of five sporadic peripheral chondrosarcomas was tested for mutations in

EXT1 and *EXT2*. The mutation status from 12 cases has been reported previously (Hameetman et al., 2007a). Mutation screening of *EXT1* or *EXT2* genes was performed and analyzed as described earlier (Hameetman et al., 2007a; Reijnders et al., 2010).

EXT tiling array

Seventeen sporadic peripheral chondrosarcomas, well-known for not showing point mutations in the *EXT* genes (Bovée et al., 1999; Hallor et al., 2009; Zuntini et al., 2010), were collected to study DNA copy-number alterations by using a custom-made Agilent oligonucleotide-based microarray containing 44 000 probes with a tiling coverage of *EXT1/2* genes and additional 68 genes involved in heparan and chondroitin sulfate biosynthesis as described by Szuhai et al. (2011). Only alterations of *EXT* genes were investigated. *EXT* tiling array in sporadic osteochondromas has been described previously by our group in a series of 11 tumors (Hameetman et al., 2007b; Reijnders et al., 2010). Labeling and hybridization of genomic DNA from freshly frozen tumor, as well as data processing, were performed as described earlier (Reijnders et al., 2010; Szuhai et al., 2011).

Fluorescent in situ hybridization

Interphase FISH on 16-µm-thick paraffin sections was performed in all 17 sporadic secondary peripheral chondrosarcomas, as described previously (Szuhai et al., 2009). The five sporadic osteochondromas used for comparison were reported previously to show homozygous deletion of *EXT1* (Hameetman et al., 2007b). Two sets of FISH probes were applied: Set 1 with the RP11-728K22 bacterial artificial chromosome clones covering the *EXT1* genomic region and Set-2 with the probe for the centromere of chromosome-8. RP11-728K22 was selected by using the UCSC Genome Browser (NCBI 36.1/hg18) (http://genome.ucsc.edu) (Figure 2). Copy-number and image analysis were performed as described by Mohseny et al. (2010) and Pansuriya et al. (2011). At least 100 cells were scored per case (more than 200 for most of the cases) counting the centromere-8 probe and the EXT1 probe. Cells with more than two centromere-8 probes were considered aneuploid; loss of one copy of *EXT1* probe was considered as a hemizygous gene loss and loss of all copies of the *EXT1* probe was considered as a homozygous deletion of the gene. Gain was defined as the presence of at least three copies of the *EXT1* probe in diploid cells. To determine the cut-off values indicating true loss of the genomic region, the percentage of gene loss was determined in two epiphyseal growth plates and two articular cartilages. From the four cases the mean (7% for hemizygous loss and 2% for homozygous loss) and the s.d. of false positive losses (2% for hemizygous loss and 1% for homozygous loss) were calculated. The mean plus three times the s.d. (15% for hemizygous loss and 6% for homozygous loss) was used as cut-off for evident loss of the gene (Table 1) (Ventura et al., 2006; Mohseny et al., 2010).

Immunohistochemistry

Immunohistochemistry was performed in all 17 sporadic secondary peripheral chondrosarcomas, as described previously (Pansuriya et al., 2011). For comparison, 10 sporadic osteochondromas were used and, for validation, 10 osteochondromas and five secondary peripheral chondrosarcomas both related to multiple osteochondromas were investigated. For EXT1, antigens were retrieved by using microwave heating with EDTA buffer for 10 min and blocked in 5% non-fat milk in phosphate-buffered saline for 30 min and incubated overnight at 4 °C with anti-EXT1 (1:400; Aviva System Biology, San Diego, CA, USA). For 10E4 (1:400; US Biological, Marblehead, MA, USA), the protocol was described earlier (Reijnders et al., 2010). Positive controls were growth plate and placenta for the EXT1 antibody, and growth plate and skin for the 10E4 antibody. Each tumor section was divided into two regions: hypertrophic layer—next to the bone of origin, morphologically constituted by medium/large and round cells; and superficial layer—near the perichondrium, constituted by spherical/flattened cells either irregularly arranged or forming clusters. Two pathologists estimated the percentage of positive cells independently (CEA and JVMGB). Results are expressed as the means with a measure of variability (s.d.). Statistical significance was calculated by one-way analysis of variance with Bonferroni's multiple comparison tests by using the SPSS 16.0 software package (IBM, Somers, NY, USA). P values <0.05 were considered significant.

Conflict of interest

The authors declare no conflict of interest.

Acknowledgements

We acknowledge the expert technical work of Marja van der Burg, Inge Briaire-de Bruijn, Maayke van Ruler and Pauline M Wijers-Koster (Leiden University Medical Center, Leiden, The Netherlands). We also thank the Netherlands Committee on Bone Tumors. Professor E Bakker is acknowledged for EXT mutation analysis. This study was supported by Netherlands Organization for Scientific Research (917-76-315 to CMAR and JVMGB) and by EuroBoNeT (a European Commission-granted European Network of Excellence for studying the pathology and genetics of bone tumors; grant number: LSHC-CT-2006-018814 (to CEA, JVMGB, DJ, KS and PCWH).

References

Bernard SA, Murphey MD, Flemming DJ, Kransdorf MJ. (2010). Improved differentiation of benign osteochondromas from secondary chondrosarcomas with standardized measurement of cartilage cap at CT and MR imaging. Radiology 255: 857–865.

Bertoni F, Bacchini P, Hogendoorn PCW. (2002). Chondrosarcoma. In: Fletcher CDM, Unni KK, Mertens F (eds). World Health Organization Classification of Tumours. Pathology and Genetics of Tumours of Soft Tissue and Bone. IARC Press: France. pp 247–251.

Bovée JVMG, Cleton-Jansen AM, Kuipers-Dijkshoorn N, Van den Broek LJCM, Taminiau AHM, Cornelisse CJ et al. (1999). Loss of heterozygosity and DNA ploidy point to a diverging genetic mechanism in the origin of peripheral and central chondrosarcoma. Genes Chromosomes Cancer 26: 237–246.

Bovee JVMG, Hogendoorn PCW, Wunder JS, Alman BA. (2010). Cartilage tumours and bone development: molecular pathology and possible therapeutic targets. Nat Rev Cancer 10: 481–488.

Bovée JVMG, van Royen M, Bardoel AFJ, Rosenberg C, Cornelisse CJ, Cleton-Jansen AM et al. (2000). Near-haploidy and subsequent polyploidization characterize the progression of peripheral chondrosarcoma. Am J Pathol 157: 1587–1595.

Bulow HE, Hobert O. (2006). The molecular diversity of glycosaminoglycans shapes animal development. Annu Rev Cell Dev Biol 22: 375–407.

Clément A, Wiweger M, von der Hardt S, Rusch MA, Selleck SB, Chien CB et al. (2008). Regulation of zebrafish skeletogenesis by ext2/dackel and papst1/pinscher. PLoS Genet 4: e1000136.

de Andrea CE, Prins FA, Wiweger MI, Hogendoorn PCW. (2011). Growth plate regulation and osteochondroma formation: insights from tracing proteoglycans in zebrafish models and human cartilage. J Pathol 224: 160–168.

de Andrea CE, Wiweger MI, Prins FA, Bovee JVMG, Romeo S, Hogendoorn PC. (2010). Primary cilia organization reflects polarity in the growth plate and implies loss of polarity and mosaicism in osteochondroma. Lab Invest 90: 1091–1101.

Dorfman HD, Czerniak B, Kotz R, Vanel D, Park YK, Unni KK. (2002). WHO classification of tumours of bone: Introduction. In: Fletcher CDM, Unni KK, Mertens F (eds). World Health Organization Classification of Tumours. Pathology and Genetics of Tumours of Soft Tissue and Bone. IARC Press: France. pp 226–232.

Evans HL, Ayala AG, Romsdahl MM. (1977). Prognostic factors in chondrosarcoma of bone. A clinicopathologic analysis with emphasis on histologic grading. Cancer 40: 818–831.

Hallor KH, Staaf J, Bovée JVMG, Hogendoorn PCW, Cleton-Jansen AM, Knuutila S et al. (2009). Genomic profiling of chondrosarcoma: chromosomal patterns in central and peripheral tumors. Clin Cancer Res 15: 2685–2694.

Hameetman L, David G, Yavas A, White SJ, Taminiau AHM, Cleton-Jansen AM et al. (2007a). Decreased EXT expression and intracellular accumulation of heparan sulphate proteoglycan in osteochondromas and peripheral chondrosarcomas. J Pathol 211: 399–409.

Hameetman L, Szuhai K, Yavas A, Knijnenburg J, van Duin M, Van Dekken H et al. (2007b). The role of EXT1 in non hereditary osteochondroma: identification of homozygous deletions. J Natl Cancer Inst 99: 396–406.

Hecht JT, Hogue D, Strong LC, Hansen MF, Blanton SH, Wagner M. (1995). Hereditary multiple exostosis and chondrosarcoma: linkage to chromosome 11 and loss of heterozygosity for EXT-linked markers on chromosomes 11 and 8. Am J Hum Genet 56: 1125–1131.

Jones KB, Piombo V, Searby C, Kurriger G, Yang B, Grabellus F et al. (2010). A mouse model of osteochondromagenesis from clonal inactivation of Ext1 in chondrocytes. Proc Natl Acad Sci USA 107: 2054–2059.

Khurana J, Abdul-Karim F, Bovée JVMG. (2002). Osteochondroma. In: Fletcher CDM, Unni KK, Mertens F (eds). World Health Organization Classification of Tumours. Pathology and Genetics of Tumours of Soft Tissue and Bone. IARC Press: France. pp 234–236.

Matsumoto K, Irie F, Mackem S, Yamaguchi Y. (2010). A mouse model of chondrocyte-specific somatic mutation reveals a role for Ext1 loss of heterozygosity in multiple hereditary exostoses. Proc Natl Acad Sci USA 107: 10932–10937.

McCormick C, Leduc Y, Martindale D, Mattison K, Esford LE, Dyer AP et al. (1998). The putative tumour suppressor EXT1 alters the expression of cell-surface heparan sulfate. Nat Genet 19: 158–161.

Mohseny AB, Tieken C, Van der Velden PA, Szuhai K, de Andrea C, Hogendoorn PCW et al. (2010). Small deletions but not methylation underlie CDKN2A/p16 loss of expression in conventional osteosarcoma. Genes Chromosomes Cancer 49: 1095–1103.

Pansuriya TC, Oosting J, Krenacs T, Taminiau AH, Verdegaal SH, Sangiorgi L et al. (2011). Genome-wide analysis of Ollier disease: is it all in the genes? Orphanet J Rare Dis 6: 2.

Raaijmakers M. (2011). Niche contributions to oncogenesis: emerging concepts and implications for the hematopoietic system. Haematologica 96: 1041–1048.

Raaijmakers MH, Mukherjee S, Guo S, Zhang S, Kobayashi T, Schoonmaker JA et al. (2010). Bone progenitor dysfunction induces myelodysplasia and secondary leukaemia. Nature 464: 852–857.

Raskind WH, Conrad EU, Chansky H, Matsushita M. (1995). Loss of heterozygosity in chondrosarcomas for markers linked to hereditary multiple exostoses loci on chromosomes 8 and 11. Am J Hum Genet 56: 1132–1139.

Reijmers RM, Groen RW, Rozemuller H, Kuil A, de Haan-Kramer A, Csikos T et al. (2010). Targeting EXT1 reveals a crucial role for heparan sulfate in the growth of multiple myeloma. Blood 115: 601–604.

Reijnders CM, Waaijer CJ, Hamilton A, Buddingh EP, Dijkstra SP, Ham J et al. (2010). No haploinsufficiency but loss of heterozygosity for EXT in multiple osteochondromas. Am J Pathol 177: 1946–1957.

Szuhai K, Ijszenga M, de Jong D, Karseladze A, Tanke HJ, Hogendoorn PCW. (2009). The NFATc2 gene is involved in a novel cloned translocation in a Ewing sarcoma variant that couples its function in immunology to oncology. Clin Cancer Res 15: 2259–2268.

Szuhai K, Jennes I, De Jong D, Bovée JVMG, Wiweger M, Wuyts W et al. (2011). Tiling resolution array-CGH shows that somatic mosaic deletion of the EXT gene is causative in EXT gene mutation negative multiple osteochondromas patients. Hum Mutat 32: 2036–2049.

van den Berg H, Kroon HM, Slaar A, Hogendoorn P. (2008). Incidence of biopsy-proven bone tumors in children: a report based on the Dutch pathology registration "PALGA". J Pediatr Orthop 28: 29–35.

Ventura RA, Martin-Subero JI, Jones M, McParland J, Gesk S, Mason DY et al. (2006). FISH analysis for the detection of lymphoma-associated chromosomal abnormalities in routine paraffin-embedded tissue. J Mol Diagn 8: 141–151.

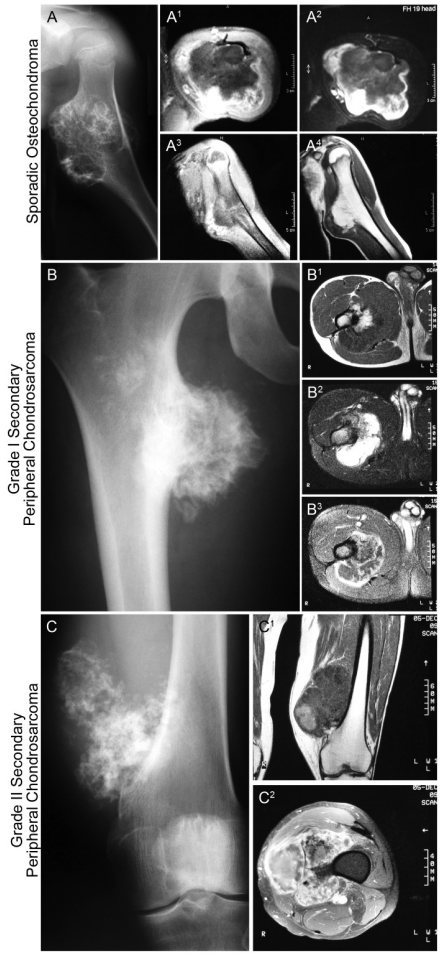
Zak BM, Crawford BE, Esko JD. (2002). Hereditary multiple exostoses and heparan sulfate polymerization. Biochim Biophys Acta 1573: 346–355.

Zuntini M, Pedrini E, Parra A, Sgariglia F, Gentile FV, Pandolfi M et al. (2010). Genetic models of osteochondroma onset and neoplastic progression: evidence for mechanisms alternative to EXT genes inactivation. Oncogene 29: 3827–3834.

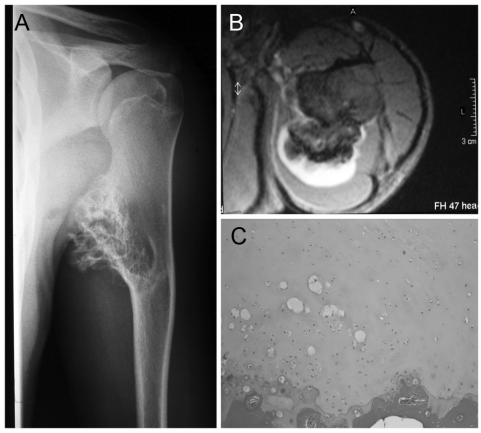
Supplementary Information

Supplementary Table 1: Summary of the immunohistochemistry results.

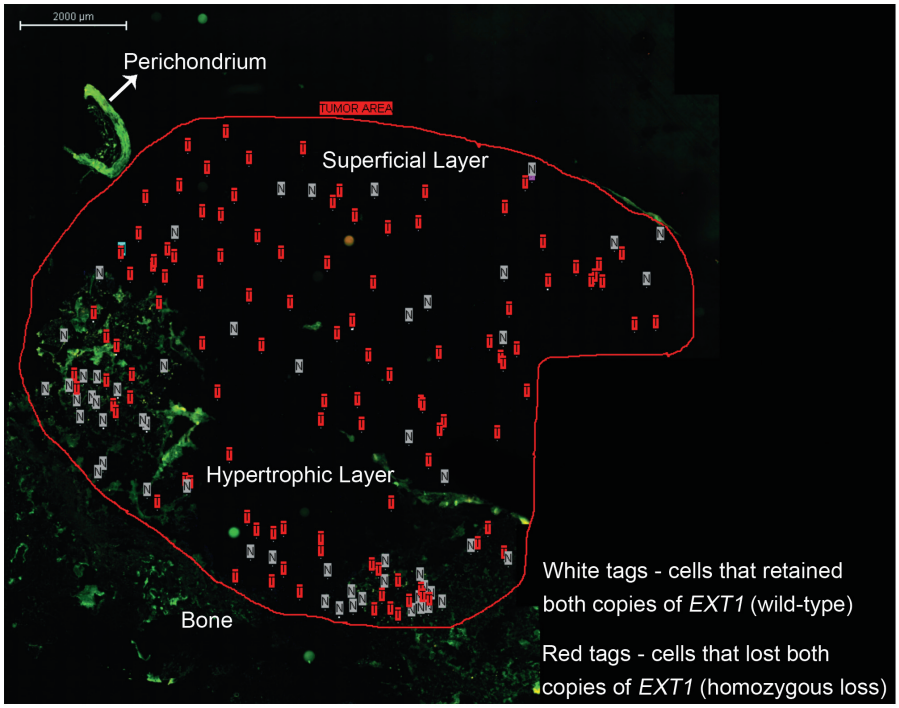
Tumor Group	EXT1		Heparan sulfate	
	Hypertrophic layer Mean (S.D.)	Superficial layer Mean (S.D.)	Hypertrophic layer Mean (S.D.)	Superficial layer Mean (S.D.)
Sporadic osteochondromas (n=10)	91 (14)	23 (12)	21 (16)	2 (5)
Grade I sporadic secondary peripheral chondrosarcomas (n=11)	90 (9)	34 (21)	18 (18)	4 (3)
Grade II sporadic secondary peripheral chondrosarcomas (n=6)	98 (3)	52 (8)	34 (34)	20 (27)
Multiple osteochondromas (n=10)	44 (21)	9 (9)	7 (7)	1 (2)
Secondary peripheral chondrosarcomas related to multiple osteochondromas (n=5)	81 (16)	46 (16)	32 (22)	32 (22)



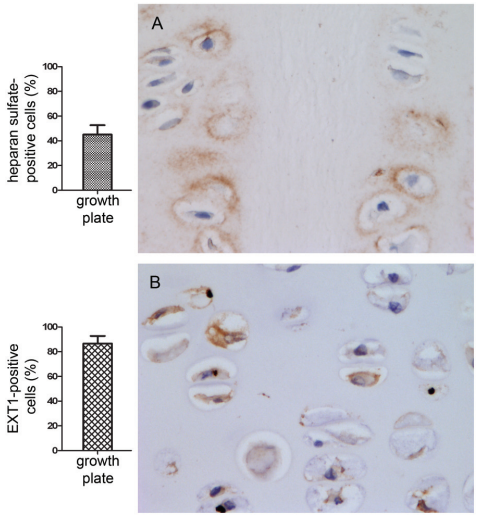
Supplementary Figure 1. (A – A4) Sporadic osteochondroma of the proximal humerus in a 12-year-old boy showing a regular lesion, with endochondral ossification, and marrow continuity with the underlying bone. The thickness of the cartilaginous cap is acceptable of the age of the patient and skeletal immaturity. (B – B3) Grade I peripheral chondrosarcoma of the proximal femur in a 21-year-old man showing a regular lesion with well-circumscribed lobular surfaces, with irregular mineralization, and continuity of the cortex with the parent bone. The thickness of the cartilaginous cap is too pronounced for the age of the patient and skeletal maturity. (C – C2) Grade II peripheral chondrosarcoma of the distal femur in a 60-year-old man showing a lesion with irregular surfaces composed by myxoid and cartilaginous nodules. Extensive invasion of the soft tissue can also be seen. On the coronal image, the stalk with continuity of the underlying marrow can be appreciated.



Supplementary Figure 2. Sporadic osteochondroma of the proximal humerus in a 18-year-old boy. (A, B) History of tumor growth on an almost mature skeleton, in which the growth plates (arrowhead) were nearly closed. (C) The histology shows no conclusive criteria for malignancy. This case was classified as a borderline lesion.



Supplementary Figure 3. Overview of a scanned FISH slide of a sporadic osteochondroma (L-1649) shows that cells with homozygous loss of the *EXT1* loci (red tag) are located in the superficial layer of the tumor. On the contrary, cells that retained both copies of *EXT1* (wild-type) are predominantly found in the hypertrophic layer of the tumor, near to the bone of origin.



Supplementary Figure 4. EXT1 (A) and 10E4 (heparan sulfate; B) immunostaining in the human epiphyseal growth plate. The percentage of EXT1-positive cells is slightly higher than the percentage of 10E4-positive cells.

Interobserver Reliability in the Histopathological Diagnosis of Cartilaginous Tumors in Patients with Multiple Osteochondromas

Carlos E. de Andrea; Herman M. Kroon; Ron Wolterbeek; Salvatore Romeo; Andrew E. Rosenberg; Barry R. DeYoung; Bernadette Liegl; Carrie Y. Inwards; Esther Hauben; Edward F. McCarthy; Miguel Idoate; Nicholas A. Athanasou; Kevin B. Jones; Pancras C. W. Hogendoorn and Judith V. M. G. Bovée

Modern Pathology; in press

Chapter 8

Abstract

The distinction between benign and malignant cartilaginous tumors located peripherally in the bone may be a challenging task in surgical pathology. The aim of this study was to investigate inter-observer reliability in histological diagnosis of cartilaginous tumors in the setting of multiple osteochondromas and to evaluate possible histological parameters that could differentiate among osteochondroma, low- and high-grade secondary peripheral chondrosarcoma. Interobserver reliability was assessed by 12 specialized bone-tumor pathologists in a set of 38 cases. Substantial agreement on diagnosis among all the reviewers was observed (intraclass correlation coefficient = 0.78). Our study confirmed that mitotic figures and nuclear pleomorphism are hallmarks of high-grade secondary peripheral chondrosarcoma. However, despite the substantial agreement, we demonstrated that histology alone cannot distinguish osteochondroma from low-grade secondary peripheral chondrosarcoma in the setting of multiple osteochondromas, since nodularity, the presence of binucleated cells, irregular calcification, cystic/mucoid changes and necrosis were not helpful to indicate malignant transformation of an osteochondroma. On the other hand, among the concordant cases, the cartilage cap in osteochondroma was significantly less thick than in low- and high-grade secondary peripheral chondrosarcoma. Therefore, our study showed that a multidisciplinary approach integrating clinical and radiographical features and the size of the cartilaginous cap in combination with a histological assessment are crucial to the diagnosis of cartilaginous tumors.

Keywords: osteochondroma, chondrosarcoma, diagnostic criteria, peripheral cartilage tumors, bone tumors.

Introduction

Multiple osteochondromas, alternatively called multiple hereditary exostoses, is an autosomal dominant disorder with a prevalence estimated at 1 in 50,000 [1], and is caused by mutations in *EXT1* at 8q24 or *EXT2* at 11p11-13 [2]. Multiple osteochondromas develops during skeletal growth and is characterized by shortened long bones and formation of multiple cartilage-capped bony projections from the metaphyses of endochondral bones adjacent to the growth plate [3]. Osteochondroma can eventually transform into a secondary peripheral chondrosarcoma in 1–3% of patients with multiple osteochondromas [2].

Secondary peripheral chondrosarcomas are malignant cartilage-producing tumors and comprise about 15% of all conventional chondrosarcomas in tertiary referral centers [4]. Patients with secondary peripheral chondrosarcomas show a diverse clinical course, ranging from slow insidious tumor growth to rapid neoplastic progression, especially when located in pelvis, shoulder and hip [5]. Secondary peripheral chondrosarcomas are often low-grade malignant tumors, i.e. grade I chondrosarcomas according to the Evans grading system [6], and are treated by limb salvage surgery with a wide or even with a marginal resection [7].

The lack of consistent and reproducible criteria to determine neoplastic transformation in multiple osteochondromas often raises diagnostic dilemmas in differentiating osteochondroma from low-grade secondary peripheral chondrosarcoma. Malignant potential of an osteochondroma is often estimated by the thickness of its cartilage cap and the evidence of tumor growth in a skeletally mature patient [8]. Cap thickness greater than 2 cm in patients with fused growth plates should be considered suspicious for progression of an osteochondroma to a chondrosarcoma [9]. Moreover, cap thickness greater than 2 cm strongly indicates secondary peripheral chondrosarcoma [10,11]. Additionally, a wide range of histological parameters is described to determine malignant transformation of an osteochondroma, ranging from the formation of nodules to the presence of mitotic figures and cystic cavities [12]. For a general pathologist, the application of these criteria is often difficult, which gives room for a subjective interpretation. Therefore, identifying stringent and reproducible histological criteria may help the interpretation of peripheral cartilaginous tumors by general pathologists.

As no “gold-standard” exists to directly assess tumor grade, prediction of peripheral cartilaginous tumor behavior cannot be ensured. Consequently, an initial step in the process of defining histological parameters for guiding the diagnosis of peripheral cartilaginous tumors in the setting of multiple osteochondromas is to assess diagnostic reliability, as measured by intraclass correlation coefficient [13]. A second step is to identify common histological criteria among the concordant cases, aiming to have histological parameters that characterize each tumor type. This study evaluated diagnostic concordance among a panel of experienced bone-tumor pathologists. Histological parameters noted to be of diagnostic value in the literature were then systematically evaluated among

the concordant cases, aiming to have histological parameters that characterize each tumor type. This study evaluated diagnostic concordance among a panel of experienced bone-tumor pathologists. Histological parameters noted to be of diagnostic value in the literature were then systematically evaluated among the concordant cases to give best guidance on diagnosing peripheral cartilaginous tumors in the setting of multiple osteochondromas.

Materials and Methods

Cases Studied

Patients with multiple osteochondromas admitted to Leiden University Medical Center between 1985 and 2009 with either osteochondroma or secondary peripheral chondrosarcoma were retrieved from our database. Cases with neither radiologic documentation nor clinical information were excluded as well as cases with local recurrences and not enough material for histological examination. All the original diagnoses were made at the Leiden University Medical Center. In addition, twenty cases were further confirmed in multidisciplinary discussions organized by the Netherlands Committee on Bone Tumors, a national multidisciplinary committee for consultation on diagnosis and treatment of musculoskeletal tumors and tumor-like lesions.

Medical records were studied to identify patient age, gender and tumor location. Imaging studies, including plain radiographs, magnetic resonance images and/or computed tomography scans, were available in 29 cases. The cartilage cap thickness was measured by a bone-tumor radiologist (H.M.K.) in accordance with Bernard et al [11]. Briefly, the cap thickness was assessed by measuring thickest portions of the cartilage cap perpendicular to the boundary between the medullary space of the osteochondroma stalk. For each case, at the minimum one complete section through the whole lesion including the maximal diameter of the cartilaginous cap was submitted for histology. Representative histological sections were subsequently selected for each case and were randomly labeled from 1 to 38. All the unique identifiers were removed to protect patient anonymity. The study was performed according to the ethical guidelines in Code for Proper Secondary Use of Human Tissue in the Netherlands (Dutch Federation of Medical Scientific Societies).

Interobserver Variability

Case series reviewers were 12 pathologists (C.E.A.; S.R.; A.E.R.; B.R.D.; B.L.A.; C.Y.I.; E.H.; E.F.M.; M.A.I.G.; N.A.A.; P.C.W.H. and J.V.M.G.B.) selected for their expertise in bone-tumor pathology. The case series consisted of (i) an Excel file with clinical information, in which the diagnosis, tumor grade and any possible remarks were asked to be filled in, (ii) digitized imaging studies, and (iii) glass slide from each case. Many pathologists classified malignant secondary peripheral cartilaginous lesions into grade-I, II or III. Many pathologists classified malignant secondary peripheral cartilaginous lesions into grade-I, II or III.

Few reviewers used grades of low-grade malignant or high-grade malignant. To have a common classification, grade- I tumors were considered low-grade malignant and grade- II and III were considered high-grade.

Table 1. Histological parameters scored among the concordant cases.

	Osteochondromas (n = 25)		Low-grade secondary peripheral chondrosarcomas (n = 3)		High-grade secondary peripheral chondrosarcomas (n = 2)		*P*
	No.	%	No.	%	No.	%	
Cellularity							0.260
Low	14	56	1	33	0		
High	11	44	2	67	2	100	
Binucleated cells							0.401
Present	18	72	3	100	2	100	
Absent	7	28	0		0		
Nuclear pleomorphism							<0.001*
Present	0		0		2	100	
Absent	25	100	3	100	0		
Calcification/ irregular mineralization							0.401
Present	18	72	3	100	NA		
Absent	7	28	0		NA		
Nodularity							0.176
Present	14	56	3	100	2	100	
Absent	11	44	0		0		
Permeation of trabecular bone							NA
Present	0		0		0		
Absent	25	100	3	100	2	100	
Cystic/mucoid changes							0.472
Present	19	76	3	100	2	100	
Absent	6	24	0		0		
Necrosis							0.401
Present	18	72	3	100	2	100	
Absent	7	28	0		0		
Mitosis							<0.001*
Present	0		0		2	100	
Absent	25	100	3	100	0		

NA, not evaluable; *, statistically significant (adjusted Chi-Square test).

Histopathology

The most common criteria noted to be of diagnostic value in the literature to distinguish osteochondroma, low-grade secondary peripheral chondrosarcoma, high-grade secondary peripheral chondrosarcoma, and dedifferentiated chondrosarcoma were evaluated among the concordant cases by 3 pathologists (C.E.A, J.V.M.G.B., and P.C.W.H.). Concordant cases were defined as agreement among the 12 pathologists greater than 75%. The list of histological parameters included: cellularity (high- or low cellular), the presence/absence of binucleated cells, nuclear pleomorphism, calcification or irregular mineralization, nodularity,

permeation of trabecular bone, cystic/mucoid changes, necrosis, and mitotic figures [3,12]. Histological parameters were defined as follows:

- Cellularity: High cellularity was defined as a cell-rich lesion with closely packed cells with scant extracellular matrix in between. Low cellularity was defined as a matrix-rich lesion in which cells were more distant from each other.

- Binucleated cells were defined as having two nuclei of a normal size sharing the same cytoplasm.

- Nuclear pleomorphism was defined as variation in nuclear size (3 times normal size) and shape.

- Irregular calcification was interpreted as coarse and irregular areas of calcification (Figure 1d).

- Nodularity was defined by the presence of nodule(s) connected with the main lesion and separated from each other by cellular fibrous septa (Figure 1a).

- Permeation of trabecular bone was defined by tumor filling up the trabecular marrow space entrapping pre-existing lamellar bone trabeculae [14].

- Cystic/mucoid changes were defined as areas or cystic spaces containing mucoid material (Figure 1b).

- Necrosis was identified by the presence of necrotic chondrocytes appearing as nuclei loosing hematoxylin staining (Figure 1c).

- Presence of mitotic figures was recorded whenever any mitotic figures were seen in any field at any rate.

Statistical Analysis

Intraclass correlation coefficients were calculated in a two-way random effects model to determine interobserver reliability among the 12 pathologists using the SPSS 16.0 software package (IBM, Somers, NY, USA). Intraclass correlations are equivalent to weighted κ coefficients with quadratic weights [13]. Intraclass correlation coefficients were calculated for the agreement on the diagnosis of osteochondroma, low-grade secondary peripheral chondrosarcoma, high-grade secondary peripheral chondrosarcoma and dedifferentiated chondrosarcoma. Interpretation of intraclass correlation coefficients was performed according to Landis and Koch [15]. A κ value below 0.20 is considered poor, 0.21 - 0.40 fair, 0.41 - 0.60 moderate, 0.61 - 0.80 substantial, and 0.81 - 1.00 very good.15 One-way ANOVA was used to evaluate statistical differences of the cartilage cap thickness among the cases. Additionally, adjusted Chi-Square test was used to determine whether there are significant differences between the histological criteria in each tumor type.

Results

Thirty-eight tumors from 29 patients were included in the study. Clinical information and thickness of the cartilage cap of the 38 cases are summarized in Figure 2. None of the studied patients showed adverse outcome (metastases or death of disease) up to the study period (range 24–312 months, mean 148.8). Two patients had local recurrence.

Interobserver variability in diagnosis

The intraclass correlation coefficient for interobserver reliability was 0.78 (95% confidence interval: 0.694 to 0.859), which indicated substantial agreement. High diagnostic concordance (agreement ≥ 75% by all the reviewers) was observed in 31 cases (Figure 2). Among these concordant cases, 25 cases were diagnosed as osteochondroma, 3 cases as low-grade secondary peripheral chondrosarcoma, 2 cases as high-grade secondary peripheral chondrosarcoma, and 1 case as dedifferentiated chondrosarcoma. Diagnostic concordance was not reached in 7 cases (agreement < 75% by all the reviewers) (Figure 2). All the non-concordant cases were diagnosed by the Netherlands Committee on Bone Tumors as being low-grade secondary peripheral chondrosarcoma. Additionally, cases number 6 and 10 were described by the Netherlands Committee on Bone Tumors as progressing to high-grade lesions. Case 6 had a cartilage cap thickness of 6 cm and neither mitotic figures nor nuclear pleomorphism were found. Case 10 had a cartilage cap thickness of 10 cm and only nuclear pleomorphism was identified. These two cases had a local recurrence after surgery. One lesion (case 9) had a large spindle cell component, which was interpreted as dedifferentiated chondrosarcoma by 10/12 pathologists.

Diagnostic value of histological parameters

All concordant cases were systematically evaluated by 3 bone-tumor pathologists (C.E.A, J.V.M.G.B., and P.C.W.H.) and data are shown in table 1. Interestingly, among osteochondromas, binucleated cells, irregular calcification and necrosis were observed in 72% of the cases (Figure 1a-d). Additionally, nodularity and cystic/mucoid changes were identified in 56% and 76% of the osteochondroma cases, respectively (Figure 1a,b). All these histological parameters were also seen in low- and high-grade secondary peripheral chondrosarcomas (Figure 3a-f). Characteristically, mitotic figures at any rate and nuclear pleomorphism were only observed in high-grade secondary peripheral chondrosarcoma. Singly or collectively, no significant differences were observed between the histological criteria in each tumor type (Table 1). Only the presence of mitotic figures and nuclear pleomorphism in high-grade secondary peripheral chondrosarcoma were significant different compared to osteochondroma and low-grade secondary peripheral chondrosarcoma ($P < 0.001$). Permeation of trabecular bone was not observed in any case.

Diagnostic value of cartilage cap thickness

The average of cartilage cap thickness was 0.82 cm (ranged from 0.1 to 2 cm) in osteochondromas, 3.83 cm (ranged from 2.5 to 5 cm) in low-grade secondary peripheral chondrosarcomas and 5.50 cm (ranged from 2 to 9 cm) in high-grade secondary peripheral chondrosarcomas. With regard to cartilage cap thickness among the concordant cases, a statistically significant difference was found in osteochondroma compared to low- and high-grade secondary peripheral chondrosarcoma (P = 0.001). In addition, among the concordant cases, no significant difference was seen between low- and high-grade secondary peripheral chondrosarcoma (P = 0.272). Among the non-concordant cases (Figure 2), the average of cartilage cap thickness varied from 1 to 10 cm.

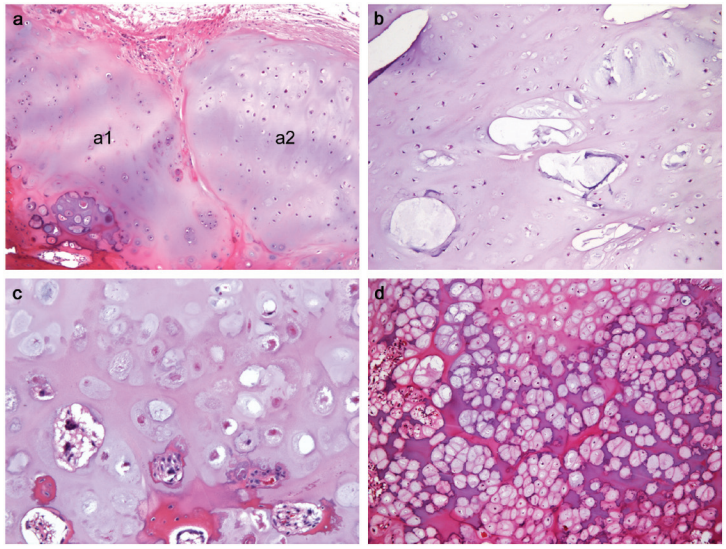


Figure 1. (a-c) Histological features often observed in lesions interpreted as osteochondromas. (a) Nodularity: a nodule is connected with the main lesion (a1) and separated from the main lesion by fibrous septa (a2). (b) Cystic changes (areas of cystic spaces containing mucoid material) are irregularly distributed in the osteochondroma cartilage cap. (c) Necrosis: necrotic chondrocytes appeared as swollen nuclei that lost haematoxylin staining. (d) Irregular calcification: coarse and irregular calcification is often seen.

Discussion

Analysis of a series of peripheral cartilaginous tumors in the setting of multiple osteochondromas by 12 experienced bone-tumor pathologists showed that there was a substantial agreement on diagnosis among all the reviewers. We here confirm that mitotic figures and nuclear pleomorphism are hallmarks of high-grade secondary peripheral. We here confirm that mitotic figures and nuclear pleomorphism are hallmarks of high-grade secondary peripheral chondrosarcoma, and that a malignant spindle cell component indicates dedifferentiated peripheral chondrosarcoma.

We previously assessed interobserver variability in central cartilaginous lesions [16,17]. Similar intraclass correlation coefficient was found for diagnosing central and peripheral lesions (in both 0.78) [17]. For central lesions, we were able to identify 5 parameters (high cellularity, presence of host bone entrapment, open chromatin, mucoid matrix quality, and age above 45 years) that could optimally differentiate between enchondroma and low-grade central chondrosarcoma, of which mucoid/myxoid matrix degenerative changes and host bone entrapment were the most important [17]. The present study however demonstrates that these criteria cannot be applied for cartilaginous tumors in the setting of multiple osteochondromas. In addition, we show that histology alone cannot distinguish osteochondroma from low-grade secondary peripheral chondrosarcoma since nodularity, the presence of binucleated cells, irregular calcification, cystic/mucoid changes and necrosis were not helpful to indicate malignant transformation of an osteochondroma.

Instead, our results emphasize that the evaluation of the size of the cartilage cap at radiology and gross pathology is crucial. Among the concordant cases, osteochondromas had a significantly thinner cartilage cap compared to secondary peripheral chondrosarcomas. This reinforces the general consensus of distinguishing osteochondroma from low-grade secondary peripheral chondrosarcoma by cartilage cap thickness [11]. A standardized measuring technique with computed tomography and magnetic resonance imaging has been described to assess the cartilage cap thickness [11].

Histologically, nodularity was observed in about half of osteochondromas. Nodules in osteochondromas have previously been considered a feature of malignant transformation [12,18]. Interestingly, cases 21, 27, and 28 showed disagreement on distinguishing benign from low-grade malignant. Although the thickness of the cartilage cap in these three cases is not increased (1 cm, 1.5 cm, and 0.5 cm, respectively), they display histological and radiological features of nodularity. The presence of nodularity in these tumors possibly led some pathologists to interpret this as suspicious for low-grade sarcoma. On the other hand, the thin cartilage cap of case 28 has probably influenced the decision of most pathologists to sign it out as a benign lesion. Although treatment planning was beyond the scope of this study, the presence of nodularity on imaging may have been interpreted as a sign suspicious of malignant transformation leading to subsequent resection. In the magnetic resonance imaging scan, nodules are often associated with vascularized septa with high intensity signal and are found in low grade chondrosarcomas and in active cartilaginous lesions [17].

Considering that Leiden University Medical Center is a tertiary hospital for treatment of bone tumors in the Netherlands, we cannot exclude that our series is slightly biased towards lesions that are more prone to malignant transformation. The major limitation of our study is the lack of “gold-standard” to distinguish osteochondroma from low-grade secondary peripheral chondrosarcoma, which has hampered the case selection. Low-grade secondary peripheral chondrosarcomas rarely metastasize and high-grade secondary

peripheral chondrosarcomas are extremely rare. A selection of a set of cases with an equal ratio of benign, low- and high-grade tumors was therefore not feasible. Despite their rarity we showed that high-grade secondary peripheral chondrosarcomas were distinguished from the low-grade lesions by the presence of mitotic figures at any rate and nuclear pleomorphism, which is in line with previous literature [12,18].

Histologically, osteochondroma and low-grade secondary peripheral chondrosarcoma in the setting of multiple osteochondromas were not distinguished by the presence of binucleated cells, irregular calcification, cystic/mucoid changes, and focal necrosis. It has been described that osteochondromas occasionally have binucleated cells [3]. Radiographically, areas of calcification in osteochondromas become disorganized and irregular, as the patient grows older [10]. Cystic/mucoid changes are related to degenerative processes, such as mucinous degeneration. Similar degenerative processes have been described in osteoarthritis [18]. Necrosis most likely is secondary to ischemia, as the cartilage cap is not vascularized and often traumatized [21].

Sporadic peripheral cartilaginous tumors are histologically indistinguishable from peripheral cartilaginous tumors occurring in the setting of multiple osteochondromas [20]. It is therefore most likely that we can extrapolate our findings indicating that histology alone is unable to confidently differentiate sporadic osteochondroma from low-grade sporadic secondary peripheral chondrosarcoma as well.

Thus, our data indicate that a multi-disciplinary team, including pathologists, radiologists, and orthopedic surgeons, is critical to establish a final diagnosis in sporadic and multiple peripheral cartilaginous tumors. Suspicious signs for malignancy in osteochondromas include: tumor growth after pubertal growth spurt and pain. Osteochondromas located in the pelvis, hips, and shoulders more often undergo malignant transformation [18].

On plain radiographs, malignant progression of osteochondroma is suggested when osteolysis or change of chondroid calcification is observed [10]. In addition, computed tomography scan might reveal new osteolytic areas and a change in the nature of calcifications in the periphery of osteochondromas [21]. Moreover, soft-tissue swelling containing calcification is very suggestive of the development of a secondary peripheral chondrosarcoma on plain radiographs and computed tomography.

The cartilage cap of peripheral cartilaginous tumors is best evaluated by magnetic resonance imaging with T2-weighted images using fat-selective pre-saturation, which allows standardized measurements of the cap. A cartilage cap thickness greater than 2 cm in a skeletally mature patient is suspicious for neoplastic transformation of osteochondroma [11]. Additionally, magnetic resonance imaging is used to delineate the extent of soft-tissue extension and its relation to the surrounding structures, specifically the neurovascular bundle [10]. Contrast-enhanced magnetic resonance imaging sequences are used to differentiate a thickened cartilage cap from an overlying bursa.

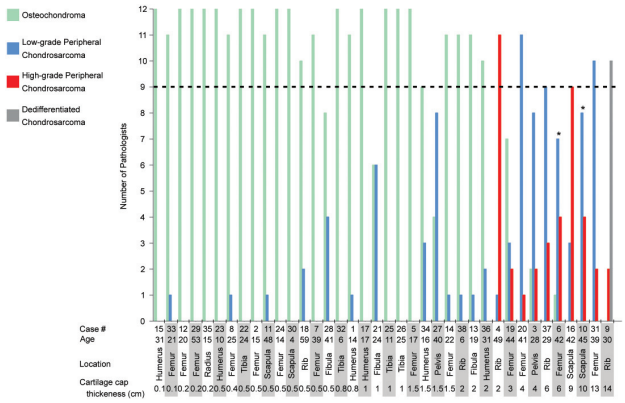


Figure 2. Chart displaying the raw data from pathologists and clinical details of the 38 cases to study interobserver reliability. Concordant cases show agreement among the 12 pathologists greater than 75% (dashed line). Asterisk indicates cases with local recurrence.

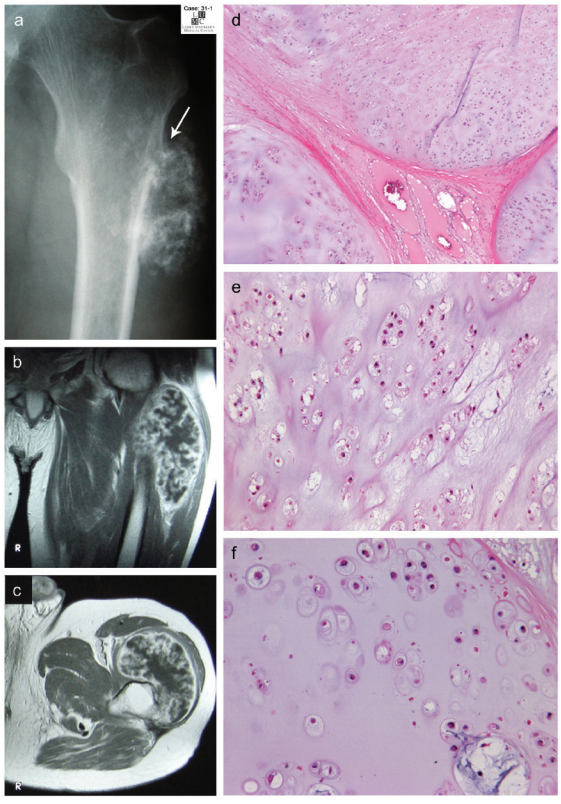


Figure 3. (a-f) Lesion interpreted as low-grade secondary peripheral chondrosarcoma by the majority of the study pathologists (Case 31). (a) Antero-posterior conventional radiograph of the proximal femur. Ossifying and calcifying mass in close relation to the surface of the femur. Arrow indicates the stalk of the original osteochondroma. (b) Coronal T1-weighted magnetic resonance imaging after intravenous administration of contrast. Large soft-tissue mass anterior and lateral to the femur with a serpentine pattern of enhancement characteristic of a chondromatous tumor, in this case the soft-tissue extension of a secondary chondrosarcoma arising from an osteochondroma. (c) Axial T1-weighted, magnetic resonance imaging after intravenous administration of contrast shows a secondary chondrosarcoma arising from an osteochondroma. The stalk of the original osteochondroma arises from the latero-posterior surface the proximal femur. Large soft-tissue mass lateral and anterior of the femur with a serpentine pattern of enhancement characteristic of a chondromatous tumor. (d) Large lobules of cartilage contained closely arranged cells in lacunae define the lesion. (e,f) Cystic changes are often observed, and no nuclear pleomorphism or mitotic figures are seen.

Whole-body bone scintigraphy in adult patients with multiple osteochondromas shows that lesions with increased uptake of the tracer may indicate malignant transformation [22].

In summary, review of 38 cases of peripheral cartilaginous tumors by 12 experienced bone-tumor pathologists showed general agreement in the diagnosis of these tumors in the setting of multiple osteochondromas. Histological parameters generally associated with malignant transformation could not reliably distinguish osteochondroma from low-grade secondary peripheral chondrosarcoma. Instead, a multidisciplinary approach integrating clinical and radiographical features and the size of the cartilaginous cap in combination with a histological assessment are crucial to the diagnosis of peripheral cartilaginous tumors.

Disclosure/Conflict of Interest

Authors declare the absence of conflicts of interest.

Acknowledgements

We acknowledge the Netherlands Committee on Bone Tumors, Dr. P.D.S. Dijkstra, Dr. E. Dootjes, and the expert technical work of Inge Briaire-de Bruijn. This study was supported by EuroBoNeT (a European Commission-granted European Network of excellence for studying the pathology and genetics of bone tumors, Grant Number: LSHC-CT-2006-018814). J.V.M.G.B. is financially supported by The Netherlands Organization for Scientific Research (Grant Number: 917-76-315).

References

1. Schmale GA, Conrad EU, Raskind WH. The natural history of hereditary multiple exostoses. J Bone Joint Surg [Am]. 1994;76:986-92.
2. Bovee JVMG, Hogendoorn PCW, Wunder JS, et al. Cartilage tumours and bone development: molecular pathology and possible therapeutic targets. Nat Rev Cancer. 2010;10:481-8.
3. Khurana J, Abdul-Karim F, Bovée JVMG. Osteochondroma. In: Fletcher CDM, Unni KK, Mertens F, (eds). World Health Organization classification of tumours. Pathology and genetics of tumours of soft tissue and bone. 3th edn. IARC Press:Lyon; 2002.pp 234-236.
4. Dorfman HD, Czerniak B, Kotz R, et al. WHO classification of tumours of bone: Introduction. In: Fletcher CDM, Unni KK, Mertens F, (eds). World Health Organization classification of tumours. Pathology and genetics of tumours of soft tissue and bone. 3th edn. IARC Press:Lyon; 2002. pp 226-232.

5. Campanacci M, Enneking WF. Peripheral Chondrosarcoma. In: Bone and Soft Tissue Tumors: Clinical Features, Imaging, Pathology and Treatment. 2nd edn. Springer-Verlag:New York; 1999. pp 335-361.
6. Evans HL, Ayala AG, Romsdahl MM. Prognostic factors in chondrosarcoma of bone. A clinicopathologic analysis with emphasis on histologic grading. Cancer. 1977;40:818-31.
7. Hogendoorn PC, Athanasou N, Bielack S, et al. Bone sarcomas: ESMO Clinical Practice Guidelines for diagnosis, treatment and follow-up. Ann Oncol. 2010;21 Suppl 5:204-213.
8. Mulder JD, Schütte HE, Kroon HM, et al. The diagnosis of bone tumors. In: Radiologic atlas of bone tumors. 2 edn. Elsevier:Amsterdam; 1993. pp 9-46.
9. Ahmed AR, Tan TS, Unni KK, et al. Secondary chondrosarcoma in osteochondroma: report of 107 patients. Clin Orthop Relat Res. 2003;411:193-206.
10. Murphey MD, Choi JJ, Kransdorf MJ, et al. Imaging of osteochondroma: variants and complications with radiologic-pathologic correlation. RadioGraphics. 2000;20:1407-34.
11. Bernard SA, Murphey MD, Flemming DJ, et al. Improved differentiation of benign osteochondromas from secondary chondrosarcomas with standardized measurement of cartilage cap at CT and MR imaging. Radiology. 2010;255:857-65.
12. Bertoni F, Bacchini P, Hogendoorn PCW. Chondrosarcoma. In: Fletcher CDM, Unni KK, Mertens F, (eds). World Health Organization classification of tumours. Pathology and genetics of tumours of soft tissue and bone. 3th edn. IARC Press:Lyon; 2002. pp 247-251.
13. Shrout PE, Fleiss JL. Intraclass correlations: uses in assessing rater reliability. Psychol Bull. 1979;86:420-8.
14. Mirra JM, Gold R, Downs J, et al. A new histologic approach to the differentiation of enchondroma and chondrosarcoma of the bones. A clinicopathologic analysis of 51 cases. Clin Orthop. 1985;201:214-37.
15. Landis JR, Koch GG. An application of hierarchical kappa-type statistics in the assessment of majority agreement among multiple observers. Biometrics. 1977;33:363-74.
16. Skeletal Lesions Interobserver Correlation among Expert Diagnosticians (SLICED) Study Group. Reliability of histopathologic and radiologic grading of cartilaginous neoplasms in long bones. J Bone Joint Surg Am. 2007;89:2113-23.
17. Eefting D, Schrage YM, Geirnaerdt MJ, et al. Assessment of interobserver variability and histologic parameters to improve reliability in classification and grading of central cartilaginous tumors. Am J Surg Pathol. 2009;33:50-57.

18. Unni KK. Chondrosarcoma (primary, secondary, dedifferentiated, and clear cell). In: Dahlin's Bone Tumors: General Aspects and Data on 11,087 Cases. 5th edn. Lippincott-Raven Publishers:Philadelphia; 1996. pp 71-108.
19. Bloem JL, Van der Woude HJ, Hogendoorn PCW. MRI of the musculoskeletal system: a teaching file. In: Deutsch AL, Mink JH, (eds). Bone tumors. 2nd edn. Lippincott-Raven Publishers:Philadelphia; 1996. pp 655-719.
20. Ledingham JM, Preston BJ, Doherty M. Cystic change in the head of the fibula in osteoarthritis. J Bone Joint Surg Br. 1993;75:429-32.
21. Carlson CS, Meuten DJ, Richardson DC. Ischemic necrosis of cartilage in spontaneous and experimental lesions of osteochondrosis. J Orthop Res. 1991;9:317-29.
22. Romeo S, Hogendoorn PC, Dei Tos AP. Benign cartilaginous tumors of bone: from morphology to somatic and germ-line genetics. Adv Anat Pathol. 2009;16:307-15.
23. Kenney PJ, Gilula LA, Murphy WA. The use of computed tomography to distinguish osteochondroma and chondrosarcoma. Radiology. 1981;139:129-37.
24. Hendel HW, Daugaard S, Kjaer A. Utility of planar bone scintigraphy to distinguish benign osteochondromas from malignant chondrosarcomas. Clin Nucl Med. 2002;27:622-4.

Peripheral chondrosarcoma progression is associated with increased type X collagen and vascularisation

Carlos E. de Andrea, Malgorzata I. Wiweger,
Judith V. M. G. Bovée, Salvatore Romeo
and Pancras C. W. Hogendoorn
Virchows Arch. 2012;460:95-102

Chapter 9

Abstract

Endochondral bone formation requires a cartilage template, known as the growth plate, and vascular invasion, bringing osteoblasts and osteoclasts. Endochondral chondrocytes undergo sequences of cell division, matrix secretion, cell hypertrophy, apoptosis, and matrix calcification/mineralisation. In this study, two critical steps of endochondral bone formation, the deposition of collagen X-rich matrix and blood vessel attraction/invasion, were investigated by immunohistochemistry. Fourteen multiple osteochondromas and six secondary peripheral chondrosarcomas occurring in patients with multiple osteochondromas were studied and compared to epiphyseal growth plate samples. Mutation analysis showed all studied patients (expect one) to harbour a germ-line mutations in either *EXT1* or *EXT2*. Here, we described that homozygous mutations in *EXT1/EXT2*, which are causative for osteochondroma formation, are likely to affect terminal chondrocyte differentiation and vascularisation in the osteocartilaginous interface. Contrastingly, terminal chondrocyte differentiation and vascularisation seem to be unaffected in secondary peripheral chondrosarcoma. In addition, osteochondromas with high vascular density displayed a higher proliferation rate. A similar apoptotic rate was observed in osteochondromas and secondary peripheral chondrosarcomas. Recently, it has been shown that cells with functional *EXT1* and *EXT2* are outnumbering *EXT1/EXT2* mutated cells in secondary peripheral chondrosarcomas. This might explain the increased type X collagen production and blood vessel attraction in these malignant tumours.

Keywords: growth plate, osteochondroma, peripheral chondrosarcoma, type X collagen, angiogenesis, bone tumour

Introduction

Elongation of long bones is a complex process that requires a cartilage template, known as the epiphyseal growth plate, and a strict coordination and synchronisation of cell–cell and cell–matrix signalling events [1]. The key events in this process can be divided into two major sequential morphogenesis phases. The first phase is characterised by the proliferation of the growth plate chondrocytes, which maintains the pool of cells needed for bone lengthening. The second phase is a multistep process characterised by the hypertrophy of proliferating chondrocytes and bone formation. Hypertrophic chondrocytes increase their volume and secrete a specialised extracellular matrix rich in type X collagen [2]. The ossifying collagen X-rich matrix attracts blood vessels and bone precursor cells, allowing bone development [3].

The process of endochondral ossification is also observed in cartilaginous tumours [4]. An active endochondral ossification takes place deep to the cartilage cap of osteochondroma and secondary peripheral chondrosarcoma [5].

Osteochondromas are the most common benign bone tumours at childhood and adolescence [6]. They can occur either as a sporadic lesion or multiple tumours in hereditary multiple osteochondromas syndrome (previously known as hereditary multiple exostoses) [7]. Osteochondromas are caused by mutations in either *EXT1* or *EXT2* genes [7]. They are pedunculated or sessile cartilage-capped bony projections from the metaphyses of endochondral bones adjacent to the growth plate [5]. In less than 1% of patients with sporadic osteochondromas and 1–3% of patients with multiple osteochondromas at the age of 30–60 years, an osteochondroma may eventually transform into a secondary peripheral chondrosarcoma [8].

Whereas osteochondromas have been linked to homozygous mutations in *EXT1* or *EXT2* genes, cells with functional *EXT1* and *EXT2* have been shown to be the predominant subclone in secondary peripheral chondrosarcomas [9].

Mutations in *EXT1* have been demonstrated to impair angiogenesis in mice [10] and to affect endochondral bone formation by reducing type X collagen deposition [11]. Endochondral bone formation has been shown to be affected in the homozygous *dak/ext2* zebrafish mutant [12].

EXT1 and *EXT2* genes encode enzymes that catalyse the biosynthesis of heparan sulphate. Heparan sulphate is a key component of the extracellular matrix acting as co-receptors for signalling molecules, including vascular endothelial growth factors (VEGF), fibroblast growth factors (FGF), and others [13, 14]. The impact of mutations in *EXT1* or *EXT2* genes with regards to production of a collagen X-rich matrix and attraction of blood vessels in osteochondromas and secondary peripheral chondrosarcomas has not been investigated so far.

Here, we describe that terminal chondrocyte differentiation and vascularisation are affected in osteochondromas. Contrastingly, these two critical steps of endochondral bone formation seem to be unaffected in secondary peripheral chondrosarcomas.

Materials and methods

Patient material

Paraffin-embedded tissues from 14 osteochondromas and 6 low-grade secondary peripheral chondrosarcomas from patients with multiple osteochondromas, collected between 1991 and 2008, were retrieved from the files of the Leiden University Medical Centre (Table 1). One patient had two tumours from distinct location included in this study. For comparison, paraffin-embedded epiphyseal growth plates (n = 3) were obtained from orthopaedic resections for pathological conditions not related to osteochondroma or chondrosarcoma. Clinical information and the thickness of the cartilage cap were obtained from pathology/radiology reports. All samples were handled in a coded fashion, and all procedures were performed according to the ethical guidelines in "Code for Proper Secondary Use of Human Tissue in the Netherlands" (Dutch Federation of Medical Scientific Societies).

Immunohistochemistry

Deparaffinised sections were treated with testicular hyaluronidase (2 mg/ml in 0.1-M Tris saline, pH 5.0; Sigma-Aldrich, St Louis, MO, USA, 60 min at 37°C) and proteinase K (5 µl/ml in 0.1-M Tris-buffered saline, pH 5.0; DakoCytomation, Carpinteria, CA, USA) followed by overnight incubation at 4°C with monoclonal antibody to collagen X (clone X53, 1:100, Quartett, Berlin, Germany), as previously described [4, 15]. Monoclonal antibody to CD31 (clone JC70A, 1:10,000, DakoCytomation, Glostrup, Denmark), cleaved caspase-3 (clone 5A1E, 1:100, Cell Signaling Technology, Danvas, MA, USA), and Ki-67 (clone MIB-1, 1:100, Dako, Glostrup, Germany) were used as earlier described [16–18]. The thickness of collagen X-rich matrix was evaluated jointly by two observers (C.E.A. and S.R.). The thickest collagen X stained area was identified in each section and measured by an eye-piece graticule, as described in Fig. 1a. The apoptotic rate was defined as the number of apoptotic cells (positive for caspase-3) out of the total number of nucleated cells. The proliferation rate was determined by counting the numbers of Ki-67-positive cells.

Estimating vascular density by Chalkley counting

The Chalkley counting method has been previously described in detail [19]. Briefly, the three most vascular areas (hot spots) of each section stained with CD31 were selected and analysed (Fig. 1b). Each vascular hotspot was viewed at × 200 magnification, and a 25-point Chalkley graticule was applied and oriented to permit the maximum number of points to hit in or within the CD31 stained blood vessels [19, 20].

Table 1. Clinical information of patients with osteochondroma and secondary peripheral chondrosarcoma

Case #	Sample	Age (years)	Gender	Location	*EXT* mutation analysis [1] (type of mutation)	Cartilage cap thickness (mm)
L-741	GP	2	M	Femur	-	-
L-996	GP	8	M	Femur	-	-
L-1142	GP	12	F	Tibia	-	-
L-1234	GP	8	F	Femur	-	-
L-298	OC	24	M	Femur	*EXT1* exon 3: c.1121G > A, p.W374X (ns) [2]	6
L-317	OC	31	M	Tibia	None in *EXT1* or *EXT2* [2]	4
L-332	OC	25	M	Femur	None in *EXT1* or *EXT2* [2]	5.5
L-523	OC	20	M	Tibia	*EXT1* del codon 235-239 (del Pro-Leu-Phe-Ser-Lys) [2]	5
L-524	OC	26	M	Tibia	*EXT1* codon 164 GAC>CAC (Asp>His),exon 1: c.1212G>C, p. D164H [2]	4.5
L-722	OC	15	F	Radius	*EXT2* IVS7 +1G>A [2]	1.5
L-726	OC	6	M	Rib	*EXT2* IVS7 +1G>A	6
L-841	OC	14	F	Femur	*EXT2* deletion exon 6 + 7 (del) [2]	8
L-1094	OC	6	M	Femur	*EXT2* del exon 6+7	3
L-1143	OC	39	M	Femur	NA	2
L-2029	OC	23	F	Femur	*EXT2* exon 7: IVS7+1 G>A	3.5
L-2069	OC	11	M	Tibia	*EXT1* exon 1 c.538_539delAG, p.Ser180fsX7 [2]	5.5
L-2160	OC	48	F	Scapula	*EXT1* exon1 c.538_539delAG, p.Ser180fsX17	6
L-2350	OC	53	F	Femur	*EXT2* exon 7: IVS7+1 G>A	1
L-951	PCH	24	M	Fibula	NA	8
L-2117	PCH	37	M	Humerus	*EXT1* exon 2: c.1056+1G>A	12
L-114	PCH	39	M	Femur	*EXT2* exon 5: 764T>C, L255P (uv) [2]	12
L-578	PCH	22	F	Femur	*EXT2* deletion exon 6 + 7 (del)	11
L-2254	PCH	33	F	Pelvis	*EXT2* exon 6 c.980delG, p.Gly327AlafsX5	8
L-2372	PCH	54	M	Rib	NA	13

GP, epiphyseal growth plate; OC, osteochondroma; PCH, low grade secondary peripheral chondrosarcoma; NA, not analysed

a - Mutation nomenclature was according to the Nomenclature Working Group [30]; ns non-sense, del deletion, uv unclassified variant, fs frame shift, pm polymorphism

b - Results of mutation previously reported [15, 23, 24]

The Chalkley count for each section was taken as the mean value of the three counts and performed by two observers independently (C.E.A. and J.V.M.G.B.).

Mutation analysis

Eleven patients were screened by direct sequencing for DNA mutations in the coding sequence of EXT1 or EXT2 genes [21]. After informed consent, DNA was isolated from resected tumours. If no alterations were found, a multiplex ligation-dependent probe amplification assay designed for EXT1 and EXT2 genes was performed to identify possible large deletions, as previously described [22]. Mutation analysis from six patients has been previously reported [15, 23, 24] (Table 1).

Statistical analysis

Results are expressed as the means with a measure of variability (standard deviation, S.D.). Statistical significance was calculated by one-way analysis of variance with Bonferroni's multiple comparison tests. Spearman's rank correlation coefficient was calculated to verify statistical dependence between two variables. Both tests were performed using the SPSS 16.0 software package (IBM, Somers, NY, USA). P values <0.05 were considered significant.

Results

Collagen X-rich matrix in peripheral cartilaginous tumours

The epiphyseal growth plate is organised in columns of stacked chondrocytes (Fig. 2a). The interface between cartilaginous and osseous parts in the growth plate (osteocartilaginous interface) was well defined and formed by hypertrophic chondrocytes immersed in a strong stained collagen X-rich matrix (Fig. 2d). In the growth plate, the collagen X-rich matrix was restricted to the hypertrophic zone and had, on average, 0.8 (± 0.47) mm thickness.

Osteochondromas showed less structured tissue organisation. The osteocartilaginous interface was also less well defined (Fig. 2b). The collagen X-rich matrix was restricted to the hypertrophic zone and had, on average, 1.5 (± 1.48) mm thickness. Additionally, in osteochondroma, not all chondrocytes with a hypertrophic morphology expressed type X collagen (Fig. 2e), and when type X collagen was present, the staining was mainly seen around the chondrocytes and not across the matrix (Fig. 2e). In osteochondromas, no correlation was found between the age of the patient and the thickness of the collagen X-rich matrix (Spearman's coefficient = 0.25).

Secondary peripheral chondrosarcomas showed no structured tissue organisation (Fig. 2c) and had an average cap thickness of 10 mm. Secondary peripheral chondrosarcomas showed a thick, uniformly and strongly stained collagen X-rich matrix (Fig. 2f) with an average 6.5 (± 3.66) mm thickness. Type X collagen expression in secondary peripheral chondrosarcomas was not restricted to the osteocartilaginous interface but was also detected throughout the extracellular tumour matrix and close to the perichondrium (data not shown). In secondary peripheral chondrosarcomas, no correlation was found between the age of the patient and the thickness of the collagen X-rich matrix (Spearman's coefficient = 0.01).

In osteochondromas and secondary peripheral chondrosarcomas, the thickness of the collagen X-rich matrix correlated with the thickness of the cartilage cap (Spearman's coefficient = 0.63) (Fig. 2g).

Similar apoptotic rates were observed in osteochondromas and secondary peripheral chondrosarcomas and had values of 35 (± 0.16) % vs. 36 (± 0.15) %, respectively (P = 0.847).

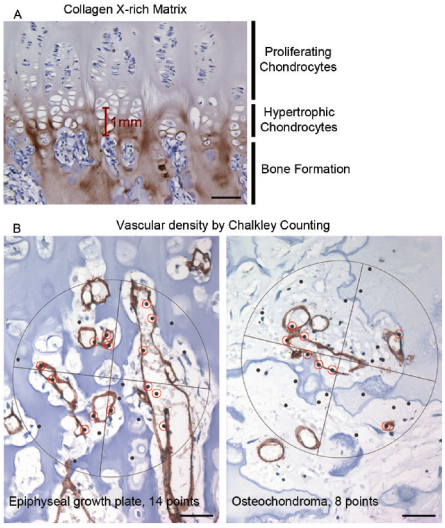


Figure 1. Collagen X-rich matrix and vascular density by Chalkley counting. Collagen X-rich matrix produced by hypertrophic chondrocytes was measured from the beginning to the end of the hypertrophic zone (a). Chalkley count reflects the number of grid points that hit CD31 stained vessels (red circles) (b). It is more of an estimate of the relative area than a true vessel count (a scale bar 10 µm; b scale bars 5 µm).

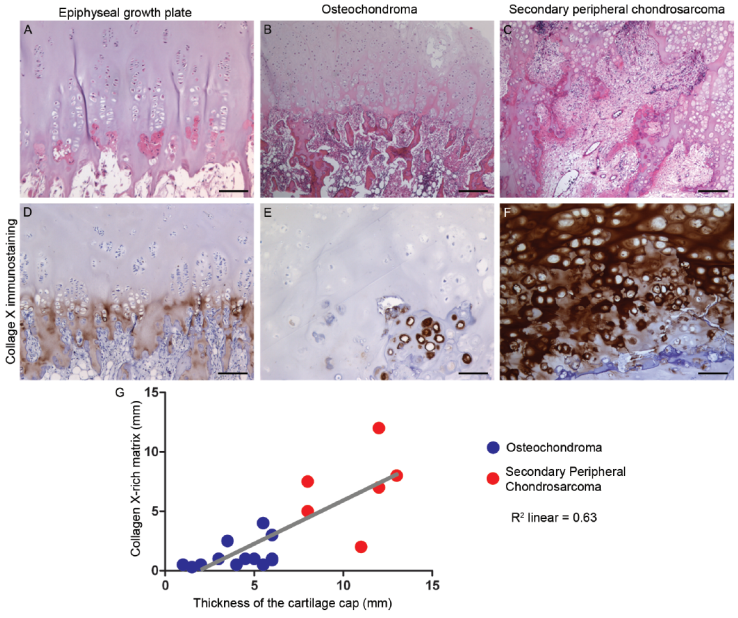


Figure 2. Collagen X-rich matrix. The epiphyseal growth plate is organised in columns of stacked chondrocytes (a). Osteochondromas show less structured organisation (b), and secondary peripheral chondrosarcomas (c) display no clear organisation. Hypertrophic chondrocytes secrete a collagen X-rich matrix, which, ultimately, is replaced by bone (d). In osteochondromas, chondrocytes with a hypertrophic morphology are not always secreting collagen X (e). In secondary peripheral chondrosarcoma, a thick layer of collagen X-rich matrix is observed (f). In osteochondromas and secondary peripheral chondrosarcomas, the thickness of the cartilage cap correlates with the thickness of collagen X-rich matrix (g) (scale bars 10 µm).

Vascular density in the ossification area

Invasion of blood vessels is a critical step towards ossification of the collagen X-rich matrix. Strong CD31 staining was observed along the cell membrane of endothelial cells in the epiphyseal growth plate, osteochondroma, and secondary peripheral chondrosarcoma. The median CD31 vascular density in the growth plate osteocartilaginous interface was significantly higher than in osteochondroma, with a value of 10.8 (± 0.83) vs. 6.1 (± 1.79), respectively (P = 0.007) (Fig. 3a, b, d). Interestingly, no differences in vascularisation of the osteocartilaginous interface were observed between the growth plate and secondary peripheral chondrosarcoma; a value of 10.8 (± 0.83) vs. 10 (± 0.70) was, respectively, found (P = 0.464) (Fig. 3a, c, d). Moreover, an irregular distribution of blood vessels was identified in the osteocartilaginous interface of osteochondromas and peripheral chondrosarcomas, but not in the epiphyseal growth plates.

In osteochondromas and secondary peripheral chondrosarcomas, no association between the age of the patient and vascular density was found (Spearman's rho correlation coefficient = 0.39 and 0.27, respectively).

In osteochondromas, the proliferation rate ranged from 0–24% in 9 cases to 25–49% in 5 cases. The cases with a higher proliferation rate (25–49%) showed a higher vascular density when compared to the cases with a lower proliferation rate (0–24%); a value of 8 (± 0.83) vs. 5.2 (± 1.58) was, respectively, found (P = 0.008).

Mutation analysis

Fifteen of 16 patients with multiple osteochondromas demonstrated a mutation in *EXT1* or *EXT2* (Table 1). One patient, from whom two distinct tumours were studied (L-317 and L-332), displayed no mutations in *EXT1* or *EXT2*. Additionally, no correlation was found between mutation type and (a) either tumour type (P = 0.564) (b) or the thickness of the collagen X-rich matrix (P = 0.564) (c) or vascular density (P = 0.556).

Discussion

In this study, two crucial steps of endochondral ossification, formation of a collagen X-rich matrix and invasion/attraction of blood vessels, were assessed and compared in the epiphyseal growth plate and peripheral cartilaginous tumours (osteochondroma and secondary peripheral chondrosarcoma). The protein expression level of type X collagen in human osteochondroma was shown to be similar to the one found in human epiphyseal growth plate [4]. Interestingly, in the EXT1 heterozygous mutant mice, in situ hybridisation studies have demonstrated that the mRNA expression of type X collagen is reduced in the growth plate as compared to wild-type mice [11, 25]. In addition, endochondral bone formation has been shown to be affected in the homozygous dak/ext2 zebrafish mutant [12].

Here, we describe that not all of the osteochondroma cells undergo terminal differentiation. These cells, although displaying a hypertrophic phenotype, do not express type X collagen (Fig. 2e). This may suggest that mutations in *EXT1* or *EXT2* genes may affect terminal chondrocyte differentiation in humans. Interestingly, progression of osteochondroma towards secondary peripheral chondrosarcoma showed an increased production of type X collagen. Therefore, the secondary peripheral chondrosarcoma cells expressing abundant type X collagen indicated that they have undergone terminal chondrocyte differentiation.

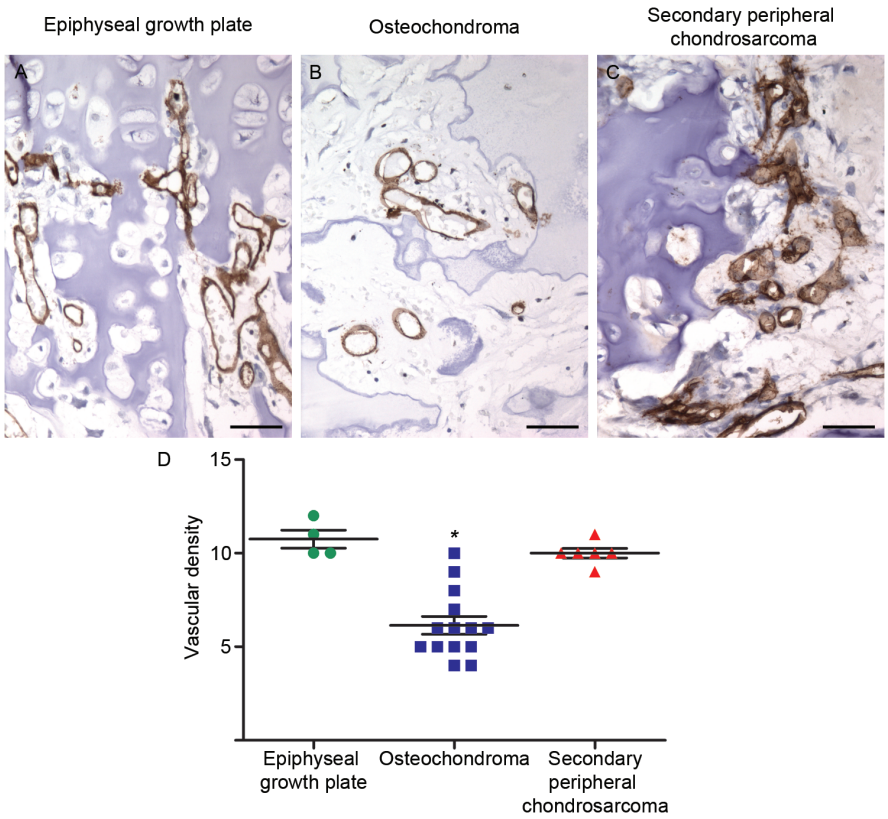


Figure 3. Vascular density in the ossification zone. The epiphyseal growth plate (a, d) and secondary peripheral chondrosarcoma (c, d) show similar vascular density. Osteochondroma displays low vascular density (b, d) (asterisk indicates $P < 0.05$; scale bars 5 µm).

Osteochondromas and secondary peripheral chondrosarcoma had a similar apoptotic rate. This indicates that, although secondary peripheral chondrosarcoma cells undergo terminal differentiation, the differentiation process does not induce apoptosis. Hence, low cell death seems to contribute to the relatively rapid growth of peripheral chondrosarcoma.

Several pro-angiogenic growth factors, such as FGF-2 and VEGFs, bind to heparan sulphate proteoglycans [26]. Heparan sulphate proteoglycans have been shown to regulate the distribution of these signalling molecules throughout the extracellular matrix and their receptor binding affinity [27]. Syndecan-2 is a cell surface heparan sulphate proteoglycan [26]. Syndecan-2 has been demonstrated to bind to VEGF, thereby regulating the distribution of VEGF nearby its receptor [28]. Interestingly, in osteochondromas, syndecan-2 is no longer located in the plasma membrane, but is shown to be accumulated in the Golgi apparatus [24]. The abnormal intracellular location of syndecan-2 may affect the distribution of VEGF, explaining the low efficiency of the osteochondroma cells in attracting blood vessels. Osteochondromas with high vascular density in the osteocartilaginous interface displayed a higher proliferation rate. This might suggest that proliferation of tumour cells is associated with increased vascularisation in the osteocartilaginous interface. Interestingly, secondary peripheral chondrosarcomas showed similar efficiency in attracting blood vessels as the epiphyseal growth plate.

We have recently shown that cells with functional *EXT1* and *EXT2* genes are the predominant subclone in secondary peripheral chondrosarcomas [9]. Therefore, the increased type X collagen deposition and blood vessel attraction in the osteocartilaginous interface of secondary peripheral chondrosarcoma are possibly associated with cells with functional *EXT1* and *EXT2* genes. In addition, collagen X-rich matrix formation and vascularisation might be useful prognostic markers of neoplastic transformation of an osteochondroma, but further validation is required before they can be proposed as a routine and as a reliable diagnostic tool.

In conclusion, we show that terminal chondrocyte differentiation and vascularisation are affected in osteochondromas, suggesting that *EXT1* and *EXT2* genes are critical for endochondral bone formation. Terminal chondrocyte differentiation and vascularisation seem to be unaffected in secondary peripheral chondrosarcomas, which might be associated with the presence of cells with functional *EXT1* and *EXT2* genes.

Acknowledgments

This work was supported by the European network of excellence EuroBoNeT (http://www.eurobonet.eu) grant number 018814 (LSHC-CT-2006-018814).

Conflict of interest

The authors declare that they have no conflict of interest.

References

1. Kronenberg HM (2003) Developmental regulation of the growth plate. Nature 423:332–336.
2. Kuhn JL, DeLacey JH, Leenellett EE (1996) Relationship between bone growth rate and hypertrophic chondrocyte volume in New Zealand white rabbits of varying ages. J Orthop Res 14:706–711.
3. Ballock RT, O'Keefe RJ (2003) The biology of the growth plate. J Bone Joint Surg Am 85-A:715–726.
4. Aigner T, Frischolz S, Dertinger S, Beier F, Girkontaité I, Von der Mark K (1997) Type X collagen expression and hypertrophic differentiation in chondrogenic neoplasias. Histochem Cell Biol 107:435–440.
5. Khurana J, Abdul-Karim F (2002) Bovée JVMG Osteochondroma. In: Fletcher CDM, Unni KK, Mertens F (eds) World Health Organization classification of tumours. Pathology and genetics of tumours of soft tissue and bone. IARC Press, Lyon (France), pp 234–236.
6. van den Berg H, Kroon HM, Slaar A, Hogendoorn P (2008) Incidence of biopsy-proven bone tumors in children: a report based on the Dutch pathology registration "PALGA". J Pediatr Orthop 28(1):29–35.
7. Bovee JVMG, Hogendoorn PCW, Wunder JS, Alman BA (2010) Cartilage tumours and bone development: molecular pathology and possible therapeutic targets. Nat Rev Cancer 10:481–488.
8. Dorfman HD, Czerniak B, Kotz R, Vanel D, Park YK, Unni KK (2002) WHO classification of tumours of bone: introduction. In: Fletcher CDM, Unni KK, Mertens F (eds) World Health Organization classification of tumours. Pathology and genetics of tumours of soft tissue and bone. IARC Press, Lyon, pp 226–232.
9. de Andrea CE, Reijnders CM, Kroon HM, de Jong D, Hogendoorn PC, Szuhai K et al (2011) Secondary peripheral chondrosarcoma evolving from osteochondroma as a result of outgrowth of cells with functional EXT. Oncogene 2012;31:1095-104.
10. Kucharzewska P, Welch JE, Birgersson J, Belting M (2010) Establishment of heparan sulphate deficient primary endothelial cells from EXT-1(flox/flox) mouse lungs and sprouting aortas. In Vitro Cell Dev Biol Anim 46:577–584.
11. Hilton MJ, Gutierrez L, Martinez DA, Wells DE (2005) EXT1 regulates chondrocyte proliferation and differentiation during endochondral bone development. Bone 36:379–386.
12. Wiweger MI, Avramut CM, de Andrea CE, Prins FA, Koster AJ, Ravelli RB et al (2011) Cartilage ultrastructure in proteoglycan-deficient zebrafish mutants brings to light new candidate genes for human skeletal disorders. J Pathol 223:531–542.

13. Hufnagel L, Kreuger J, Cohen SM, Shraiman BI (2006) On the role of glypicans in the process of morphogen gradient formation. Dev Biol 300:512–522.
14. Hacker U, Nybakken K, Perrimon N (2005) Heparan sulphate proteoglycans: the sweet side of development. Nat Rev Mol Cell Biol 6:530–541.
15. Reijnders CM, Waaijer CJ, Hamilton A, Buddingh' EP, Dijkstra SP, Ham J et al (2010) No haploinsufficiency but loss of heterozygosity for EXT in multiple osteochondromas. Am J Pathol 177:1946–1957.
16. Verbeke SL, Fletcher CD, Alberghini M, Daugaard S, Flanagan AM, Parratt T et al (2010) A reappraisal of hemangiopericytoma of bone; analysis of cases reclassified as synovial sarcoma and solitary fibrous tumor of bone. Am J Surg Pathol 34:777–783.
17. Schrage YM, Machado I, Meijer D, Briaire-de Bruijn I, van den Akker B, Taminiau AHM et al (2010) COX-2 expression in chondrosarcoma: a role for celecoxib treatment? Eur J Cancer 46:616–624.
18. de Andrea CE, Wiweger M, Prins F, Bovee JVMG, Romeo S, Hogendoorn PCW (2010) Primary cilia organization reflects polarity in the growth plate and implies loss of polarity and mosaicism in osteochondroma. Lab Invest 90:1091–1101.
19. Vermeulen PB, Gasparini G, Fox SB, Toi M, Martin L, McCulloch P et al (1996) Quantification of angiogenesis in solid human tumours: an international consensus on the methodology and criteria of evaluation. Eur J Cancer 32A:2474–2484.
20. Hansen S, Grabau DA, Sorensen FB, Bak M, Vach W, Rose C (2000) The prognostic value of angiogenesis by Chalkley counting in a confirmatory study design on 836 breast cancer patients. Clin Cancer Res 6:139–146.
21. Vink GR, White SJ, Gabelic S, Hogendoorn PCW, Breuning MH, Bakker E (2004) Mutation screening of EXT1 and EXT2 by direct sequence analysis and MLPA in patients with multiple osteochondromas: splice site mutations and exonic deletions account for more than half of the mutations. Eur J Hum Genet 13:470–474.
22. White SJ, Vink GR, Kriek M, Wuyts W, Schouten J, Bakker B et al (2004) Two-color multiplex ligation-dependent probe amplification: detecting genomic rearrangements in hereditary multiple exostoses. Hum Mutat 24:86–92.
23. Bovee JVMG, Cleton-Jansen AM, Wuyts W, Caethoven G, Taminiau AHM, Bakker E et al (1999) EXT-mutation analysis and loss of heterozygosity in sporadic and hereditary osteochondromas and secondary chondrosarcomas. Am J Hum Genet 65:689–698.
24. Hameetman L, David G, Yavas A, White SJ, Taminiau AHM, Cleton-Jansen AM et al (2007) Decreased EXT expression and intracellular accumulation of HSPG in osteochondromas and peripheral chondrosarcomas. J Pathol 211:399–409.

25. Koziel L, Kunath M, Kelly OG, Vortkamp A (2004) EXT1-dependent heparan sulfate regulates the range of Ihh signaling during endochondral ossification. Dev Cell 6:801–813.
26. Iozzo RV (2001) Heparan sulfate proteoglycans: intricate molecules with intriguing functions. J Clin Invest 108:165–167.
27. Bernfield M, Gotte M, Park PW, Reizes O, Fitzgerald ML, Lincecum J et al (1999) Functions of cell surface heparan sulfate proteoglycans. Annu Rev Biochem 68:729–777.
28. Chen E, Hermanson S, Ekker SC (2004) Syndecan-2 is essential for angiogenic sprouting during zebrafish development. Blood 103:1710–1719.

Summary and Concluding Remarks

I. Zebrafish as a model system to study human skeletal disorders
II. Developmental regulation of the epiphyseal growth plate in relation to the formation of osteochondroma
III. The role of EXT1 and EXT2 genes in the formation of a secondary peripheral chondrosarcoma
IV. Clues to the mechanisms of neoplastic transformation of osteochondroma towards secondary peripheral chondrosarcoma
VI. Conclusions

Chapter 10

I. Zebrafish as a model system to study human skeletal disorders

Mutations in the exostosin genes, *dackel* (*dak/ext2*) and *boxer* (*box/exlt3*), cause defects in zebrafish cartilage that strongly resemble those seen in patients with multiple osteochondromas [1;2]. **Chapters 3**, **4** and **5** address the use of the dak mutant zebrafish as a model to understand the formation of human osteochondroma.

Cartilage is formed by the interweaving of collagen fibres and proteoglycans. Polyethyleneimine (PEI) is a well-described cationic dye used in reflection contrast- and electron microscopy. PEI binds to anionic sites on proteoglycans and allows visualisation and quantification of the negatively charged sites at the ultrastructural level. Using PEI pre-embedding staining, we showed wild-type zebrafish and fish mutants with a mild cartilage phenotype display proteoglycans distributed in a gradient fashion throughout the cartilaginous extracellular matrix (**Chapter 5**). A similar pattern of distribution was observed in normal human growth plate. In contrast, chondrocytes from *dak* mutant fish did not display proteoglycans distributed in a gradient fashion throughout the cartilaginous extracellular matrix (**Chapter 5**) which was similar to human osteochondroma in which gradients were also absent. Interestingly, only a subset of osteochondroma cells displayed absence of extracellular gradients of proteoglycans, which suggests that those cells have homozygous inactivation of *EXT1/EXT2*. Moreover, these homozygous mutant cells have been shown to be intermingled with a population of cells that appeared to have an intact distribution of proteoglycans in a gradient fashion (**Chapter 5**). Therefore, the distinct subset of cells that compose an osteochondroma indicate that this bone tumour is a mosaic of *EXT1/EXT2* mutant and wild-type cells. The mosaic cell population of osteochondroma has been also elegantly reported by Jones et al. using a conditional mouse model for *Ext1* [3]. Additionally, using these mutant zebrafish, we showed that heparan sulphate controls mesenchymal differentiation towards the osteoblastic lineage (**Chapter 4**). Our data suggest that heparan sulphate is involved in the “bone-to-fat” switch during mesenchymal differentiation, without affecting chondrogenic- or muscle lineages. The over-expression of PPAR-γ signalling is possibly involved in the inhibition of osteoblastogenesis in zebrafish. However, it still remains to be established how exactly heparan sulphate controls the “bone-to-fat” switch. Whether this phenomenon plays a role in human osteochondroma formation is so far unclear.

II. Developmental regulation of the epiphyseal growth plate in relation to the formation of osteochondroma

The growth and structure of the epiphyseal growth plate is regulated by short and long range signalling molecules. The diffusion of these molecules across the cartilaginous extracellular matrix is shown to be mediated by proteoglycans [4].

Proteoglycans are distributed across the cartilaginous extracellular matrix in a gradient fashion, as was shown in **Chapter 5**. Nevertheless, the question remains: how the gradients of proteoglycans are formed?

Proteoglycans are polyanionic chains. Their molecules have negatively charged sites that arise from their sulphate and carboxyl groups. In solution, the mutual repulsion of these negative charges causes an aggregated proteoglycan molecule to spread out and occupy a large volume [5]. This mutual repulsion of negative charges may partially explain the formation of gradients of proteoglycans across the cartilaginous extracellular matrix.

Osteochondromas have been linked to loss-of-function mutations in *EXT1/EXT2*. The *EXT* genes encode glycosyltransferases involved in heparan sulphate biosynthesis. The mechanism by which alterations in heparan sulphate biosynthesis lead to osteochondroma is not entirely understood. As heparan sulphate acts as a co-receptor for fibroblast growth factors and BMPs [6], and regulates the diffusion of Ihh [7] and members of the Wnt family [8], improper elongation of heparan sulphate chains may result in loss of extracellular gradients of proteoglycans as well as in a variety of growth factor signalling defects and impaired cell-cell and cell-matrix interactions, which ultimately may result in osteochondroma formation.

Cells with homozygous inactivation of *EXT1/EXT2* are thought to disrupt gradients of signalling molecules, by affecting the gradient distribution of proteoglycans (**Chapter 2** and **5**). As heparan sulphate modulates the formation of gradients of Ihh and Wnt, altered gradients may disturb these pathways, which may contribute to the initiation of an osteochondroma. The diffusion of Ihh molecules and their ligand-receptor interaction have been demonstrated to be affected by the dysfunction of *Ext1* in chondrocytes during endochondral ossification [9]. Additionally, improper diffusion of Ihh may affect osteogenesis at the perichondrium. The perichondrium then fails form a bone collar, which may facilitate the formation of an osteochondroma. The gradients of Wnt signalling are involved in planar cell polarity, providing positional information to govern morphogenesis [10]. Planar cell polarity has been linked to a microtubule-based subcellular organelle that projects from the surface of the cell called the primary cilium [11]. Primary cilia function as a signalling apparatus of the cell that receives and transduces mechanical and chemical signals from the neighbouring cells and the extracellular matrix. In the proliferating and hypertrophic chondrocytes of the epiphyseal growth plate, primary cilia are polarized and oriented parallel to the longitudinal axis of the bone (**Chapter 6**). Shorter heparan sulphate chains produced by osteochondroma cells may affect the formation of gradients of Wnt signalling. Hypothetically, the lack of adequate positional information may impair the polarity function of primary cilia in osteochondroma cells. The loss of cell/tissue polarity may contribute to osteochondroma formation (**Chapters 2** and **6**).

III. The role of EXT1 and EXT2 genes in the formation of a secondary peripheral chondrosarcoma

Neoplastic transformation of an osteochondroma occurs in less than 1% of patients with sporadic osteochondromas and 1-3% of patients with multiple osteochondromas [12].

A custom-made oligonucleotide-based microarray with a tiling coverage of *EXT1/EXT2* genes was used to detect deletions involving any part of *EXT1* or *EXT2* genes. We showed that, unlike in osteochondromas, homozygous deletions of *EXT1/EXT2* are rare events in sporadic secondary peripheral chondrosarcomas (**Chapter 7**). FISH with an EXT1 probe showed that cells with retention of one-, or both copies of *EXT1* constitute the major population of cells in the tumour. As cells carrying a homozygous deletion (having no copies of the involved genomic region left at all) are not able to regain the lost alleles during neoplastic progression, the cellular origin of secondary peripheral chondrosarcomas is possibly the wild-type cells located either in the osteochondroma cap or in the neighbouring tissue. The presence of these wild-type cells in the cartilage cap of osteochondroma was suggested earlier by the PEI- and primary cilia studies (**Chapters 5** and **6**) as well as in mice using a conditional model for *Ext1* [3]. Using FISH, we showed the wild-type cells to predominate in the hypertrophic zone of osteochondroma (**Chapter 7**). Consequently, while homozygous inactivation of *EXT1/EXT2* is essential for osteochondroma formation, *EXT1* and *EXT2* seem not to play a role in the formation of most secondary peripheral chondrosarcomas (**Chapter 7**).

V. Clues to the mechanisms of neoplastic transformation of osteochondroma towards secondary peripheral chondrosarcoma

We have shown that morphological parameters alone cannot distinguish between osteochondroma and low-grade peripheral chondrosarcoma (**Chapter 8** and **9**). It remains very difficult and observer dependent to identify early malignant progression of an osteochondroma. We could not formulate a set of reliable histological criteria based upon a large multinational study (**Chapter 8**). On the other hand, we showed that malignant progression of an osteochondroma is associated with increased expression of type X collagen and increased vascularisation (**Chapter 9**). Formation of a collagen X-rich matrix and increased vascularisation might be useful prognostic markers of neoplastic transformation of an osteochondroma, but further validation is required before they can be proposed as a routine and reliable diagnostic tool.

Malignant progression of secondary peripheral chondrosarcoma is characterized by a high percentage of loss of heterozygosity (i.e., *CDKN2A/p16*, *TP53*, *RB1*) and ploidy ranging from half to twice the normal DNA content [13-15]. Therefore, during neoplastic transformation of most osteochondromas, the *EXT* wild-type cells may acquire genetic alterations in *p16*, *p53*, *RB1*, or an as yet not identified gene to give rise to secondary

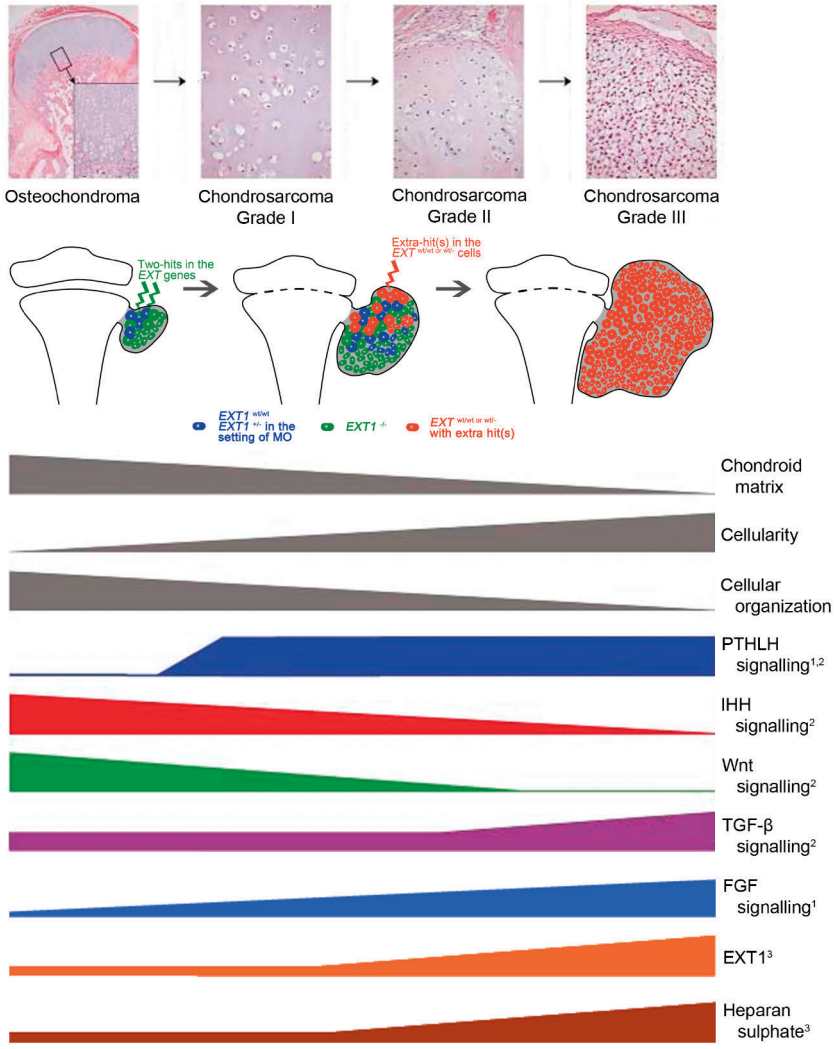


Figure 1. Schematic representation of changes in morphology and expression of signalling pathways during neoplastic transformation of an osteochondroma. Different tumours are represented by their histology. Progression towards secondary peripheral chondrosarcoma is characterized by a decrease in chondroid matrix and an increase in cellularity and cellular disorganization. Clonal cell selection occurs during the formation of a secondary peripheral chondrosarcoma. *EXT*-null cells (green cells) and *EXT* wild-type cells (blue cells) compose the osteochondroma cap. The *EXT*-null cells acquire genetic alteration(s) to give rise to a secondary peripheral chondrosarcoma. The chondrosarcoma cells (red cells) get a proliferative advantage, overgrowing the osteochondroma *EXT*-null cells. During neoplastic transformation/progression, PTHLH, TGF-β and FGF signalling increase. Similar increase is found for EXT1 and heparan sulphate. In addition, IHH and Wnt signalling decrease. (Adapted from Hameetman L et al. 2006). Figure references:

1- Bovee JVMG, et al. Lab Invest 2000;80:1925-33.
2- Hameetman L, et al. J Pathol 2006;209:501-11.
3- de Andrea CE, et al. Oncogene 2012;31:1095-104.

peripheral chondrosarcomas. While mutations in *IDH1/IDH2* have been associated with enchondromas and central chondrosarcomas [16;21], these genes are not involved in osteochondromas and peripheral chondrosarcomas [17;18], again proving their different genetic make up as compared to central cartilaginous tumours.

Previously, we have described that signalling pathways dependent on heparan sulphate, such as fibroblast growth factor (FGF) and parathyroid hormone-related protein (PTHLH), are inactive in osteochondromas and active in secondary peripheral chondrosarcomas [17;18]. We have shown that cells with functional *EXT1* and *EXT2* are the predominant clone in secondary peripheral chondrosarcomas (**Chapter 7**). Probably, these *EXT1/EXT2* wild-type cells synthesize heparan sulphate with normal chain length, which may explain the active PTHLH and FGF in secondary peripheral chondrosarcomas (Figure 1).

The contribution of FGFs and PTHLH to secondary peripheral chondrosarcoma formation is still unclear. In the epiphyseal growth plate, PTHLH suppresses chondrocyte differentiation into hypertrophic chondrocytes [19] and FGF regulates chondrocyte proliferation and differentiation [20].

VI. Conclusions

In the epiphyseal growth plate, the way that chondrocytes interact with each other and with their micro-environment via extracellular matrix has gradually been unveiled. In the epiphyseal growth plate, these interactions lead to the formation of a polarized tissue structure. Cells in the epiphyseal growth plate harbouring homozygous mutations in *EXT1/EXT2* disrupt the diffusion gradients and signal transduction, leading to the loss of cell polarity, which may contribute to the formation of an osteochondroma. In addition, osteochondroma may act as a permissive environment, which facilitates *EXT1/EXT2* wild-type cells located in its cartilage cap to acquire genetic changes to form a secondary peripheral chondrosarcoma.

References

1. Clément A, Wiweger M, von der Hardt S., Rusch MA, Selleck SB, Chien CB, et al. Regulation of zebrafish skeletogenesis by ext2/dackel and papst1/pinscher. PLoS Genet 2008;4:e1000136.
2. Wiweger MI, Avramut CM, de Andrea CE, Prins FA, Koster AJ, Ravelli RB, et al. Cartilage ultrastructure in proteoglycan-deficient zebrafish mutants brings to light new candidate genes for human skeletal disorders. J Pathol 2011;223:531-42.
3. Jones KB, Piombo V, Searby C, Kurriger G, Yang B, Grabellus F, et al. A mouse model of osteochondromagenesis from clonal inactivation of Ext1 in chondrocytes. Proc Natl Acad Sci U S A 20108;107:2054-9.
4. Wu Y, Belenkaya TY, Lin X. Dual roles of Drosophila glypican Dally-like in Wingless/Wnt signaling and distribution. Methods Enzymol 2010;480:33-50.

5. Mansour JM. Biomechanics of cartilage. In: Oatis C, editor. Kinesiology: The Mechanics and Pathomechanics of Human Movement. 2 ed. ed. Philadelphia, PA: Lippincott Williams and Wilkins; 2008. p. 66-79.
6, Bernfield M, Gotte M, Park PW, Reizes O, Fitzgerald ML, Lincecum J, et al. Functions of cell surface heparan sulfate proteoglycans. Annu Rev Biochem 1999;68:729-77.
7. Cortes M, Baria AT, Schwartz NB. Sulfation of chondroitin sulfate proteoglycans is necessary for proper Indian hedgehog signaling in the developing growth plate. Development 2009;136:1697-706.
8. Fuerer C, Habib SJ, Nusse R. A study on the interactions between heparan sulfate proteoglycans and Wnt proteins. Dev Dyn 2010;239:184-90.
9. Koziel L, Kunath M, Kelly OG, Vortkamp A. Ext1-dependent heparan sulfate regulates the range of Ihh signaling during endochondral ossification. Dev Cell 2004;6:801-13.
10. Gao B, Song H, Bishop K, Elliot G, Garrett L, English MA, et al. Wnt signaling gradients establish planar cell polarity by inducing Vangl2 phosphorylation through Ror2. Dev Cell 2011;20:163-76.
11. Jones C, Roper VC, Foucher I, Qian D, Banizs B, Petit C, et al. Ciliary proteins link basal body polarization to planar cell polarity regulation. Nat Genet 2008;40:69-77.
12. Bertoni F, Bacchini P, Hogendoorn PCW. Chondrosarcoma. In: Fletcher CDM, Unni KK, Mertens F, editors. World Health Organisation classification of tumours. Pathology and genetics of tumours of soft tissue and bone.Lyon: IARC Press; 2002. p. 247-51.
13. Hallor KH, Staaf J, Bovée JVMG, Hogendoorn PCW, Cleton-Jansen AM, Knuutila S, et al. Genomic Profiling of Chondrosarcoma: Chromosomal Patterns in Central and Peripheral Tumors. Clin Cancer Res 2009;15:2685-94.
14. Bovée JVMG, Royen Mv, Bardoel AFJ, Rosenberg C, Cornelisse CJ, Cleton-Jansen AM, et al. Near-haploidy and subsequent polyploidization characterize the progression of peripheral chondrosarcoma. Am J Pathol 2000;157:1587-95.
15. Bovée JVMG, Sciot R, Dal Cin P, Debiec-Rychter M, Van Zelderen-Bhola SL, Cornelisse CJ, et al. Chromosome 9 alterations and trisomy 22 in central chondrosarcoma: a cytogenetic and DNA flow cytometric analysis of chondrosarcoma subtypes. Diagn Mol Pathol 2001;10:228-36.
16. Pansuriya TC, van ER, d'Adamo P, van Ruler MA, Kuijjer ML, Oosting J, et al. Somatic mosaic IDH1 and IDH2 mutations are associated with enchondroma and spindle cell hemangioma in Ollier disease and Maffucci syndrome. Nat Genet 2011;43:1256-61.

17. Bovee JVMG, Van den Broek LJCM, Cleton-Jansen AM, Hogendoorn PCW. Up-regulation of PTHrP and Bcl-2 expression characterizes the progression of osteochondroma towards peripheral chondrosarcoma and is a late event in central chondrosarcoma. Lab Invest 2000;80:1925-33.
18. Hameetman L, Rozeman LB, Lombaerts M, Oosting J, Taminiau AHM, Cleton-Jansen AM, et al. Peripheral chondrosarcoma progression is accompanied by decreased Indian Hedgehog (IHH) signalling. J Pathol 2006;209:501-11.
19. Vortkamp A, Lee K, Lanske B, Segre GV, Kronenberg HM, Tabin CJ. Regulation of rate of cartilage differentiation by indian hedgehog and PTH-related protein. Science 1996;273:613-22.
20. Kronenberg HM. Developmental regulation of the growth plate. Nature 2003 May 15;423(6937):332-6.
21. Amary MF, Bacsi K, Maggiani F et al. IDH1 and IDH2 mutations are frequent events in central chondrosarcoma and central and periosteal chondromas but not in other mesenchymal tumours. J Pathol 2011; 224:334-343.

Inhoud

I. De zebravis als een modelsysteem voor de studie van menselijke skelet aandoeningen
II. Epifysaire groeischijf ontwikkelingsregulatie en de vorming van het osteochondroom
III. De rol van EXT1 en EXT2 genen bij de vorming van een secundair perifeer chondrosarcoom
IV. Mogelijke oplossingen voor de mechanismen van neoplastische transformatie van osteochondromen naar perifere chondrosarcomen
V. Conclusies

Nederlandse samenvatting

I. De zebravis als een modelsysteem voor de studie van menselijke skelet aandoeningen

Mutaties in de exostosin genen, dackel (dak/ext2) en boxer (box/exlt3), leiden tot defecten in zebravis kraakbeen, die sterk lijken op de afwijkingen in patiënten met multipele osteochondromen. De **hoofdstukken 3**, **4** en **5** hebben betrekking op het gebruik van de dak mutant zebravis als model voor de vorming van de menselijke osteochondroom.

Kraakbeen wordt gevormd door de verwevenheid van collageen vezels en proteoglycanen. Polyethyleenimine (PEI) is een goed gedefiniëerde kationische kleurstof voor toepassing in reflectiecontrast- en elektronenmicroscopie. PEI bindt aan anionische sites op proteoglycanen en maakt visualisatie en kwantificering van de negatief geladen sites op het ultrastructurele niveau mogelijk. Met behulp van PEI pre-embedding kleuring toonden we aan dat in wild-type zebravissen en in mutanten met een mild fenotype de proteoglycanen in een gradient gedistribueerd zijn over de gehele kraakbenige extracellulaire matrix (**hoofdstuk 5**). Een soortgelijk patroon van de distributie werd waargenomen in de normale humane groeischijf. Chondrocyten van de dak mutant vertoonden daarentegen geen gradueel verdeelde proteoglycanen (**hoofdstuk 5**). Dit was vergelijkbaar met het humane osteochondroom waarin de gradiënten ook afwezig waren. Interessant is dat slechts een deel van de osteochondroom cellen de extracellulaire gradiënten van proteoglycanen missen, wat doet vermoeden dat alleen die cellen homozygote inactivatie van *EXT1/EXT2* hebben. De homozygoot mutant cellen bleken gemengd te zijn met een populatie van cellen met een correcte verdeling van proteoglycanen in een gradiënt (**hoofdstuk 5**). Het lijkt er derhalve op dat de verschillende cellen die het osteochondroom vormen bestaan uit een mozaïek van *EXT1/EXT2* mutant en het wild-type cellen. De mozaïek celpopulatie van het osteochondroom is ook fraai gerapporteerd door Jones et al. met een conditioneel muismodel voor *Ext1*. Bovendien hebben we met deze mutant zebravis aangetoond dat heparansulfaat de mesenchymale differentiatie naar de osteoblastische lijn controleert (**hoofdstuk 4**). Onze gegevens suggereren dat heparansulfaat betrokken is bij de “bot-naar-vet”-schakelaar tijdens de mesenchymale differentiatie, zonder dat dit invloed heeft op de ontwikkeling van chondrocyten of spiercellen. De over-expressie van *PPAR-γ* signaaltransductie is mogelijk betrokken bij de inhibitie van osteoblast ontwikkeling in de zebravis. Er is nog niet precies vastgesteld hoe heparansulfaat de “bot-naar-vet” schakelaar controleert. Of dit verschijnsel een rol speelt in het humane osteochondroom is tot dusver onduidelijk.

II. Epifysaire groeischijf ontwikkelingsregulatie en de vorming van het osteochondroom

De groei en structuur van de epifysaire groeischijf worden geregeld door korte en lange afstand signaalmoleculen. De diffusie van deze moleculen in de kraakbeenachtige extracellulaire matrix wordt gemediëerd door proteoglycanen. Proteoglycanen zijn verdeeld

over de kraakbenige extracellulaire matrix in een gegradeerd verloop, zoals bleek in **hoofdstuk 5**. Toch blijft de vraag hoe de gradiënten van proteoglycanen worden gevormd.

Proteoglycanen zijn polyanionische ketens van moleculen met negatief geladen gebieden bestaand uit de sulfaat en carboxylgroepen. In opgeloste vorm zorgt ,de onderlinge afstoting van de negatieve lading ervoor dat de geaggregeerde proteoglycaan molecule uitspreiden en een groot volume innemen. Deze wederzijdse afstoting van negatieve ladingen kan deels de vorming van gradiënten van proteoglycanen in het kraakbeen extracellulaire matrix verklaren.

Osteochondromen worden geassocieerd met verlies-van-functie mutaties in *EXT1/EXT2*. De *EXT* genen coderen voor glycosyltransferases die betrokken zijn bij de heparansulfaat biosynthese. Het mechanisme hoe veranderingen in heparansulfaat biosynthese leiden tot het osteochondroom is niet volledig begrepen. Aangezien heparansulfaat werkt als een co-receptor voor fibroblast groeifactoren en BMP's, en het de diffusie van Ihh en leden van de Wnt-familie reguleert, kan een verkeerde verlenging van heparansulfaat ketens leiden tot verlies van extracellulaire proteoglycaan gradiënten. Dit resulteert dan in verschillende groeifactor signaleringsdefecten en verminderde cel-cel en cel-matrix interacties en uiteindelijk een osteochondroom.

Er wordt gedacht dat de gradiënten van signaalmoleculen rond cellen met homozygote inactivatie van *EXT1/EXT2* verstoord zijn, omdat daar de gradiënt distributie van proteoglycanen is aangetast (**hoofdstuk 2** en **5**). Aangezien heparansulfaat de vorming van gradiënten van IHH en Wnt moduleert, kunnen veranderingen in de gradiënten deze routes verstoren, en zo bijdragen aan het ontstaan van een osteochondroom. De diffusie van Ihh moleculen en hun ligand-receptor interactie toont aan dat zij worden beïnvloed door de dysfunctie van *Ext1* in chondrocyten tijdens de endochondrale ossificatie. Daarnaast geeft foute diffusie van Ihh een afwijking van de osteogenese bij het perichondrium. Het perichondrium kan dan geen bot kraag maken, wat bijdraagt aan de vorming van een osteochondroom. De gradiënten van Wnt signalering zijn betrokken bij "planar cell polarity", een proces wat zorgt voor positionering van de morfogenese. "Planar cell polarity" is gekoppeld aan een op een microtubulair gebaseerd subcellulair organel, het primaire cilium, wat uitsteekt aan de oppervlakte van de cel. Primaire cilia werken als een communicatie apparaat van de cel en ontvangen en transduceren mechanische en chemische signalen van de naburige cellen en van de extracellulaire matrix. In proliferende en hypertrofe chondrocyten van de epifysaire groeischijf zijn de primaire cilia gepolariseerd en evenwijdig aan de lengteas van het bot (**hoofdstuk 6**). Kortere heparansulfaat ketens die worden geproduceerd door osteochondroom cellen kunnen de vorming van gradiënten voor Wnt signalering beïnvloeden. Hypothetisch zou het gebrek aan adequate positionele informatie afbreuk kunnen doen aan de polariteit functie van primaire cilia in osteochondroom cellen.

Het verlies van cel/weefsel polariteit kan zo bijdragen aan de vorming van een osteochondroom (**hoofdstukken 2** en **6**).

III. De rol van *EXT1* en *EXT2* genen bij de vorming van een secundair perifeer chondrosarcoom

Neoplastische transformatie van een osteochondroom komt voor bij minder dan 1% van de patiënten met sporadische osteochondromen en bij 1-3% van de patiënten met meerdere osteochondromen.

Een op maat gemaakte oligonucleotide-gebaseerde microarray met een overlappende dekking van *EXT1/EXT2* genen werd gebruikt om deleties in elk stukje van de *EXT1* of *EXT2* genen op te sporen. We toonden aan dat, anders dan in osteochondromen, homozygote deleties van *EXT1/EXT2* zelden voorkomen in sporadische perifere chondrosarcomen (**hoofdstuk 7**). FISH met een EXT1 probe toonde aan dat cellen met behoud van één of beide kopieën van *EXT1* een grote populatie van cellen vormt in de tumor. Aangezien cellen met een homozygote deletie (die derhalve geen kopieën van de betrokken genomische regio meer hebben) niet in staat zijn om de verloren allelen tijdens neoplastische progressie terug te krijgen, moet de cellulaire oorsprong van perifere chondrosarcomen misschien wel te zoeken zijn in de wild-type cellen welke zich bevinden zich in de kap van het osteochondroom of in het naburige weefsel. De aanwezigheid van deze wild-type cellen in de kraakbeenkap van osteochondroom is eerder gesuggereerd door de PEI- en de primaire cilia studies (**hoofdstuk 5** en **6**) en ook in muizen met een conditioneel *Ext1* gen. Met behulp van FISH toonden we aan dat de wild-type cellen in de meerderheid zijn in de hypertrofische zone van osteochondromen (**hoofdstuk 7**). Daarom, terwijl de homozygote inactivatie van *EXT1/EXT2* essentieel is voor het osteochondroom, lijken *EXT1* en *EXT2* geen rol te spelen in de vorming van de meeste perifere chondrosarcomen (**hoofdstuk 7**).

IV. Mogelijke oplossingen voor de mechanismen van neoplastische transformatie van osteochondromen naar perifere chondrosarcomen

We hebben aangetoond dat morfologische parameters alleen geen onderscheid maken tussen osteochondromen en laaggradige perifere chondrosarcomen (**hoofdstuk 8** en **9**). Het blijft heel moeilijk en afhankelijk van de waarnemer om vroege kwaadaardige progressie van een osteochondroom te identificeren. We konden het geen betrouwbare histologische criteria fomuleren op basis van een grote multinationale studie (**hoofdstuk 8**). Echter, we hebben wel aangetoond dat kwaadaardige progressie van een osteochondroom geassocieerd is met verhoogde expressie van type X collageen en met verhoogde vascularisatie (**hoofdstuk 9**). De vorming van een collageen X-rijke matrix en een verhoogde vascularisatie kunnen bruikbare prognostische markers zijn van de neoplastische transformatie van een osteochondroom, maar verdere validatie is vereist voordat ze klinisch kunnen worden toegpast.

Kwaadaardige progressie van perifere chondrosarcomen wordt gekenmerkt door een hoog percentage van verlies van heterozygotie (bijvoorbeeld *CDKN2A/p16*, *TP53*, *RB1*) waarbij de ploïdie variëert van half tot tweemaal het normale DNA-gehalte. Daarom kunnen de *EXT* wild-type cellen in de meeste osteochondromen tijdens neoplastische transformatie genetische veranderingen oplopen in *p16*, *p53*, *RB1* of een nog niet geïdentificeerd gen, wat leidt tot de vorming van perifere chondrosarcomen. Terwijl de mutaties in *IDH1/IDH2* zijn geassocieerd met enchondromen en centrale chondrosarcomen, blijken deze genen niet betrokken bij de osteochondromen en perifere chondrosarcomen. Dit toont opnieuw de verschillende genetische make-up aan ten opzichte van centrale kraakbeen tumoren.

Eerder hebben wij beschreven dat signaaltransductie routes die afhankelijk zijn van heparansulfaat, zoals fibroblastgroeifactor (FGF) en parathyroïde hormoon-gerelateerde eiwit (PTHLH), inactief zijn in osteochondromen en actief in perifere tumoren. We hebben aangetoond dat cellen met functionele *EXT1* en *EXT2* genen de belangrijkste kloon vormen in perifere chondrosarcomen (**hoofdstuk 7**). Waarschijnlijk synthetiseren deze *EXT1/EXT2* wild-type cellen heparansulfaat met een normale ketenlengte, die de activiteit van PTHLH en FGF in perifere tumoren (figuur 10.1) kunnen verklaren.

De bijdrage van FGF en PTHLH aan secundair perifeer chondrosarcoom formatie is nog onduidelijk. In de epifysaire groeischijf onderdrukt PTHLH chondrocyten differentiatie in hypertrofische chondrocyten en FGF regelt chondrocyten proliferatie en differentiatie.

V. Conclusies

In de epifysaire groeischijf is geleidelijk onthuld hoe chondrocyten met elkaar en met de micro-omgeving communiceren via extracellulaire matrix. Deze interacties in de epifysaire groeischijf leiden tot de vorming van een gepolariseerde weefselstructuur. Cellen in de epifysaire groeischijf hebben homozygote mutaties in *EXT1/EXT2* wat de gradiënten en daardoor de signaaltransductie verstoort, en wat uiteindelijk leidt tot het verlies van celpolariteit. ,Dit kan dan bijdragen tot de vorming van een osteochondroom. Bovendien kan osteochondroom werken als een permissieve omgeving, waarin *EXT1/EXT2* wild-type cellen in de kraakbeenkap genetische veranderingen ondergaan en ontaaarden in een perifeer chondrosarcoom.

List of Publications

de Andrea CE, Kroon HM, Wolterbeek R, Romeo S, Rosenberg AE, DeYoung BR,Liegl B, Inwards CY, Hauben E, McCarthy EF, Idoate M, Athanasou NA, Jones KB, Hogendoorn PCW, Bovée JVMG. Interobserver reliability in the histopathological diagnosis of cartilaginous tumors in patients with multiple osteochondromas. *Mod Pathol.* 2012; *in press*.

de Andrea CE, Wiweger MI, Bovée JV, Romeo S, Hogendoorn PC. Peripheral chondrosarcoma progression is associated with increased type X collagen and vascularisation. *Virchows Arch.* 2012;460:95-102.

de Andrea CE, Hogendoorn PC. Epiphyseal growth plate and secondary peripheral chondrosarcoma: the neighbours matter. *J Pathol.* 2012;226:219-28.

de Andrea CE, Reijnders CM, Kroon HM, de Jong D, Hogendoorn PC, Szuhai K, Bovée JV. Secondary peripheral chondrosarcoma evolving from osteochondroma as a result of outgrowth of cells with functional EXT. *Oncogene*. 2012;31:1095-104.

de Andrea CE, Prins FA, Wiweger MI, Hogendoorn PC. Growth plate regulation and osteochondroma formation: insights from tracing proteoglycans in zebrafish models and human cartilage. *J Pathol.* 2011;224:160-8.

de Andrea CE, Petrilli AS, Jesus-Garcia R, Bleggi-Torres LF, Alves MT. Large and round tumor nuclei in osteosarcoma: good clinical outcome. *Int J Clin Exp Pathol.* 2011;4:169-74.

Wiweger MI, Avramut CM, de Andrea CE, Prins FA, Koster AJ, Ravelli RB, Hogendoorn PC. Cartilage ultrastructure in proteoglycan-deficient zebrafish mutants brings to light new candidate genes for human skeletal disorders. *J Pathol.* 2011;223:531-42.

Mohseny AB, Tieken C, van der Velden PA, Szuhai K, de Andrea C, Hogendoorn PC, Cleton-Jansen AM. Small deletions but not methylation underlie CDKN2A/p16 loss of expression in conventional osteosarcoma. *Genes Chromosomes Cancer.* 2010;49:1095-103.

de Andrea CE, Wiweger M, Prins F, Bovée JV, Romeo S, Hogendoorn PC. Primary cilia organization reflects polarity in the growth plate and implies loss of polarity and mosaicism in osteochondroma. *Lab Invest.* 2010;90:1091-101.

Curriculum Vitae

Carlos E. de Andrea was born on November 1st, 1978 in Curitiba, Brazil. He did his secondary undergraduate education at Bom Jesus High School (Curitiba, Brazil) and graduated in 1996. Subsequently, from 1997 to 2002, he attended **University of Parana** (Curitiba, Brazil) from where he received his Medicinæ Doctor degree, and then pursued Anatomic Pathology training at the same university. In 2005, he began a visiting resident program in bone and soft tissue pathology at **Mayo Clinic** (Rochester, MN, USA) under the supervision of **Dr. Krishnan K. Unni**. Subsequently, he resumed his training in bone pathology at **Federal University of Sao Paulo** under the supervision of **Dr. Maria T.S. Alves**. From 2008 to 2011, Carlos performed the research described in this thesis at the Department of Pathology, Leiden University Medical Center (Leiden, the Netherlands) under the supervision of **Prof. Dr. Pancras C.W. Hogendoorn**. In 2011, he received **the Pathologist-in-Training Award** from the International Society of Bone and Soft Tissue Pathology and **the Stowell Orbison Certificate of Merit** at the 100th United States and Canadian Academy of Pathology (USCAP) annual meeting. Since 2012, Carlos has been working as an Assistant Professor at Department of Histology and Pathology at **University of Navarra** (Pamplona, Spain).

Acknowledgments

I would like to thank the many people who have encouraged and assisted me throughout my pursuit of my doctorate. **Pancras C.W. Hogendoorn** has been a great mentor, given me valuable assistance and kept me focused on the individual tasks that together comprise a thesis. I would like to acknowledge and express my appreciation to the following people who have contributed their energies, experience and knowledge to me and my work during this rewarding process: **Anne-Marie Cleton-Jansen**, **Judith V.M.G. Bovee**, **Karoly Szuhai, Malgorzata I. Wiweger** and **Salvatore Romeo** for their direction, suggestions, and interest both professional and personal; **Alex B. Mohseny** and **Twinkal C. Pansuriya** for marshalling these extraordinary forces and mitigating the stress that can easily accompany a project of such scope; **Dina Ruano** for her sympathetic ear and her professional and personal skills in assisting me in any possible way; **Brendy van den Akker**, **Daniëlle de Jong**, **Frans Prins**, **Herman H. Kroon**, **Inge Briaire-de Bruijn**, **Maayke van Ruler** and **Pauline Wijers-Koster** for their contributions in time, energy and technical skills; all the **PhD students** and **Post-docs** of our research group for invaluable input; to my **friends** in and out of academia, whose generosity contributed in uncounted measure to the completion of my degree; and to all my **family**, especially my **mother** and **father**, who knew enough to take me to medicine and science in the first place.